SOLID STATE APPLICATIONS OF DIRECT ENERGY CONVERSION AND HEAT PUMPING FOR A SMALL AUTOMOTIVE VEHICLE

Thomas Constantine Tsoukalas

NAVAL POSTGRADUATE SCHOOL
Monterey, California

THESIS

SOLID STATE APPLICATIONS
OF DIRECT ENERGY CONVERSION AND HEAT PUMPING
FOR A SMALL AUTOMOTIVE VEHICLE

by

Thomas Constantine Tsoukalas

September 1975

Thesis Advisor: M.L. Wilcox

Approved for public release; distribution unlimited.

REPORT DOCUMENTATION PAGE

READ INSTRUCTIONS BEFORE COMPLETING FORM

1. REPORT NUMBER

2. GOVT ACCESSION NO.

3. RECIPIENT'S CATALOG NUMBER

4. TITLE (and Subtitle)

Solid State Applications of Direct Energy Conversion and Heat Pumping for a Small Automotive Vehicle

5. TYPE OF REPORT & PERIOD COVERED
Engineer's Thesis; September 1975

6. PERFORMING ORG. REPORT NUMBER

7. AUTHOR(s)

Thomas Constantine Tsoukalas

8. CONTRACT OR GRANT NUMBER(s)

9. PERFORMING ORGANIZATION NAME AND ADDRESS
Naval Postgraduate School
Monterey, California 93940

10. PROGRAM ELEMENT, PROJECT, TASK AREA & WORK UNIT NUMBERS

11. CONTROLLING OFFICE NAME AND ADDRESS
Naval Postgraduate School
Monterey, California 93940

12. REPORT DATE
September 1975

13. NUMBER OF PAGES
141

14. MONITORING AGENCY NAME & ADDRESS(if different from Controlling Office)

15. SECURITY CLASS. (of this report)
Unclassified

15a. DECLASSIFICATION/DOWNGRADING SCHEDULE

16. DISTRIBUTION STATEMENT (of this Report)

Approved for public release; distribution unlimited.

17. DISTRIBUTION STATEMENT (of the abstract entered in Block 20, if different from Report)

18. SUPPLEMENTARY NOTES

19. KEY WORDS (Continue on reverse side if necessary and identify by block number)

20. ABSTRACT (Continue on reverse side if necessary and identify by block number)

The feasibility of solid state application for electrical power generation and heat pumping in small automotive vehicles has been examined. A new geometric configuration for the thermoelectric couple was introduced and the heat

(20. ABSTRACT Continued)

flow problem has been solved analytically in detail. The obtained results appeared promising for future developments in this area.

Solid State Applications of Direct Energy Conversion and Heat Pumping For a Small Automotive Vehicle

by

Thomas Constantine Tsoukalas
Lieutenant, Hellenic Navy
B.S., Hellenic Naval Academy, 1964
M.S., Naval Postgraduate School, 1974

Submitted in partial fulfillment of the
requirements for the degree of

ELECTRICAL ENGINEER

from the

NAVAL POSTGRADUATE SCHOOL
September 1975

ABSTRACT

The feasibility of solid state application for electrical power generation and heat pumping in small automotive vehicles has been examined. A new geometric configuration for the thermoelectric couple was introduced and the heat flow problem has been solved analytically in detail. The obtained results appeared promising for future developments in this area.

TABLE OF CONTENTS

I. INTRODUCTION ---------- 8

II. STEADY STATE HEAT FLOW IN THE SEMICONDUCTOR ELEMENT ---------- 12

III. THERMOELECTRIC COOLER ---------- 18

A. ANALYSIS OF THE ELEMENTARY COOLER --------- 18

B. CONDITIONS FOR MAXIMUM HEAT PUMPING RATE -- 22

C. CONDITIONS FOR MAXIMUM COEFFICIENT OF PERFORMANCE ---------- 25

D. COMPARISON OF THE EXTERNAL CONDITIONS ----- 27

E. ESTIMATION OF TEMPERATURES OF OPERATION --- 30

IV. COOLER DESIGN ---------- 35

A. GENERAL CONSIDERATIONS ---------- 35

B. COOLER DESIGN BASED ON MAXIMUM COP. ------- 40

1. Thermoelectric Couple ---------- 40

2. Cold Side Heat Exchanger ---------- 42

3. Hot Side Heat Exchanger ---------- 51

V. THERMOELECTRIC GENERATOR ---------- 54

A. ANALYSIS OF ELEMENTARY GENERATOR ---------- 54

B. CONDITIONS FOR MAXIMUM EFFICIENCY --------- 59

C. OPTIMIZATION OF THE SEGMENTED T.E. GENERATOR ---------- 63

D. T.E. GENERATOR DESIGN ---------- 71

E. ESTIMATION OF AVAILABLE HEAT POWER FROM THE EXHAUST GASSES ---------- 86

1. Preliminary Calculations ---------- 86

2. Released Heat from Converter Action --- 90

3. Estimation of Available Heat from Hot Gasses ---------- 94

F. FINAL CONSIDERATIONS ON GENERATOR -------- 96

VI. CONCLUSIONS AND RECOMMENDATIONS FOR FURTHER STUDY ---------- 101

APPENDIX A. APPROXIMATE ANALYTIC SOLUTION OF HEAT BALANCE EQUATION ---------- 105

1. Influence of Thomson Effect on Heat Conduction ---------- 108

2. Influence of the Joule Effect on Heat Conduction ---------- 111

3. Composite Solution ---------- 116

APPENDIX B. SOLUTION OF SIMPLIFIED HEAT BALANCE EQUATION ---------- 122

COMPUTER PROGRAMS ---------- 126

LIST OF REFERENCES ---------- 140

INITIAL DISTRIBUTION LIST ---------- 141

ACKNOWLEDGEMENT

I would like to express my deepest appreciation for Professor Milton. L. Wilcox considered advice and help. For without them, this paper would not have been possible.

I, also, want to thank Ford Motor Company for providing necessary data which made the study realistic.

I. INTRODUCTION

In recent years the great expansion in the development of semiconducting materials with acceptable thermoelectric characteristics has made them attractive for, in special applications, direct energy conversion and heat pumping.

Thermoelectric power sources and heat pumping devices can offer significant advantages with respect to long life, years of unattended operation, freedom from environmental restraints, and unusually favorable specific power ratios.

It is true that even now thermoelectric cooling and power sources are not serious competitors of powerful heat pumps and conventional power apparatus, but they are irreplaceable in those cases where the overriding requirements are small size, simplicity of construction, quiet operation, weight, etc.

Various microrefrigerators, used in radio engineering, medicine and industrial design, have received proper recognition. Fueled portable thermoelectric generators, especially for military applications, are already used.

In the present work an attempt is made to design, at least theoretically, a thermoelectric air cooling device servicing the passenger compartment of a small automotive vehicle, in conjunction with a thermoelectric generator using the waste heat of the exhaust gasses of the engine to provide a portion of the required electrical power.

The feasibility of the replacement of the conventional alternator by a thermoelectric generator is also examined.

The introduction of the thermoelectric generator will improve the coefficient of performance of the thermoelectric cooler, and will also increase the initial installation cost.

The design was developed from the macroscopic point of view, considering the present state of the art of thermoelectric materials.

The total work is divided into five sections:

1) The heat flow analysis for the semiconductor material under a temperature gradient and internally generated heat due to the flow of electric current. The results of this analysis are almost common to the thermoelectric cooler and generator. In this section a differential equation, which describes the heat balance in the thermoelement has been derived. In this equation, the cross section of the thermoelement is treated as a function of the length and the properties of the material, as thermal conductivity, Thomson coefficient, etc., are treated as functions of temperature.

2) The analysis and design of the thermoelectric cooler. A detailed analysis of the T.E. cooler is made for both modes of operation, maximum heat pumping rate and maximum coefficient of performance. The analysis is closed with comparison between the two modes and the selection of max COP as the most suitable for the present application.

The analysis is followed by an indicated design of a cooler with a capacity of 7000 BTU/hour which, from a quick

estimation, was found to be satisfactory for the selected environmental conditions.

3) The analysis and design of the thermoelectric generator. The analysis is conducted from the standpoint of maximum efficiency mode. It is followed by selection of the proper thermoelectric materials for the assumed conditions. Computer techniques are employed for estimation of the temperature relations of the thermoelectric material properties. The analysis is closed with the estimation of the available heat power from the exhaust gasses. The attempted design concerns a segmented type thermoelectric generator which is carried out exclusively by a computer program.

4) Conclusions and recommendations for further study.

5) Appendices

Generally, the proposed configuration would be as it is shown in Figure 1.

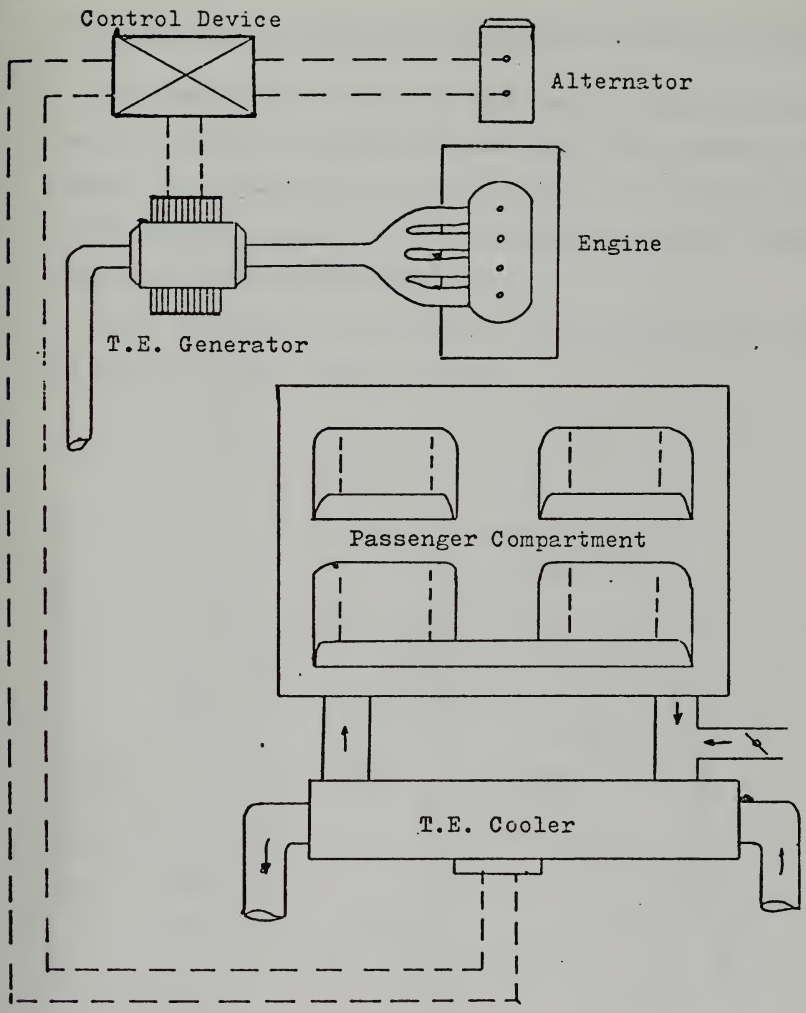

FIGURE I

DIAGRAMMATIC ARRANGEMENT OF THE PROPOSED SYSTEM

II. STEADY STATE HEAT FLOW IN THE SEMICONDUCTOR ELEMENT

The derivation of the heat flow balance equation through the thermoelement is presented when the cross section of the element is a function of the length and the characteristics of the material, electrical resistivity and thermal conductivity are functions of temperature.

Under the proposed geometry of the semiconductor, the one dimension heat flow is evident.

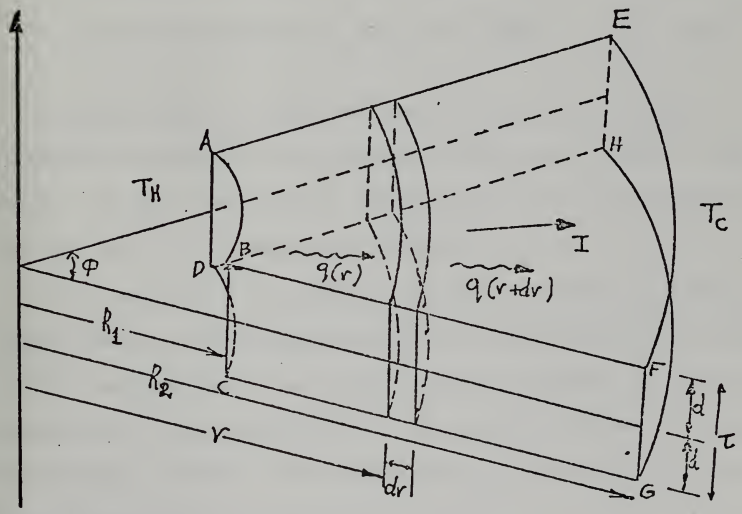

FIGURE 2

PROPOSED GEOMETRY OF THERMOELECTRIC SEGMENT

The semiconductor is considered to be adiabatically insulated on all sides except side ABCD and EFGH.

The temperature of the solid is assumed to be T_H at the front side (ABCD) and T_C at the rear side (EFGH), when T_H is greater than T_C. The characteristics of the material are considered to be variable and more specifically to be functions of temperature which can be expressed as:

1) Conductivity $\lambda(T) = a_0 + a_1T + a_2T^2$

2) Resistivity $\rho(T) = b_0 + b_1T + b_2T^2$

3) Seebeck coefficient $\alpha(T) = c_0 + c_1T + c_2T^2$

4) Thomson coefficient $\sigma(T) = T\frac{da(T)}{dT} = c_1T + 2c_2T^2$

Considering the part of the semiconductor which is confined between the cylindrical surfaces of radii r and r+dr, let q(r) and q(r+dr) be the rates of heat flowing in and out of the differential element.

If a current I is flowing through the semiconductor Joule heat will be generated due to the electrical resistance of the semiconductor and heat will be released or absorbed — depending on the direction of the flowing current — due to the Thomson effect. The differential of the Joule heat generation rate is given as:

$$q_J = I^2 \frac{\rho(T)}{A(r)} dr \qquad (1\text{-}1)$$

where A(r) is the surface of the differential solid element at radius r.

Also the differential form of the Thomson effect is given as:

$$q_T = I\sigma(T)dT \tag{1-2}$$

Consider now, for balance the rate of heat flow out of the differential solid element must be equal to the rate of heat flow in, plus the rate of heat generation in the element. These can be expressed as:

$$q(r+dr) = q(r) + q_J \pm q_T \tag{1-3}$$

But q(r+dr) can be expanded in a series of the form:

$$q(r+dr) = q(r) + \frac{\partial q(r)}{\partial r}dr + \cdots \tag{1-4}$$

If the first two terms will be considered, then equation (1-3) can be written as:

$$\frac{\partial q(r)}{\partial r}dr = q_J \pm q_T \tag{1-5}$$

Substituting the equivalent relations for q_J and q_T equation (1-5) becomes

$$\frac{dq(r)}{dr} = I^2\frac{\rho(T)}{A(r)} \pm I\sigma(T)\frac{dT}{dr} \tag{1-6}$$

The conduction heat – rate of flow – q(r) is given by:

$$q(r) = -\lambda(T)A(r)\frac{dT}{dr} \tag{1-7}$$

By differentiation in respect to r equation (1-7) becomes:

$$\frac{dq(r)}{dr} = -\frac{d[\lambda(T)]}{dT}\frac{dT}{dr}A(r)\frac{dT}{dr} - \lambda(T)\frac{d[A(r)]}{dr}\frac{dT}{dr} - \lambda(T)A(r)\frac{d^2T}{dr^2} \tag{1-8}$$

By substituting of equation (1-8), equation (1-6) becomes:

$$\lambda(T)A(r)\frac{d^2T}{dr^2} + \frac{d[\lambda(T)]}{dT}A(r)\left[\frac{dT}{dr}\right]^2 + \lambda(T)\frac{d[A(r)]}{dr}\frac{dT}{dr} \pm I\sigma(T)\frac{dT}{dr} + I^2\frac{\rho(T)}{A(r)} = 0 \tag{1-9}$$

For the geometric configuration of Figure 2 the cross section area A(r) is a linear function of radius r:

$$A(r) = \phi\tau r \tag{1-10}$$

$$A(r) = mr \tag{1-10a}$$

where $m = \phi\tau$.

Using the above expression for the cross section, equation (1-9) becomes:

$$\lambda(T)mr\frac{d^2T}{dr^2} + \frac{d[\lambda(T)]}{dT}mr\left[\frac{dT}{dr}\right]^2 + \left[\lambda(T)m \mp I\sigma(T)\right]\frac{dT}{dr} + I^2\frac{\rho(T)}{mr} = 0 \tag{1-11}$$

Equation (1-11) is the differential equation which describes the rate of heat flow through the semiconductor material, with the geometry of Figure 2 and the conditions stated before, when a temperature gradient is impressed and an electrical current is allowed to flow.

This equation is non-linear and at least a rigorous analytic solution is not obvious.

If in the range of temperature, when the thermoelectric couple is operated, the characteristics of the semiconductor material are constant or reasonably can be assumed to be constant, then equation (1-11) is greatly simplified and takes the following form:

$$\frac{d^2T}{dr^2} + \frac{1}{r}\frac{dT}{dr} + \frac{I^2\varrho}{\lambda m^3 r^2} = 0 \qquad (1\text{-}12)$$

Since the temperature gradient under which the thermoelectric element of a cooler is operating is small, equation (1-12) reasonably can be used as the basic equation for the design.

This is not the case for the thermoelectric generator where the range of temperature is quite extended, and the material characteristics present sufficient deviations from the corresponding values at low temperatures.

For this, equation (1-11) will be used as the basis for the thermoelectric generator design.

An analytic solution of equation (1-11) is given in APPENDIX A under certain assumptions. APPENDIX B provides the analytic solution of equation (1-12).

III. THERMOELECTRIC COOLER

A. ANALYSIS OF THE ELEMENTARY COOLER

The operation of the thermoelectric cooler is based on the Peltier effect, which was discovered in the eighteen-thirties. This phenomenon was explained correctly by Lenz in 1838. When an electric current I flows through a contact between two conductors, a certain amount of heat is either evolved or absorbed at the contact, depending on the directions of the current. This heat is known as the Peltier heat Q_Π.

Becquerel and others established that Q_Π is directly proportional to the current I:

$$Q_\Pi = \Pi(T) I \tag{3-1}$$

where $\Pi(T)$ is the so-called Peltier coefficient.

It has also been shown that if the current flowing through the junction has the same direction as heat flow which is due to the heating of this junction then the Peltier heat is absorbed; while in the opposite case, heat is evolved.

The Peltier effect has been observed in a great variety of materials, and the Peltier coefficient has been found to be dependent on temperature in a complex fashion.

The thermocouple is considered under steady state conditions with its hot junction at a temperature T_H and the cold junction at T_C.

Electric current is considered flowing through the couple in the direction opposite to its Seebeck voltage.

The arrangement is shown in Figure 3.

The law of conservation of energy gives:

$$q_{I_1} - q_{I_0} = W \tag{3-2}$$

where q_o is the rate of heat absorption at the cold junction, q_I is the rate of heat which is evolved at the hot junction, and W is the electric power.

An important efficiency index of the thermocouple is the coefficient of performance which is defined by:

$$COP = \frac{q_o}{W} \tag{3-3}$$

Another important index is the heat pumping rate — or the refrigerating effect — q_o which can be expressed by:

$$q_{I_o} = \Pi(T_c)I + \lambda_P(T)A_P(r)\left.\frac{dT}{dr}\right|_{r=R_1} + \lambda_N(T)A_N(T)\left.\frac{dT}{dr}\right|_{r=R_1} \tag{3-4}$$

The thermoelectric coolers are usually operating under a small temperature difference. This is particularly true in the air conditioning applications. Under these small

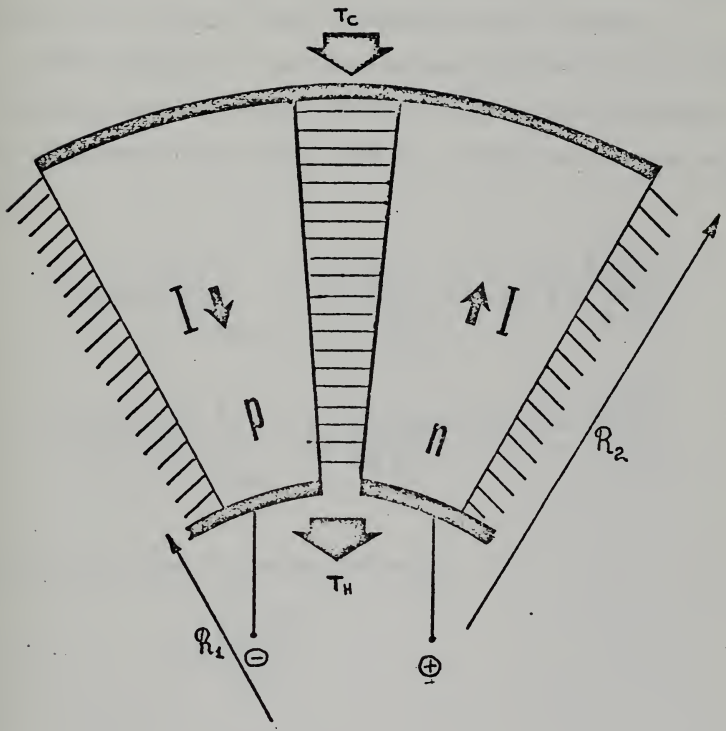

FIGURE 3

ELEMENTARY THERMOELECTRIC COUPLE

temperature ranges, the variations of the properties of the semiconducting materials are limited, and the use of average values introduces slight errors of the order of one percent.

The use of average values simplifies the analysis of the system and they are used throughout this section.

From APPENDIX B the rate of heat flowing to the cold junction, because of the existing temperature gradient and the generated Joule heat, for the P-type and N-type segments is:

$$-\bar{\lambda}_P A_P(r)\frac{dT}{dr}\bigg|_{r=R_1} = -\bar{\lambda}_P \frac{(\phi\tau)_P}{\ln\left(\frac{R_2}{R_1}\right)}\Delta T - \frac{1}{2}I^2\bar{\rho}_P\frac{\ln\left(\frac{R_2}{R_1}\right)}{(\phi\tau)_P} \tag{3-5}$$

$$-\bar{\lambda}_N A_N(r)\frac{dT}{dr}\bigg|_{r=R_1} = -\bar{\lambda}_N \frac{(\phi\tau)_N}{\ln\left(\frac{R_2}{R_1}\right)}\Delta T - \frac{1}{2}I^2\bar{\rho}_N\frac{\ln\left(\frac{R_2}{R_1}\right)}{(\phi\tau)_N} \tag{3-6}$$

Introducing the following variables:

$$x = \frac{\ln\left(\frac{R_2}{R_1}\right)}{(\phi\tau)_P} \tag{3-7}$$

$$y = \frac{\ln\left(\frac{R_2}{R_1}\right)}{(\phi\tau)_N} \tag{3-8}$$

$$\Pi(T_c) = \bar{\alpha}(T_c)T_c = \left(|\alpha_P(T_c)| + |\alpha_N(T_c)|\right)T_c \tag{3-9}$$

equation (3-4) becomes:

$$q_o = \bar{\alpha}(T_c) I T_c - \left[\frac{\bar{\lambda}_P}{X} + \frac{\bar{\lambda}_N}{Y}\right]\Delta T - \frac{1}{2} I^2 \left[\bar{\rho}_P X + \bar{\rho}_N Y\right] \qquad (3\text{-}10)$$

The work done by the electric source, per unit time, consists of the Joule heat evolved in the thermocouple arms, and the work done against the thermo-e.m.f $I\bar{\alpha}\Delta T$

$$W = I\bar{\alpha}\Delta T + I^2 R \qquad (3\text{-}11)$$

where R is the ohmic resistance of the couple. The coefficient of performance can be written as:

$$COP = \frac{\bar{\alpha}(T_c) I - \left[\frac{\bar{\lambda}_P}{X} + \frac{\bar{\lambda}_N}{Y}\right]\Delta T - \frac{1}{2} I^2 \left[\bar{\rho}_P X + \bar{\rho}_N Y\right]}{I\bar{\alpha}\Delta T + I^2 \left[\bar{\rho}_P X + \bar{\rho}_N Y\right]} \qquad (3\text{-}12)$$

$$COP = \frac{q_o}{I\bar{\alpha}\Delta T + I^2 R} \qquad (3\text{-}13)$$

B. CONDITIONS FOR MAXIMUM HEAT PUMPING RATE

The heat pumping rate of the elementary thermoelectric cooler, as it appears in equation (3-10), is a function of X, Y, and I. Relative maximum can be found by the Lagrange multiplier technique using as constraint function:

$$R = \bar{\rho}_P X + \bar{\rho}_N Y \qquad (3\text{-}14)$$

Thus the following conditions must be satisfied:

$$\frac{\partial q_o}{\partial x} + h\bar{\rho}_P = 0 \tag{3-15}$$

$$\frac{\partial q_o}{\partial y} + h\bar{\rho}_N = 0 \tag{3-16}$$

$$\frac{\partial q_o}{\partial I} = 0 \tag{3-17}$$

where h is the Lagrange multiplier.

Eliminating h from equations (3-15) and (3-16) the first condition for q_o to be maximum is found to be:

$$\frac{x}{y} = \left[\frac{\bar{\rho}_N \bar{\lambda}_P}{\bar{\rho}_P \bar{\lambda}_N}\right]^{1/2} \tag{3-18}$$

By substitution of equations (3-7) and (3-8), equation (3-18) becomes:

$$\frac{(\Phi\tau)_N}{(\Phi\tau)_P} = \left[\frac{\bar{\rho}_N \bar{\lambda}_P}{\bar{\rho}_P \bar{\lambda}_N}\right]^{1/2} \tag{3-19}$$

The second condition for the maximum heat pumping rate is found from equation (3-17):

$$I_{opt} = \frac{\bar{\alpha} T_c}{R} \tag{3-20}$$

The voltage to be applied to the thermocouple is given by:

$$V = \bar{\alpha}\Delta T + I_{opt} R \tag{3-21}$$

Substituting the expression for I from equation (3-2) in the above equation it is found:

$$V = \bar{\alpha} T_H \tag{3-22}$$

The required electrical power for the couple is:

$$P = VI = \bar{\alpha} T_H I_{opt} \tag{3-23}$$

The maximum heat pumping rate q_{max} is found from equation (3-10) after the substitution of equations (3-18) and (3-20).

$$q_{max} = \frac{\bar{\alpha}^2 T_c^2 (D-J)(D+J)}{2R\,(D-1)(D+1)} \tag{3-24}$$

where

$$D = \left[1 + g\right]^{1/2} \tag{3-25}$$

$$g = \frac{\bar{\alpha}^2}{\left[\sqrt{\bar{\rho}_p \lambda_p} + \sqrt{\bar{\rho}_N \bar{\lambda}_N}\right]^2} \frac{T_H + T_c}{2} \tag{3-26}$$

$$J = \frac{T_H}{T_c} \tag{3-27}$$

The coefficient of performance under the maximum heat pumping rate conditions is found from equation (3-13) after transforming it by means of equations (3-18) and (3-20).

$$COP = \frac{(D-J)(D+J)}{2J\,(D-1)(D+1)} \tag{3-28}$$

The rate of heat rejection is determined with the help of equations (3-3), (3-28) and (3-24).

$$q_1 = \frac{\bar{\alpha}^2 T_c^2}{2R} \left[\frac{(D-J)(D+J)}{(D-1)(D+1)} + 2J \right] \tag{3-29}$$

C. CONDITIONS FOR MAXIMUM COEFFICIENT OF PERFORMANCE

As it was in the case of maximum heat pumping rate, the coefficient of performance equation (3-13), is also a function of x, y, and I.

Applying the same technique, the following conditions must be satisfied:

$$\frac{\partial K}{\partial x} + h\bar{\rho}_P = 0 \tag{3-30}$$

$$\frac{\partial K}{\partial y} + h\bar{\rho}_N = 0 \tag{3-31}$$

$$\frac{\partial K}{\partial I} = 0 \tag{3-32}$$

Where the notation K instead of COP, for the coefficient of performance is introduced for convenience, and h again represents the Lagrange multiplier. Elimination of h between equations (3-30) and (3-31) gives exactly the condition of equations (3-18) and (3-19).

By algebraic manipulation the following expressions are obtained:

$$I = \frac{\bar{\alpha}\,\Delta T}{(D-1)\,R} \tag{3-33}$$

$$V = \frac{\bar{\alpha}\,\Delta T\,D}{(D-1)} \tag{3-34}$$

$$COP_{max} = \frac{T_c}{\Delta T}\left[\frac{D - \frac{T_H}{T_c}}{D+1}\right] \tag{3-35}$$

It is obvious that equation (3-25) goes to zero when:

$$D = \frac{T_H}{T_c} \tag{3-36}$$

and it goes to infinity when:

$$\Delta T = 0 \tag{3-37}$$

Combining equations (3-10), (3-18) and (3-33), the heat pumping rate becomes:

$$q_0 = \frac{\bar{\alpha}^2 D}{R(D-1)^2(D+1)}(T_H - T_c)(T_c D - T_H) \tag{3-38}$$

D. COMPARISON OF THE EXTERNAL CONDITIONS

The two cases of maximum heat pumping rate and maximum coefficient of performance differ very markedly as regards both the working conditions — voltage required — and the efficiency indices.

Comparing the values of q_{max} and q_o in Figure 4, it is seen that q_{max} is greater than q_o and consequently, in order to have the same heat pumping rate for thermocouples working under conditions of q_{max} and COP_{max} it is necessary to use a larger number of thermoelectric units in the second case than in the first. This aspect is not decisive because from the efficiency point of view it is first of all necessary to ensure that the coefficient of performance is sufficiently high, since it is this coefficient which governs the electrical power consumed in a cooling device. On the other hand, it follows from Figure 5 that the coefficient of performance at the COP_{max} is greater than COP and that this difference can not be compensated at all. The preferable conditions are those when the coefficient of performance is a maximum since the materials known at present do not give such a high coefficient of performance that it can be afforded to have it lower, even for the purpose of economy of material.

Designs based on the maximum heat pumping rate could be used only for the rapid cooling of an enclosure or for cooling it to a lower temperature at the cost of additional electrical power consumption.

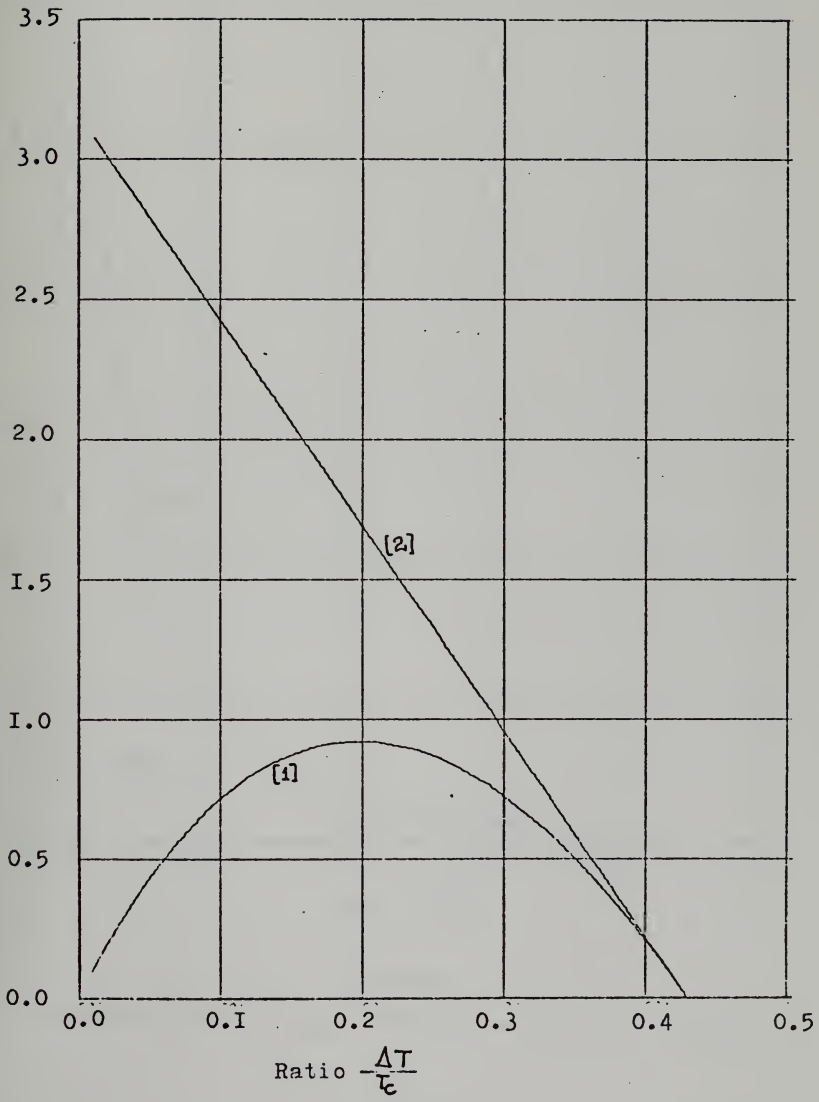

FIGURE 4

COMPARISON OF q_{max} - CURVE 2 - AND q_o - CURVE I

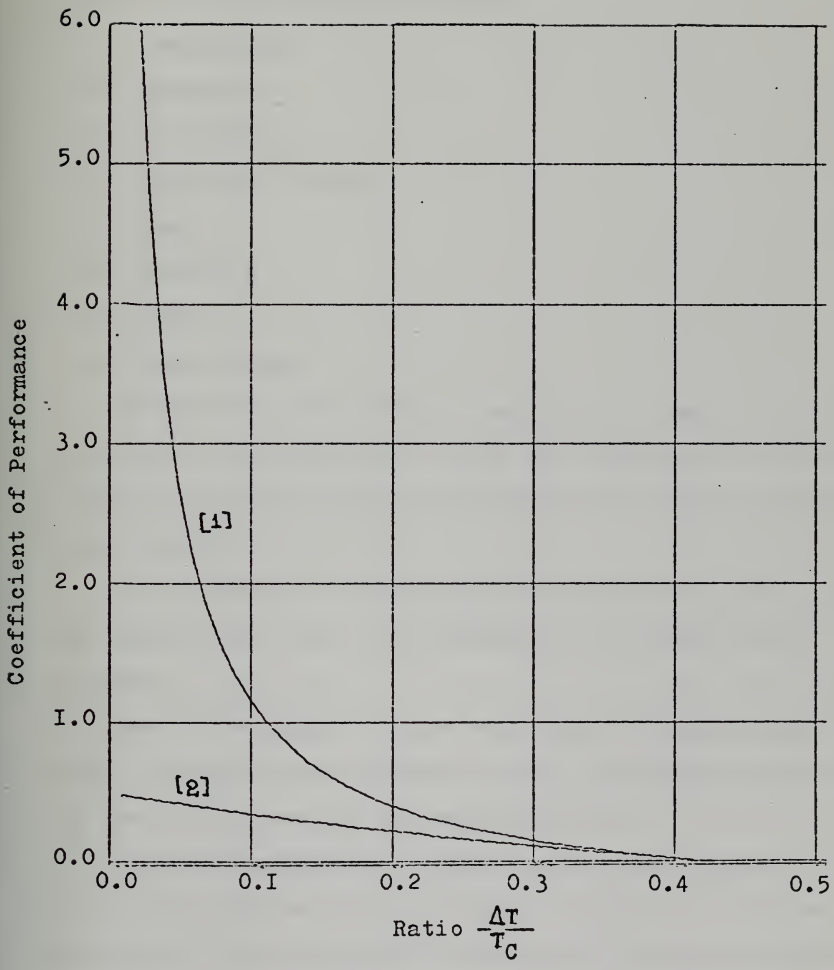

FIGURE 5

COMPARISON OF COP_{MAX} - CURVE I - AND COP - CURVE 2

E. ESTIMATION OF TEMPERATURES OF OPERATION

Complete air conditioning involves the simultaneous control of the following factors:

1) Temperature
2) Humidity
3) Air motion
4) Air distribution
5) Dust
6) Bacteria
7) Odors
8) Toxic gasses

Of these the first three, temperature, humidity, and air motion, are paramount, and no air conditioning system deserves the name unless it satisfactorily controls those three factors.

In the present work the thermoelectric air conditioning is examined only from the standpoint of the air cooling process.

The device should be also considered as equally applicable for air heating process by just reversing the direction of the current through the thermoelements.

From the standpoint of human comfort, the object of the air cooling device is not to cool the body but to control its rate of heat loss within reasonable limits by methods that are known to be the most conductive to comfort.

There are four factors which, by their combined effect, determine the cooling power of the atmosphere upon the human

body. They are temperature, humidity, air motion and radiation.

The effect of humidity and air movement are matters of common experience. When the indoor air is very dry, a higher temperature is necessary for comfort because of the greater cooling effect of the dry air. The evaporation of the perspiration with which the human body is always partially covered has a marked influence upon the rate of heat loss, and the rate of evaporation is dependent upon the humidity of the surrounding atmosphere.

The cooling action of air motion upon the skin increases heat removal by the increased evaporative effect and by an increase in the convection effect as the layer of air in contact with the skin is repeatedly renewed.

Loss of heat by radiation from the exposed body and clothing depends on the temperature of the surrounding walls and is independent of air temperature.

Air movement reduces to some extent the radiation loss by lowering the surface temperature of the body. The rate of heat loss varies according to Steffen's fourth power law and is dependent upon the difference in temperature between the surface of the body and the mean temperature of the environment. This latter temperature is referred to as the mean radiant temperature.

Experiments made on a large number of human subjects have demonstrated that there is a consistent relation between

the temperature, humidity and air motion in their effect upon comfort. When the results of such observations are plotted on a psychometric chart, it is found that the points representing conditions of equal warmth fall in approximately straight lines. These straight lines are called "effective temperature lines". For moving air the effective temperature for a given temperature and humidity is lower than that corresponding to still air. The effective temperature is the only true index of human comfort that is now available. Neither the dry-bulb nor the wet-bulb thermometer alone trully indicates the conditions of the air from a comfort standpoint.

The optimum conditions for human comfort at summer time are considered to be 71 F° effective temperature and air movement of 15 to 35 feet per minute for an outdoor temperature of 80 F°.

The following table gives the corresponding effective temperatures for several outdoor dry-bulb temperatures.

OUTSIDE DRY-BULB TEMPERATURE (F°)	EFFECTIVE TEMPERATURE (F°)
105	75.5
100	75
95	74
90	73
85	72
80	71

TABLE 1

These effective temperatures are the statistical results of extensive experimental work, where several factors were considered, between them the stress which a human body suffers when it is moving from low to high temperature environments and vice versa.

The outdoor conditions to be assumed in the calculations of the cooling and dehumidifying load should not be the highest recorded temperature in a location which usually exist for only a few hours during the year. They should be chosen as conditions which may be exceeded for a few days during the summer.

In every large city a certain design dry-bulb and wet-bulb temperature which are readily ascertained, have become established and generally adopted. The following table gives these temperatures for a few cities of the U.S.A.

LOCATION	DESIGN TEMPERATURES	
	DRY-BULB	WET-BULB
New York City	95	75
Chicago	95	75
Philadelphia	95	78
Detroit	95	75
Cleveland	95	75
St. Louis	95	78
Washington	95	78
New Orleans	95	79
San Francisco	90	65
Dallas	100	78
Jacksonville	95	78

TABLE 2

Since an automobile is not designed to operate in a certain place, the worst case outdoor conditions are selected as those corresponding to the city of Dallas.

So, outdoor dry-bulb temperature is 100 F° and indoor maintained-effective-temperature the corresponding 75 F°.

IV. COOLER DESIGN

A. GENERAL CONSIDERATIONS

The design is based on the worst case which corresponds to an outdoor temperature of 100 F° and an effective temperature, for human comfort, of 75 F°. This means that the temperature of the incoming air in the hot side of the thermo elements would be 100 F° and the maintained temperature in the passenger's compartment of the vehicle would be 75 F°.

The proposed configuration of the thermoelectric cooler is shown in Figures 6a, 6b. It consists of radially arranged thermocouples, forming rings. A number of such rings are assembled to form the annular configuration. Fins have been introduced in both sides of the thermocouples to increase the rate of heat transfer. The outer annular finned space forms the heat absorbing exchanger and the inner cylindrical finned space forms the heat rejecting exchanger. The cooling medium is air which flows by means of fans, one for every heat exchanger. When the vehicle is moving with a speed higher than a certain level, there is no need for operation of the heat rejecting exchanger fan.

It is also assumed that the vehicle has been parked for a long period under the sun and the temperature of the indoor air has reached 100 F°.

The temperatures of the hot and cold side of the thermoelements, T_H, T_C, can be estimated if the desired logarithmic

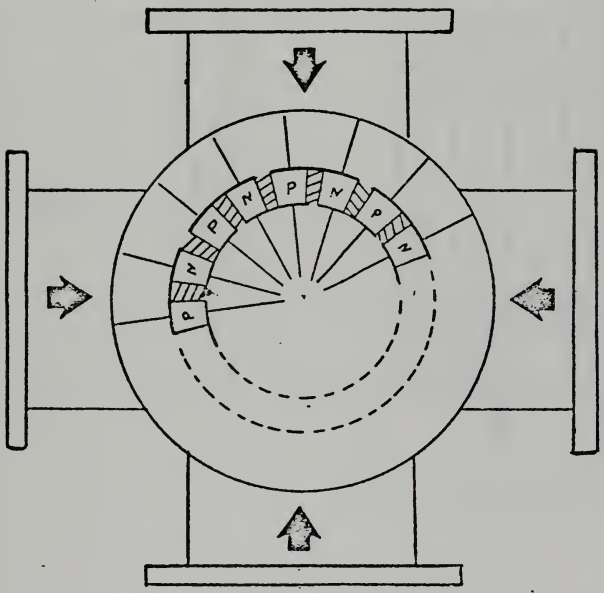

FIGURE 6a

CROSS SECTION OF T.E. COOLER

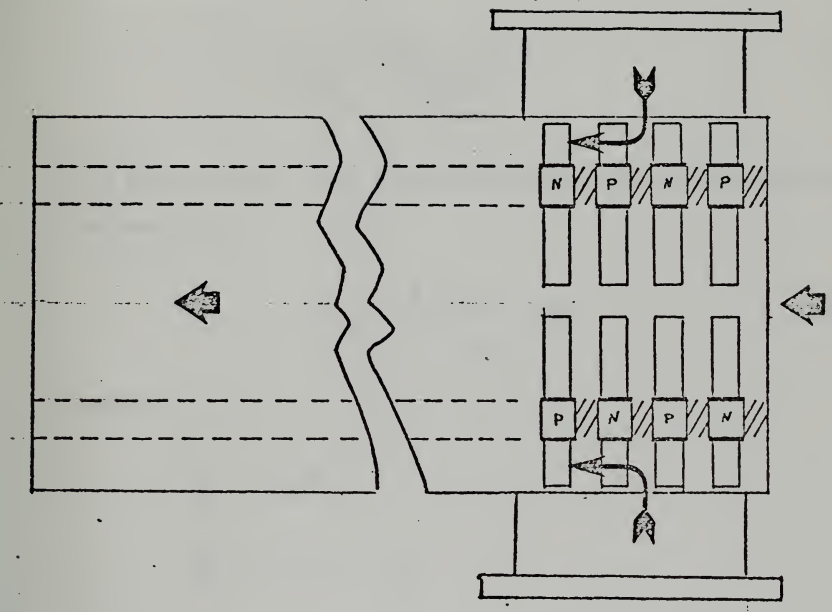

FIGURE 6b

LONGITUDINAL CROSS SECTION OF T.E. COOLER

mean and output temperatures of the cooling air, in both sides of the thermocouples are selected.

According to the definition of mean logarithmic temperature:

$$\Delta T_{ln} = \frac{\theta_{max} - \theta_{min}}{ln \frac{\theta_{max}}{\theta_{min}}} \qquad (4\text{-}1)$$

the hot and cold shoe temperatures of the thermocouples are estimated as:

$$T_{c,H} = \frac{A T_{out} - T_{in}}{A - 1} \qquad (4\text{-}2)$$

where:

$A = e^{\frac{\Delta T}{K}}$

$\Delta T = T_{in} - T_{out}$

K = desired value of logarithmic mean temperature

θ_{min}, θ_{max} = temperature differences as shown in Figure 7.

The cooling capacity of the thermoelectric cooler is selected to be 7000 BTU per hour. This figure is considered as a moderate value, sufficient to serve a small vehicle carrying four passengers under the climatological conditions described previously.

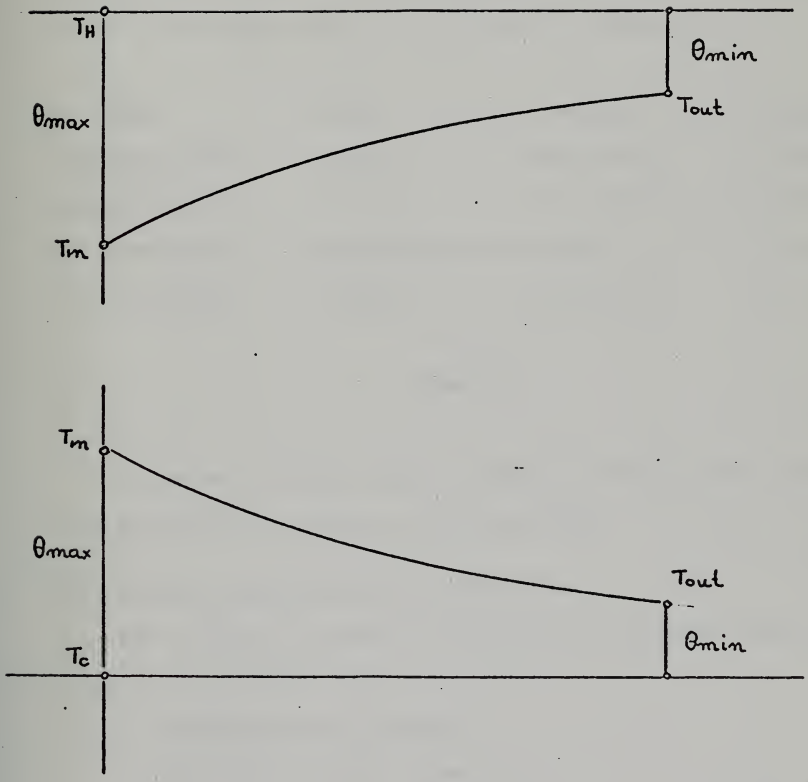

FIGURE 7

ASSUMED TEMPERATURE DISTRIBUTION FOR DETERMINATION OF LOG. MEAN TEMPERATURES

As the most suitable thermoelectric material for cooling application selected a bismuth – tellurium – antimony compound for the P-type semiconductor, and a bismuth – tellutium – selenium compound for the N-type. These materials have been developed since 1968 from Westinghouse. The average properties of the materials are displayed in Table 3.

ITEM	UNITS	P-type	N-type
Seebeck Coeff.	V/deg K	205×10^{-6}	-220×10^{-6}
Resistivity	ohm-cm	1.2×10^{-3}	1.08×10^{-6}
Th. Conductiv.	watts/deg c-cm	0.0121	0.0149
Fig. of merit	1/deg K	2.82×10^{-3}	3.0×10^{-3}

TABLE 3

In order to obtain good mechanical strength the materials are processed by pressure and sintering.

B. COOLER DESIGN BASED ON MAXIMUM COP

This design is based on the results obtained from the analysis in Section III-C.

1. Thermoelectric Couple

The coefficient of performance, as was defined in Section III-C, is independent of the geometric configuration of the thermoelectric couple. It is only a function of hot and cold shoe temperature and of the material properties. The heat pumping rate and the optimum current depend on the

total electrical resistance of the thermocouple which is a strong function of geometry. From this standpoint, an optimization of the geometry had been attempted using iterative computer techniques and the selected dimensions in Table 4.

ITEM	UNITS	P-type segment	N-type segment
R_1	cm (in.)	7.0 (2.756)	7.0 (2.756)
R_2	cm (in.)	8.5 (3.346)	8.5 (3.346)
ϕ	degrees	10.0	11.0
τ	cm (in.)	1.0 (0.3937)	1.0 (0.3937)

TABLE 4

The calculated cooling and electrical characteristics of the thermocouple are shown in Table 5.

ITEM	UNIT	VALUE
Electrical Resistance	ohm	2.31×10^{-3}
Hot shoe temp. T_H	degr. K	322.73
Cold shoe temp. T_C	degr. K	291.5
Electrical current	amperes	14.4
Applied Voltage	volts	0.048
COP	dimensionless	1.13534
Required Power	watts	0.691
Heat pumping rate	watts	0.74466
Heat rejection rate	watts	1.43569

TABLE 5

For the cooling load of 7000 BTU per hour a total number of 2754 thermocouples is required. If a nine degree wedge of insulation is provided for each thermocouple, then 12 couples form one ring and the total number of rings is determined as 230. Each ring, according to Table 4, has width 1.0 cm. Allowing insulation of 0.3 cm between the rings, the total length of the configuration is 299 cm.

Four units, each having a length of 74.75 cm and consisting of 57.5 rings, will satisfy the requirements. The externally supplied electrical power is calculated to be:

$$2754 \times 0.691 = 1903 \text{ watts}$$

and the heat rejection rate:

$$2754 \times 1.43569 = 3954 \text{ watts or } 13504 \text{ BTU/hour}$$

2. Cold Side Heat Exchanger

The introduction of extended surfaces, in the form of fins with rectangular cross section, increases the exchange surface of the heat exchanger. The fins have an efficiency given by:

$$\eta_f = \frac{\tanh(mb)}{mb} \qquad (4\text{-}3)$$

where

$$m = \sqrt{\frac{2h}{\lambda \delta}} \qquad (4\text{-}4)$$

Figure 8b shows the variation of n_f as a function of for several values of h. The cooling medium is air with average properties displayed in Table 6.

SYMBOL	ITEM	UNITS	VALUE
λ	Thermal conductivity	BTU/ft-hour-F°	0.015
μ	Dynamic viscosity	lbm/ft-sec.	1.7×10^{-5}
ρ	Density	lbm/ft^3	0.075
c_p	Thermal capacity	BTU/lbm-F°	0.24

TABLE 6

Figure 9 shows the heat exchanger arrangement. The long fins form four different types of air ducts, namely A, B, C, and D.

Each air duct has an equivalent hydraulic diameter given by:

$$D_e = \frac{4\ S}{P} \qquad (4\text{-}5)$$

where S is the cross section and P the perimeter of the duct.

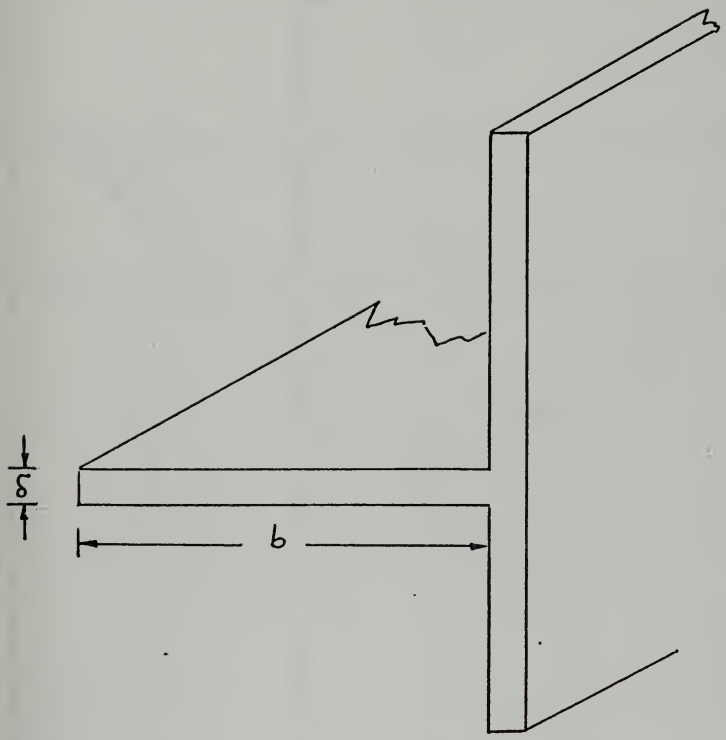

FIGURE 8a

LONGITUDINAL FIN ARRANGEMENT

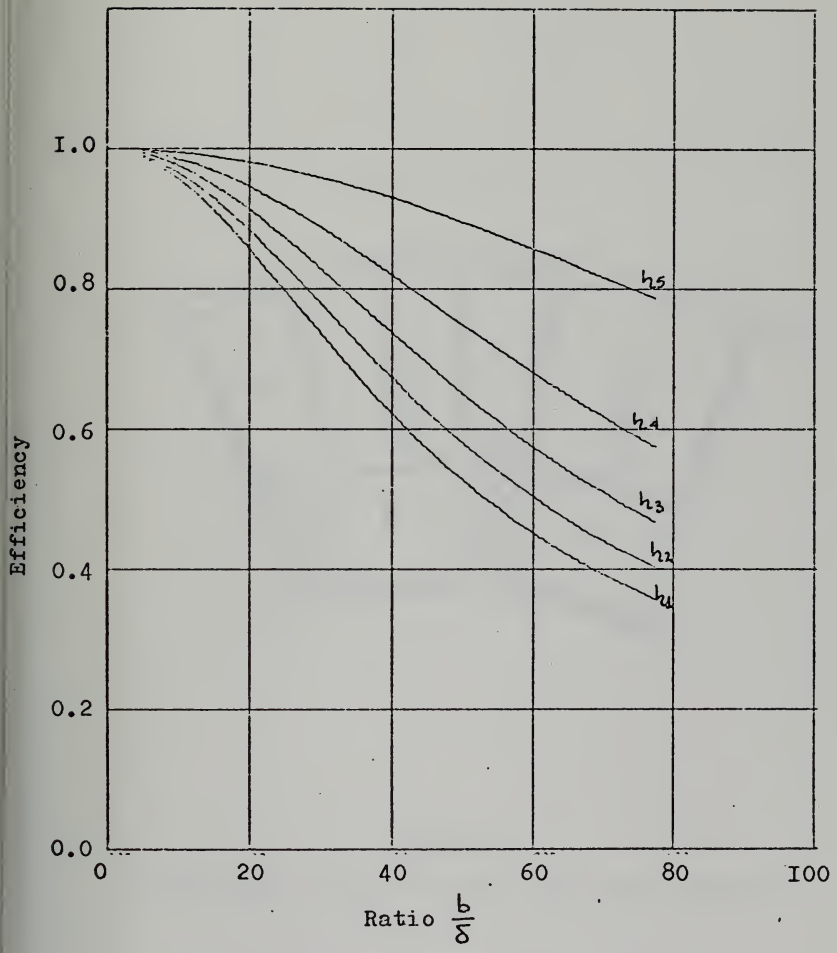

FIGURE 8b

FIN EFFICIENCY

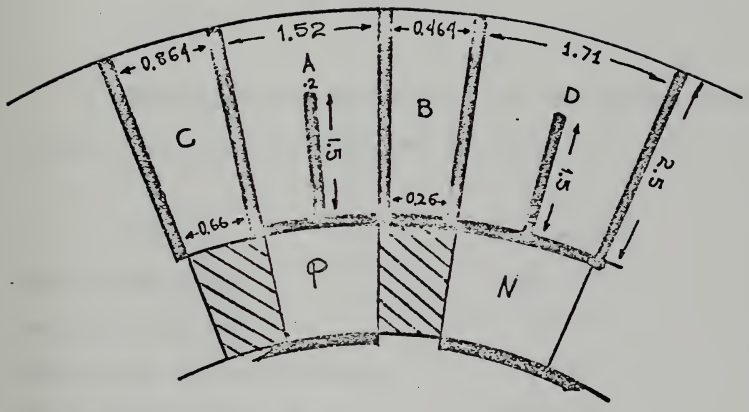

FIGURE 9

ELEMENTARY SECTION OF COLD SIDE HEAT EXCHANGER

The calculated equivalent diameters for each duct type are:

$$(D_e)_A = 48.284 \times 10^{-3} \text{ ft}$$

$$(D_e)_B = 43.89 \times 10^{-3} \text{ ft}$$

$$(D_e)_C = 43.89 \times 10^{-3} \text{ ft}$$

$$(D_e)_D = 62.26 \times 10^{-3} \text{ ft}$$

The selected temperatures for the air and thermocouple cold shoe are displayed in Table 7.

ITEM	TEMPERATURE
Incoming hot air	100 F°
Outgoing cold air	70 F°
Maintained room environment	75 F°
Thermocouple cold shoe	291.5 K°

TABLE 7

For operation at low noise level, air velocity is selected to be 1800 feet per minute.

The Reynold's number is determined from:

$$N_{RE} = \frac{\rho D_e v}{\mu} \qquad (4\text{-}6)$$

Using the air properties of Table 7 the corresponding value of N_{RE} for each type of duct is calculated as:

$$(N_{RE})_A = 9285$$

$$(N_{RE})_B = 8440$$

$$(N_{RE})_C = 8440$$

$$(N_{RE})_D = 11973$$

These values are indicative of turbulent flow. The calculation of the convection heat transfer coefficients is based on the Dittus and Boelter equation:

$$N_{NU} = 0.0265 \ (N_{RE})^{0.8} \ (N_{pr})^{0.3} \qquad (4\text{-}7)$$

where N_{NU} and N_{pr} are the Nusselt's and Prandtl's number correspondingly, given by:

$$N_{Nu} = \frac{h D_e}{\lambda} \qquad (4\text{-}8)$$

$$N_{Pr} = \frac{c_p \mu}{\lambda} \qquad (4\text{-}9)$$

For a Prandtl's number almost equal to 0.7 the Nusselt's number, for the different type of air ducts, is:

$$(N_{NU})_A = 35.1428$$

$$(N_{NU})_B = 32.56$$

$$(N_{NU})_C = 32.56$$

$$(N_{NU})_D = 43.07$$

The corresponding convection heat transfer coefficients are found from Equation (4-8) as:

$$h_A = 10.92$$

$$h_B = 11.128$$

$$h_C = 11.128$$

$$h_D = 10.376$$

Using the above values for the convection heat transfer coefficient and assuming aluminum as the fins material, with thermal conductivity 92 BTU/ft-hour-F°, the efficiency of the long and short fins, according to Equation (4-3), is:

$$n_{fl} = 0.9256 \quad \text{and} \quad n_{fs} = 0.9716$$

correspondingly.

The rate of heat absorption is calculated from the following equation:

$$q = \Delta T_{ln} \sum_j h_j S_j \qquad (4\text{-}10)$$

where the subscript j corresponds to different types of air ducts of the heat exchanger. Analytically the exchange effective surfaces per thermocouple column are:

$S_A = (5n_{fl} + 3n_{fs} + 1.08)\ 230 = 1983.2\ cm^2 = 2.135\ ft^2$

$S_B = (5n_{fl} + 0.26)\ 230 = 1124.24\ cm^2 = 1.21\ ft^2$

$S_C = 5n_{fl} 230 = 1064.44\ cm^2 = 1.146\ ft^2$

$S_D = (5n_{fl} + 3n_{fs} + 1.232)\ 230 = 2018.2\ cm^2 = 2.172\ ft^2$

From the temperatures of Table 2 the logarithmic mean temperature of the cooling air, according to Equation (4-1), is found to be:

$$\Delta T_{ln} = 15.0$$

Substitution of the determined values for S_j and h_j in Equation (4-10) gives:

$$q = (2.135 \cdot 10.92 + 1.21 \cdot 11.128 + 1.146 \cdot 11.128 + 2.172 \cdot 10.376)\ \Delta T_{ln} = 1081\ \text{BTU/hour}$$

For the 12 thermocouple columns of the device, the capacity of the heat absorbing exchanger is found:

$$q_{TOT} = 12792 \text{ BTU/hour}$$

The above figure for the heat exchanger's capacity offers a margin factor of 1.85 which ensures satisfactory operation under even, not considered, worse conditions.

The air flow requirements can be determined from:

$$\dot{m} = \frac{q}{c_p (t_{in} - t_{out})} \qquad (4\text{-}11)$$

for q = 12,792 BTU/hour, c_p = 0.28 BTU/lbm-F°, t_{in} = 100 F°, and t_{out} = 70 F°, the rate of air flow is determined as:

$$\dot{m} = 1522.8 \text{ lbm/hour}$$

For the air density $\rho = 0.075 \text{ lbm/ft}^3$

$$\dot{m} = 5.64 \text{ ft}^3/\text{sec}$$

3. Hot Side Heat Exchanger

This is also a finned type heat exchanger. It consists of a tube with radially introduced fins of two different lengths. The fin's material is assumed to be aluminum

with thermal conductivity 92 BTU/hour-ft-F°. Following the same procedure as in the cold side heat exchanger the obtained results are displayed in Table 8.

ITEM		UNIT	VALUE
Required capacity		BTU/hour	13,503
Hot shoe		F°	121.5
Temperature	Incoming air	F°	100
	Outgoing air	F°	110
	Log. mean difference	F°	16
Tube diameter		ft	0.4462
Long fin length		ft	0.1833
Short fin length		ft	0.082
Number of air ducts		-	24
Duct equivalent diameter		ft	0.03784
Duct length		ft	9.55
Air velocity		ft/sec	86
Reynold's number		-	20,860
Nusselt's number		-	67.15
Prandtl's number		-	0.7
Convection coefficient		BTU/ft^2-hour-F°	26.6
Long fin efficiency		-	0.6296
Short fin efficiency		-	0.882
Calculated capacity		BTU/hour	18,983
Security factor		-	1.4
Volumetric rate of flow		ft^3/sec	9.4

TABLE 8

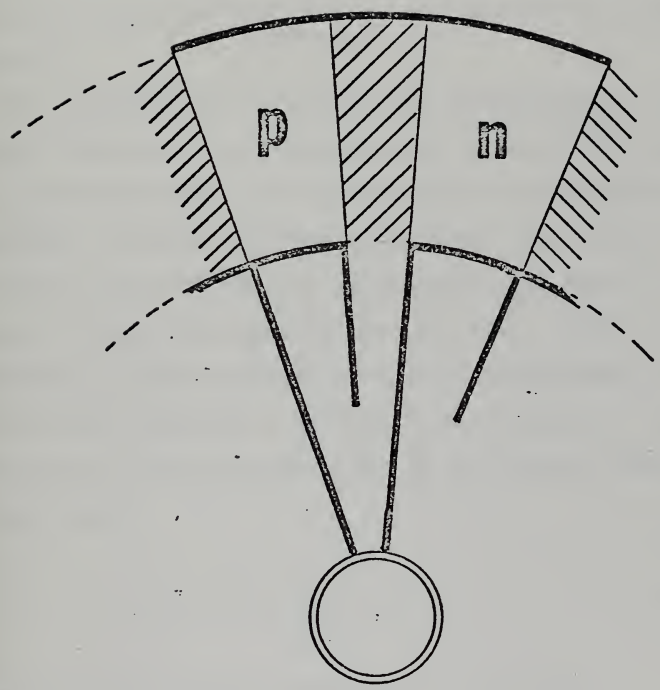

FIGURE 10

ELEMENTARY T.C.-HOT SIDE
HEAT EXCHANGER

V. THERMOELECTRIC GENERATOR

A. ANALYSIS OF ELEMENTARY GENERATOR

The elementary thermoelectric generator, which is operating under steady state conditions, consists of a thermocouple externally connected to a resistive load, as it is shown in Figure 11.

The operation of the device can be described as follows: the hot junction of the thermocouple is assumed at temperature T_C. The thermocouple arms are assumed to be adiabatically insulated, and heat exchange takes place only at the junctions. At the hot junction heat q_o is absorbed, and heat q_1 is evolved at the cold junction per unit time. Under these conditions, a thermo-e.m.f. $E = \alpha \Delta T$ is established in the circuit and it maintains an electrical current I. The coefficient in the thermo-e.m.f. is the Seebeck coefficient of the couple

$$\alpha = \left| \alpha_p(T) \right| + \left| \alpha_n(T) \right| \qquad (5\text{-}1)$$

From the law of energy conservation it follows:

$$q_o - q_1 = W \qquad (5\text{-}2)$$

where W is the available electrical power at the external load.

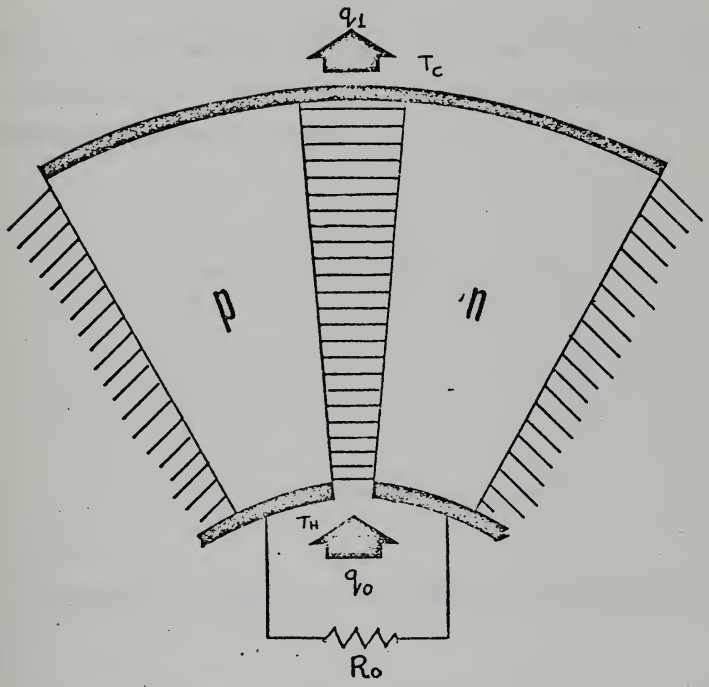

FIGURE II

ELEMENTARY T.E. GENERATOR

$$W = I^2 R_o$$

$$W = IE - I^2 R \qquad (5\text{-}3)$$

$$W = I\alpha \Delta T - I^2 R$$

where R is the total electrical resistance of the thermocouple.

Equations (5-3) suggest the electrical equivalent of the thermocouple shown in Figure 12.

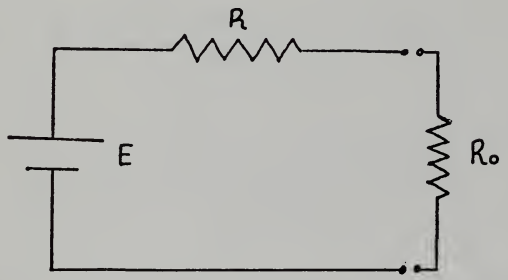

Figure 12: Electrical equivalent of thermoelectric couple.

The general expression for the heat flow rate q_0 has the following form:

$$q_{o} = \pi(T_H)I - \left[\lambda_p(T)A_p(r)\frac{dT}{dr}\bigg|_{\substack{r=R_1 \\ T=T_H}}\right] - \left[\lambda_N(T)A_N(r)\frac{dT}{dr}\bigg|_{\substack{r=R_1 \\ T=T_H}}\right] \qquad (5\text{-}4)$$

This expression is reduced to a more practical form by introducing the estimate of the rate of heat flow in the conducting solid, as it is determined in Appendix A

$$-\lambda(T)A(r)\frac{dT}{dr}\bigg|_{\substack{r=R_1\\T=T_H}} = \bar{\lambda}\frac{(\phi\tau)}{\ln\left(\frac{R_2}{R_1}\right)}\Delta T - I^2\frac{\ln\left(\frac{R_2}{R_1}\right)}{(\phi\tau)}\hat{\rho} \pm I\hat{\sigma}\Delta T \qquad (5\text{-}5)$$

where

$$\bar{\lambda} = \frac{1}{\Delta T}\int_{T_c}^{T_H}\lambda(T)\,dT$$

$$\hat{\rho} = \frac{\int_{T_c}^{T_H}\rho(T)\lambda(T)\left(\int_{T_c}^{T}\lambda(T)dT\right)dT}{\left[\int_{T_c}^{T_H}\lambda(T)dT\right]^2} \qquad (5\text{-}6)$$

$$\hat{\sigma} = \frac{1}{\Delta T}\,\frac{\int_{T_c}^{T_H}\sigma(T)\left(\int_{T_c}^{T}\lambda(T)dT\right)dT}{\int_{T_c}^{T_H}\lambda(T)dT}$$

The plus or minus sign in equation (5-5) allows for two possible directions of the electrical current: the minus sign representing the current in the P-type segment and the plus sign giving the current in the N-type segment. As it is shown in Appendix A, the value of $\hat{\rho}$ is very close to half of the average resistivity for the range of temperature T_H, T_C.

For convenience in further calculations, it is desirable to replace equation (5-5) with a less exact but much simpler expression:

$$-\lambda(T)A(r)\left.\frac{dT}{dr}\right|_{\substack{r=R_1\\T=T_H}} = \bar{\lambda}\frac{(\phi\tau)}{\ln\left(\frac{R_2}{R_1}\right)}\Delta T - \frac{1}{2}I^2\bar{\rho}\frac{\ln\left(\frac{R_2}{R_1}\right)}{(\phi\tau)} \pm I\hat{\epsilon}\Delta T \qquad (5\text{-}7)$$

where:

$$\bar{\rho} = \frac{1}{\Delta T}\int_{T_c}^{T_H}\rho(T)\,dT$$

Combining equations (5-4) and (5-7), the rate of heat flow at the hot shoe of the thermocouple becomes:

$$q_0 = \pi(T_H)I + \left[\bar{\lambda}_P(\phi\tau)_P + \bar{\lambda}_N(\phi\tau)_N\right]\frac{\Delta T}{\ln\left(\frac{R_2}{R_1}\right)} - \frac{1}{2}I^2\left[\frac{\bar{\rho}_P}{(\phi\tau)_P} + \frac{\bar{\rho}_N}{(\phi\tau)_N}\right]\ln\left(\frac{R_2}{R_1}\right) - I(\hat{\epsilon}_P - \hat{\epsilon}_N)\Delta T \qquad (5\text{-}8)$$

Introducing the Kelvin's relation, equation (5-8) becomes:

$$q_0 = \bar{\alpha}T_H I + \left[\frac{\bar{\lambda}_P}{x} + \frac{\bar{\lambda}_N}{y}\right]\Delta T - \frac{1}{2}I^2\left[\bar{\rho}_P x + \bar{\rho}_N y\right] - I\left[\hat{\epsilon}_P - \hat{\epsilon}_N\right]\Delta T \qquad (5\text{-}9)$$

where

$$x = \frac{\ln\left(\frac{R_2}{R_1}\right)}{(\phi\tau)_P} \qquad y = \frac{\ln\left(\frac{R_2}{R_1}\right)}{(\phi\tau)_N}$$

and (5-10)

$$\bar{\alpha} = \frac{1}{\Delta T}\int_{T_c}^{T_H}\left[(\alpha_P(T)) - (\alpha_N(T))\right]dT$$

The efficiency of the elementary thermoelectric generator is defined as:

$$\eta = \frac{\alpha I \Delta T - I^2\left[\bar{\rho}_P x + \bar{\rho}_N y\right]}{\alpha T_H I + \left[\frac{\bar{\lambda}_P}{x} + \frac{\bar{\lambda}_N}{y}\right]\Delta T - \frac{1}{2} I^2\left[\bar{\rho}_P x + \bar{\rho}_N y\right] - I(\hat{\sigma}_P - \hat{\sigma}_N)\Delta T} \qquad (5\text{-}11)$$

If I and ΔT are considered as constants, then the efficiency η is a function of x and y which determine the geometry of the P and N type segments.

Figure 13 shows the three dimensional representation of efficiency as it is interpreted in (5-11), for a certain temperature range and $S_i G_e$ as thermoelectric material.

B. CONDITIONS FOR MAXIMUM EFFICIENCY

Equation (5-11) is a function of geometric variables x, y and of the electrical current I, for a given temperature range. Using the Lagrange multiplier technique again, the necessary conditions for maximum efficiency are defined as:

$$\frac{\partial \eta}{\partial x} + h\bar{\rho}_P = 0 \qquad (5\text{-}12a)$$

$$\frac{\partial \eta}{\partial y} + h\bar{\rho}_N = 0 \qquad (5\text{-}12b)$$

$$\frac{\partial \eta}{\partial I} = 0 \qquad (5\text{-}12c)$$

where h is again the Lagrange multiplier and R = is the constraint function.

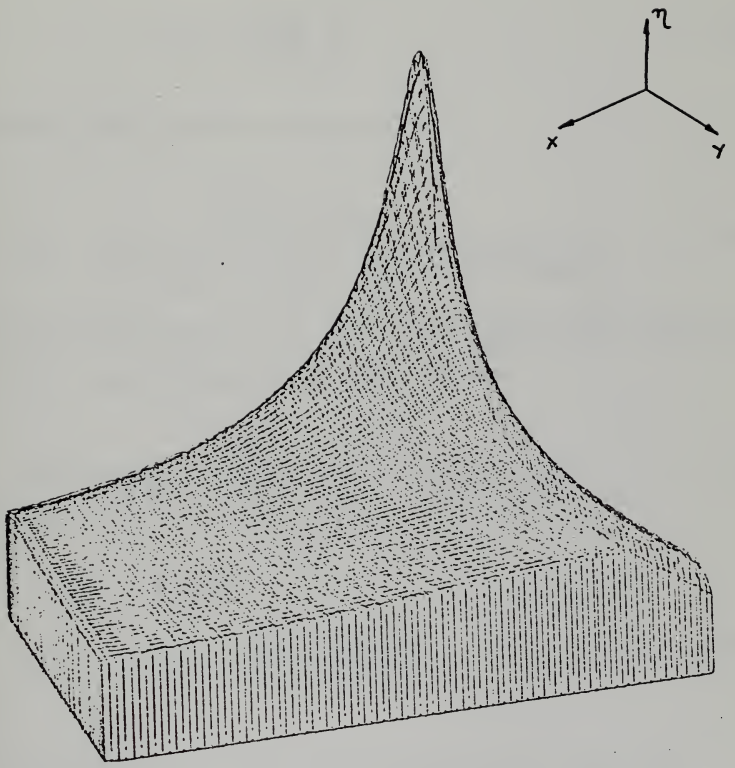

FIGURE I3

THREE DIMENSION REPRESENTATION OF EFFICIENCY

Elimination of h from equations (5-12a) and (5-12b) gives the already found condition

$$\frac{x}{y} = \left[\frac{\bar{\lambda}_P \bar{\rho}_N}{\bar{\lambda}_N \bar{\rho}_P}\right]^{1/2} \tag{5-13}$$

Equation (5-11) can be written as:

$$\eta = \frac{\bar{\alpha} I \Delta T - I^2 R}{\bar{\alpha} T_H I + \left[\frac{\bar{\lambda}_P}{x} + \frac{\bar{\lambda}_N}{y}\right]\Delta T - \frac{1}{2} I^2 R - I(\hat{\epsilon}_P - \hat{\epsilon}_N)\Delta T} \tag{5-14}$$

Multiplying and dividing by R and introducing the condition of (5-13), the efficiency equation becomes:

$$\eta = \frac{\bar{\alpha} f \Delta T - f^2}{\bar{\alpha} T_H f + \beta^2 \Delta T - \frac{1}{2} f^2 - f(\hat{\epsilon}_P - \hat{\epsilon}_N)\Delta T} \tag{5-15}$$

where

$$f = IR$$

$$\beta^2 = \left(\sqrt{\bar{\rho}_P \bar{\lambda}_P} + \sqrt{\bar{\rho}_N \bar{\lambda}_N}\right)^2 \tag{5-16}$$

Optimization of (5-15) with respect to f gives the condition:

$$f = \frac{\bar{\alpha}\,\Delta T}{C_T + 1} \tag{5-17}$$

where:

$$G = \left(1 + \frac{\bar{\alpha}^2}{\beta^2} T_{av} - \frac{\alpha}{\beta^2} \frac{1}{\Delta T}\right)^{1/2}$$

$$T_{av} = \frac{1}{2}(T_H + T_C) \qquad (5\text{-}18)$$

The optimum current is:

$$I_{opt} = \frac{\bar{\alpha} \Delta T}{R(G+1)} \qquad (5\text{-}19)$$

The optimum effective voltage is:

$$V = \frac{\bar{\alpha} G \Delta T}{G+1} \qquad (5\text{-}20)$$

When the conditions (5-13) and (5-17) are satisfied, the efficiency reaches its maximum value, which is found from equations (5-15) and (5-17):

$$\eta_{max} = \frac{\Delta T}{T_H} \frac{(G-1)}{\left(G + \frac{T_C}{T_H}\right)} \qquad (5\text{-}21)$$

The electrical power dissipated in the external circuit is found from equation (5-19) and (5-20).

$$W = \frac{\bar{\alpha}^2 G (\Delta T)^2}{R(G+1)^2} \qquad (5\text{-}22)$$

The formulae developed above show that the efficiency of a thermocouple and its power output increase with increase of the working range of temperatures. The thermocouple efficiency,

like the cooler C.O.P., depends only the the ratio T_C/T_H and the quality factor G, which is slightly different from the quality factor D for the thermoelectric cooler.

For the present application the working temperatures of the thermoelectric generator are varying as the temperature of the exhaust gasses varies for different power level operation of the automobile engine. In the present state of material development, no single thermoelectric material is satisfactory for use over the complete temperature range. Therefore, it is necessary to use different materials in each temperature range. One way to accomplish this, is to form each leg of the couple by joining different materials in series; that is, forming a sandwich structure of the appropriate thermoelectric materials for each temperature range.

C. OPTIMIZATION OF THE SEGMENTED T.E. GENERATOR

In Figure 14 two P-type materials, P_1 and P_2, are connected in series to form a positive thermoelectric arm and two N-type materials, N_1 and N_2, form the negative arm of the thermocouple.

The optimization problem is to maximize the thermal efficiency, subject to specification of the interface temperatures T_x and T_y over the equivalent length of thermocouple, $L = \ln\left(\frac{R_2}{R_1}\right)$, equivalent cross sectional area $A_p=(\Phi\tau)_p$, and the temperature averaged material properties.

The reciprocal of the thermal efficiency, as defined in equation (5-11), is:

$$\frac{1}{\eta} = \frac{\bar{\alpha} T_H I + (T_H - T_x) K_{P1} + (T_H - T_y) K_{N1} - \frac{1}{2} I^2 (R_{P1} + R_{N1}) - I(\hat{\sigma}_P - \hat{\sigma}_N)\Delta T}{I^2 R_o} \quad (5\text{-}23)$$

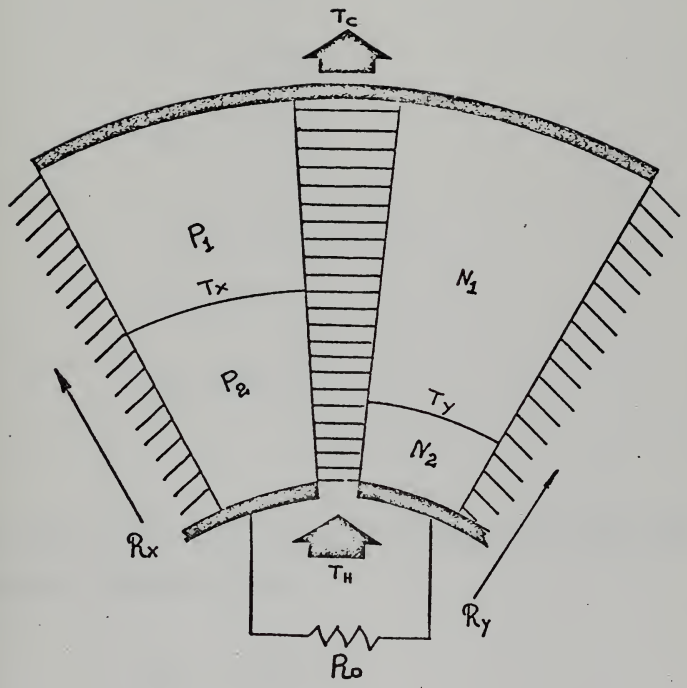

FIGURE I4

ELEMENTARY SEGMENTED GENERATOR

Introducing the concept of equivalent length and cross section for the P-type and N-type segment as:

$$\ell_{P1} = \ell_n\left(\frac{R_x}{R_1}\right)$$

$$\ell_{P2} = \ell_n\left(\frac{R_2}{R_x}\right)$$

$$\ell_{N1} = \ell_n\left(\frac{R_y}{R_1}\right) \qquad (5\text{-}24)$$

$$\ell_{N2} = \ell_n\left(\frac{R_2}{R_y}\right)$$

$$L = \ell_{P1} + \ell_{P2} = \ell_{N1} + \ell_{N2}$$

$$A_P = (\Phi\tau)_P$$

$$A_N = (\Phi\tau)_N$$

The terms in the numerator of equation (5-23) have the following interpretations:

$$K_{P1} = \bar{\lambda}_{P1}\frac{A_P}{\ell_{P1}}$$

$$K_{N1} = \bar{\lambda}_{N1}\frac{A_N}{\ell_{N1}} \qquad (5\text{-}25)$$

$$R_{P1} = \bar{\rho}_{P1}\frac{\ell_{P1}}{A_P}$$

$$R_{N1} = \bar{\rho}_{N1}\frac{\ell_{N1}}{A_N}$$

$$\hat{\sigma}_{P1} = \frac{1}{\Delta T} \frac{\int_{T_x}^{T_H} \sigma_{P1}(T) \int_{T_x}^{T} \lambda_{P1}(T) dT dT}{\int_{T_x}^{T_H} \lambda_{P1}(T) dT}$$

$$\hat{\sigma}_{N1} = \frac{1}{\Delta T} \frac{\int_{T_y}^{T_H} \sigma_{N1}(T) \int_{T_y}^{T} \lambda_{N1}(T) dT dT}{\int_{T_y}^{T_H} \lambda_{N1}(T) dT} \qquad (5\text{-}25)$$

The electrical current I in equation (5-23) is given by:

$$I = \frac{E}{R + R_o} \qquad (5\text{-}26)$$

where: $R = R_{P1} + R_{P2} + R_{N1} + R_{N2} = R_P + R_N$ is the total electrical resistance of the thermocouple and E is the circuit voltage produced by the cumulative Seebeck effect in the positive and negative elements. The segmented elements may be considered as batteries connected in series.

The voltage E is given by:

$$E = \alpha'(T_H - T_C) \qquad (5\text{-}27)$$

where:

$$\alpha' = \frac{1}{\Delta T} \left[\int_{T_x}^{T_H} \alpha_{P1}(T) dT + \int_{T_c}^{T_x} \alpha_{P2}(T) dT - \int_{T_y}^{T_H} \alpha_{N1}(T) dT - \int_{T_c}^{T_y} \alpha_{N2}(T) dT \right]$$

Substituting equation (5-26) into (5-23), the latter becomes:

$$\frac{1}{\eta} = \frac{(T_H - T_x)K_{P1} + (T_H - T_y)K_{N1} + \bar{\alpha} T_H \frac{E}{R+R_o} - \frac{E^2(R_{P1}+R_{N1})}{2(R+R_o)^2} - (\hat{\epsilon}_{P1} - \hat{\epsilon}_{N1})\frac{E}{R+R_o}}{\frac{E^2 R_o}{(R+R_o)^2}} \quad (5\text{-}28)$$

With the variables θ_P and θ_N defined by the equations:

$$\theta_P = \frac{T_H - T_x}{T_H - T_c}$$

$$\theta_N = \frac{T_H - T_y}{T_H - T_c} \quad (5\text{-}29)$$

and multiplying the numerator and denominator of equation (5-28) by $(R+R_o)^2$, equation (5-28) becomes:

$$\frac{1}{\eta} = \frac{(T_H - T_c)\left[\theta_P K_{P1} + \theta_N K_{N1}\right](R+R_o)^2 + \bar{\alpha} T_H E (R+R_o) - \frac{1}{2}E^2(R_{P1}+R_{N1})}{E^2 R_o} - \quad (5\text{-}30)$$

$$- \frac{E(\hat{\epsilon}_{P1} - \hat{\epsilon}_{N1})(R+R_o)}{E^2 R_o}$$

With the quantities R'_P, R'_N, K'_{P1}, K'_{N1} defined by the equations:

$$R'_P = R_P A_P$$

$$R'_N = R_N A_N \quad (5\text{-}31)$$

$$K'_{P1} = \frac{K_{P1}}{A_P}$$

$$K'_{N1} = \frac{K_{N1}}{A_N}$$

equation (5-30) becomes:

$$\frac{1}{\eta} = \frac{(T_H - T_C)\left[\theta_P K'_{P1} A_P + \theta_N K'_{N1} A_N\right]\left(\frac{R'_P}{A_P} + \frac{R'_N}{A_N}\right)\left(1 + \frac{R_o}{R}\right)\left(1 + \frac{R}{R_o}\right)}{E^2} +$$

(5-32)

$$+ \frac{\bar{\alpha} T_H \left(1 + \frac{R}{R_o}\right)}{\alpha'(T_H - T_C)} - \frac{(R_{P1} + R_{N1})}{2R_o} - \frac{(\hat{\epsilon}_{P1} - \hat{\epsilon}_{N1})\left(1 + \frac{R}{R_o}\right)}{\alpha'(T_H - T_C)}$$

or:

$$\frac{1}{\eta} = \frac{(T_H - T_C)\left[\theta_P K'_{P1} R'_P + \theta_P K'_{P1} R'_N \left(\frac{A_P}{A_N}\right) + \theta_N K'_{N1} R'_P \left(\frac{A_N}{A_P}\right) + \theta_N K'_{N1} R'_N\right]\left(1 + \frac{R_o}{R}\right)\left(1 + \frac{R}{R_o}\right)}{}$$

(5-33)

$$+ \frac{\bar{\alpha} T_H \left(1 + \frac{R}{R_o}\right)}{\alpha'(T_H - T_C)} - \frac{(R_{P1} + R_{N1})}{2R_o} - \frac{(\hat{\epsilon}_{P1} - \hat{\epsilon}_{N1})\left(1 + \frac{R}{R_o}\right)}{\alpha'(T_H - T_C)}$$

Assuming $\frac{R_o}{R} = f\left(\frac{A_N}{A_P}\right)$, minimization of equation (5-33) with respect to $\left(\frac{A_N}{A_P}\right)$, gives:

$$\frac{\partial\left(\frac{1}{\eta}\right)}{\partial\left(\frac{A_N}{A_P}\right)} = \theta_N K'_{N1} R'_P - \theta_P K'_{P1} R'_N \left(\frac{A_P}{A_N}\right)^2 = 0 \qquad (5\text{-}34)$$

From equation (5-34) the condition is obtained:

$$\frac{A_N}{A_P} = \left[\frac{\theta_P K'_{P1} R'_N}{\theta_N K'_{N1} R'_P}\right]^{1/2} \tag{5-35}$$

Applying condition (5-35) to equation (5-33), the latter becomes:

$$\frac{1}{\eta} = \frac{\left[(\theta_P R'_P K'_{P1})^{1/2} + (\theta_N R'_N K'_{N1})^{1/2}\right]^2 (1+\frac{R_o}{R})(1+\frac{R}{R_o})}{E^2} + \tag{5-36}$$

$$+ \frac{\bar{\alpha} T_H (1+\frac{R}{R_o})}{\alpha'(T_H - T_c)} - \frac{(R_{P1} + R_{N1})}{2R_o} - \frac{(\hat{\sigma}_{P1} - \hat{\sigma}_{N1})(1+\frac{R}{R_o})}{\alpha'(T_H - T_c)}$$

With the figure of merit defined as:

$$M = \frac{(\alpha')^2 T_H}{4\left[(\theta_P R'_P K'_{P1})^{1/2} + (\theta_N R'_N K'_{N1})^{1/2}\right]} \tag{5-37}$$

equation (5-36) becomes:

$$\frac{1}{\eta} = \frac{T_H (1+\frac{R_o}{R})(1+\frac{R}{R_o})}{4M(T_H - T_c)} + \frac{T_H \bar{\alpha}(1+\frac{R}{R_o})}{\alpha'(T_H - T_c)} - \tag{5-38}$$

$$- \frac{(R_{P1} + R_{N1})}{2R_o} - \frac{(\hat{\sigma}_{P1} - \hat{\sigma}_{N1})(1+\frac{R}{R_o})}{\alpha'(T_H - T_c)}$$

With the partial derivative of $(\frac{1}{\eta})$ with respect to $\frac{R_o}{R}$ set equal to zero, the following condition is obtained:

$$\frac{R_o}{R} = \left[\frac{T_H \left(\frac{1}{4M} + \frac{\bar{\alpha}}{\alpha'} \right)}{\left(\frac{T_H}{4M} - \frac{(\hat{\epsilon}_{P1} - \hat{\epsilon}_{N1})}{\alpha'} \right)} \right]^{1/2} \tag{5-39}$$

Substitution of (5-39) into equation (5-38) gives the minimum $\frac{1}{\eta}$ or the maximum efficiency.

Summarizing, the maximization problem of the segmented generator efficiency can be stated as follows: Given the values of $\bar{\alpha}_{ij}$, $\bar{\rho}_{ij}$, ΔT_{ij}, T_H, T_C, A_p, and L determine the values of A_N, ℓ_{ij}, R, R_o, I, and η, where i = P, N and j = 1, 2.

Solution of the problem requires that the following equations be satisfied:

$$I = \frac{\alpha' (T_H - T_c)}{R + R_o} \tag{5-40}$$

$$\frac{A_N}{A_P} = \left[\frac{\theta_P K'_{P1} R'_N}{\theta_N K'_{N1} R'_P} \right]^{1/2} \tag{5-41}$$

$$M = \frac{(\alpha')^2 T_H}{4 \left[(\theta_P R'_P K'_{P1})^{1/2} + (\theta_N R'_N K'_{N1})^{1/2} \right]^2} \tag{5-42}$$

$$\frac{R_o}{R} = \left[\frac{T_H \left(\frac{1}{4M} + \frac{\bar{\alpha}}{\alpha'} \right)}{\left(\frac{T_H}{4M} - \frac{(\hat{\epsilon}_{P1} - \hat{\epsilon}_{N1})}{\alpha'} \right)} \right]^{1/2} \tag{5-43}$$

$$L = \ell_{P1} + \ell_{P2} = \ell_{N1} + \ell_{N2} \tag{5-44}$$

$$R = R_{P1} + R_{P2} + R_{N1} + R_{N2} \tag{5-45}$$

$$\frac{1}{2} I^2 R_{P1} + \frac{1}{2} I^2 R_{P2} - (\bar{\alpha}_{P2} - \bar{\alpha}_{P1}) T_H I - (\hat{\epsilon}_{P1} + \hat{\epsilon}_{P2}) I + \bar{\lambda}_{P1} \frac{A_P}{\ell_{P1}} (T_H - T_x) = \bar{\lambda}_{P2} \frac{A_P}{\ell_{P2}} (T_x - T_c) \tag{5-46}$$

$$\frac{1}{2} I^2 R_{N1} + \frac{1}{2} I^2 R_{N2} + (\bar{\alpha}_{N2} - \bar{\alpha}_{N1}) T_H I + (\hat{\epsilon}_{N1} + \hat{\epsilon}_{N2}) I + \bar{\lambda}_{N1} \frac{A_N}{\ell_{N1}} (T_H - T_y) = \bar{\lambda}_{N2} \frac{A_N}{\ell_{N2}} (T_y - T_c) \tag{5-47}$$

Equations (5-46) and (5-47) represent the energy balance for the interfaces between elements P_1, P_2 and N_1, N_2. They state that the amount of energy flowing to interface, plus or minus the amounts of energy generated or absorbed at the interface is equal to the amount of energy flowing from the interface.

D. T.E. GENERATOR DESIGN

The design of the segmented thermoelectric generator is implemented by computer aided iteration methods. Such methods have been coded for the IBM-360 as it is displayed in program Number one. The procedure consists of several steps:

1) For the selected materials, calculation of $\bar{\alpha}_{ij}$, $\bar{\rho}_{ij}$, $\bar{\lambda}_{ij}$, $\hat{\epsilon}_{ij}$ for i = P,N and j = 1,2.

2) Calculation of α', θ_P, θ_N.

3) Initial estimation of ℓ_{P1}, ℓ_{P2}, ℓ_{N1}, ℓ_{N2} from:

$$\bar{\lambda}_{P1} \frac{A_P}{\ell_{P1}} (T_H - T_X) = \bar{\lambda}_{P2} \frac{A_P}{\ell_{P2}} (T_X - T_C)$$

$$\bar{\lambda}_{N1} \frac{A_N}{\ell_{N1}} (T_H - T_Y) = \bar{\lambda}_{N2} \frac{A_N}{\ell_{N2}} (T_Y - T_C)$$

$$L = \ell_{P1} + \ell_{P2} = \ell_{N1} + \ell_{N2}$$

4) Calculation of R'_P, R'_N, K'_{P1}, K'_{P2}.

5) Calculation of $\frac{A_N}{A_P}$, from Equation (5-41) and for selected value of A_P determination of A_N.

6) Determination of figure of merit M from Equation (5-37).

7) Calculation of $\frac{R_O}{R}$ from Equation (5-42).

8) Calculation of R from equation:

$$R = (\bar{\rho}_{P1} \ell_{P1} + \bar{\rho}_{P2} \ell_{P2}) \frac{1}{A_P} + (\bar{\rho}_{N1} \ell_{N1} + \bar{\rho}_{N2} \ell_{N2}) \frac{1}{A_N}$$

9) Calculation of current I from Equation (5-40).

10) Calculation of both sides of Equations (5-46) and (5-47). If their differences are greater than a predetermined figure, then a new set of l_{P1}, l_{N1} is estimated and the procedure is repeated until the wanted accuracy is obtained.

11) Calculation of R_{Pl}, R_{Nl}.

12) Calculation of efficiency from Equation (5-38).

The procedure is based on an "in advance" selection of the interface temperatures T_X and T_Y with the criterion of safe behavior of the materials at the extreme operating temperatures.

When the lengths of the P and N type segments are calculated for the extreme temperatures, the problem of re-estimation of the interface temperatures, for different hot junction temperatures, is encountered by modification of the iteration procedure in step 10. That is, for the calculated lengths, T_X and T_Y are varying until Equations (5-46) and (5-47) are satisfied.

The adverse operating conditions of the thermoelectric generator — high hot junction temperatures and extended operating range — impose restrictions in the selection of the best available thermoelectric material for energy conversion.

All thermoelectric materials represent the best of their characteristics in a quite narrow range of temperatures. This problem is partially encountered by the segmented type generator design, where the one material acts as the complement of the other in regions of poor characteristics.

For the present application, the selected thermoelectric materials and some of their properties are displayed in Table 9.

ITEM	MATERIAL	MAX OPERAT. TEMPERATURE
P_1	Ag Sb Te_2	900 (K°)
P_2	25% Bi_2Te_3 + 75% Sb_2Te_3	600 (K°)
N_1	Pb Te (25% Sn Te)	900 (K°)
N_2	75% Bi_2Te_3 + 25% Bi_2Se	700 (K°)

TABLE 9

With proper dopants the maximum operating temperature of P_1 and N_1 materials can be considerably extended.

The thermoelectric properties of the materials are displayed in Figures 15 through 21. The data have been taken from Reference [1] and [2] and the corresponding temperature relations developed using the "best fit polynomial" technique as it is shown in Program 2.

With these data supplied, the computer runs through the iteration procedure described earlier, and solves for the optimum thermal efficiency and the optimum design parameters. The optimum solution is displayed in Table 10.

The maximum and minimum values for efficiency, current, and voltage in Table 10 are associated with the highest and lowest hot junction temperature.

Figures 22 through 24 shows the variation of efficiency, voltage, and current with respect to hot junction temperature T_H.

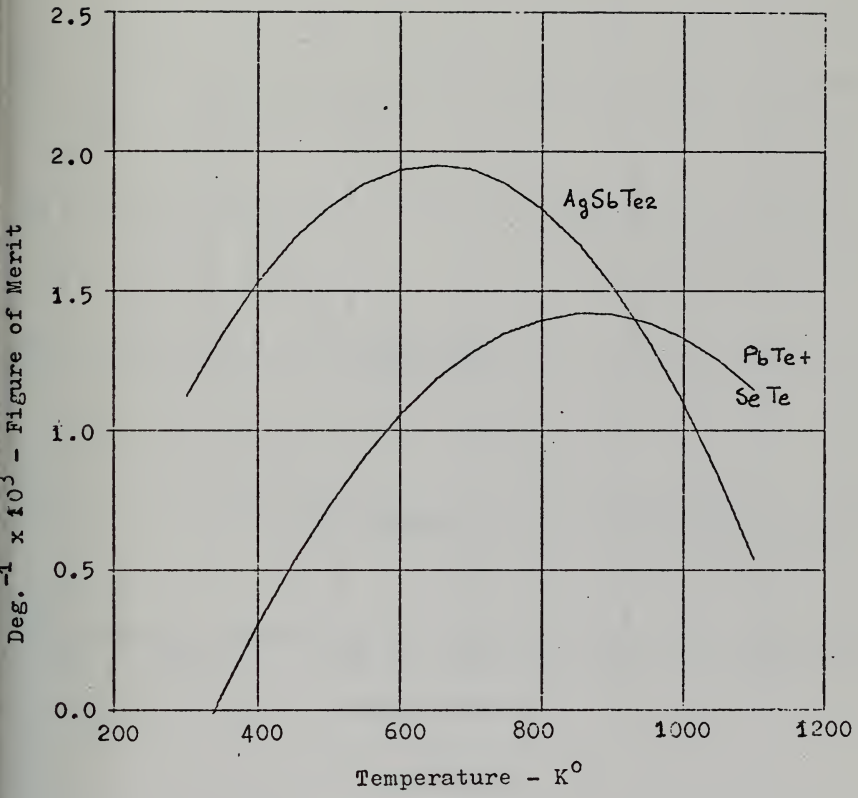

FIGURE 15

FIGURE OF MERIT

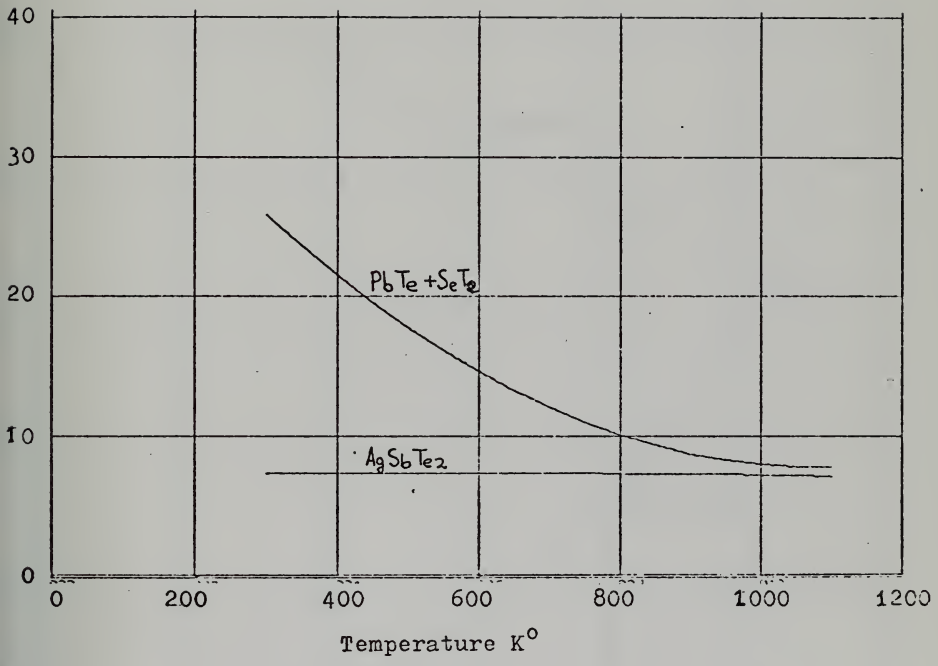

FIGURE 16

THERMAL CONDUCTIVITY

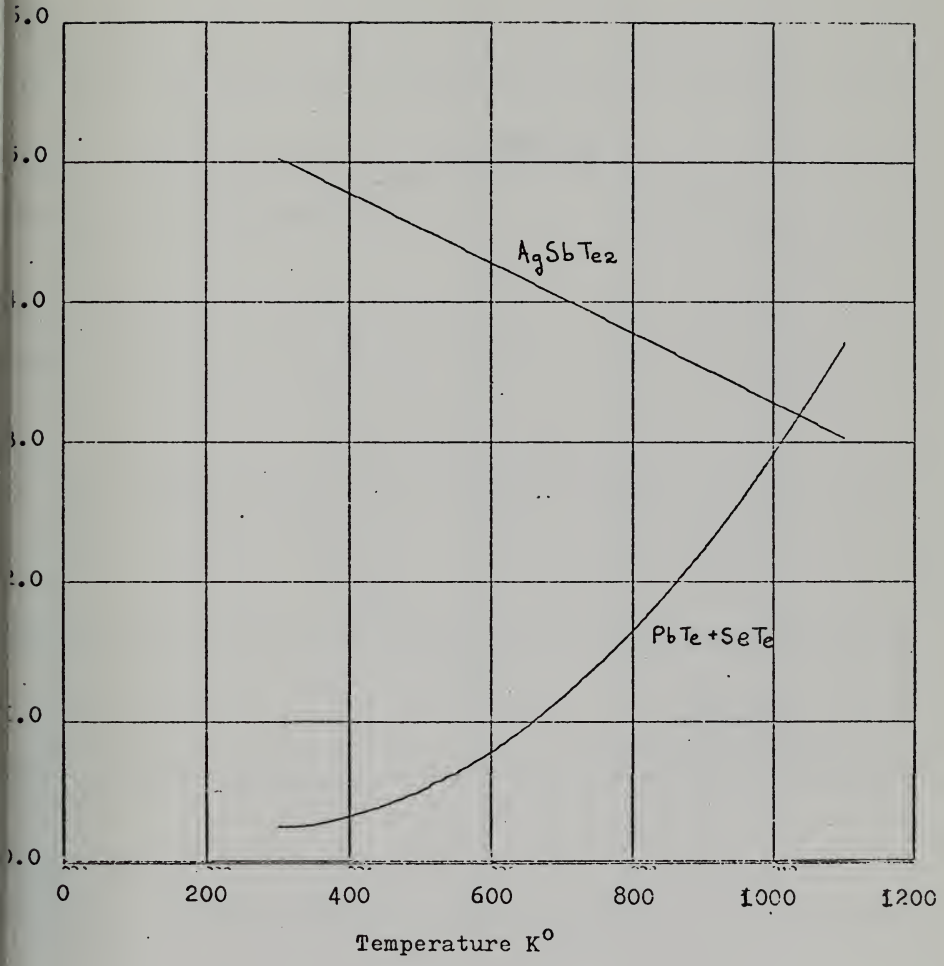

FIGURE 17

ELECTRICAL RESISTIVITY - OHM - CM x 10^3

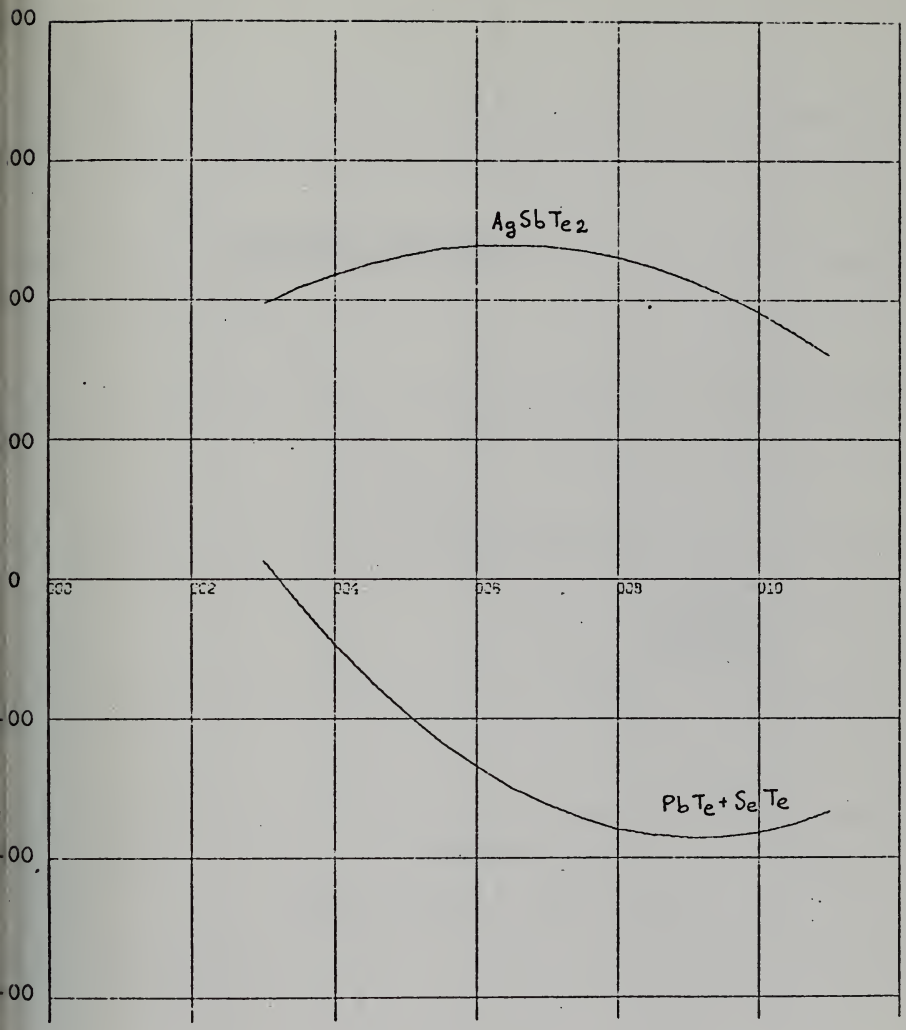

Temperature - K^{o} x 100

FIGURE 18

SEEBECK COEFFICIENT ($\mu v/K^{o}$)

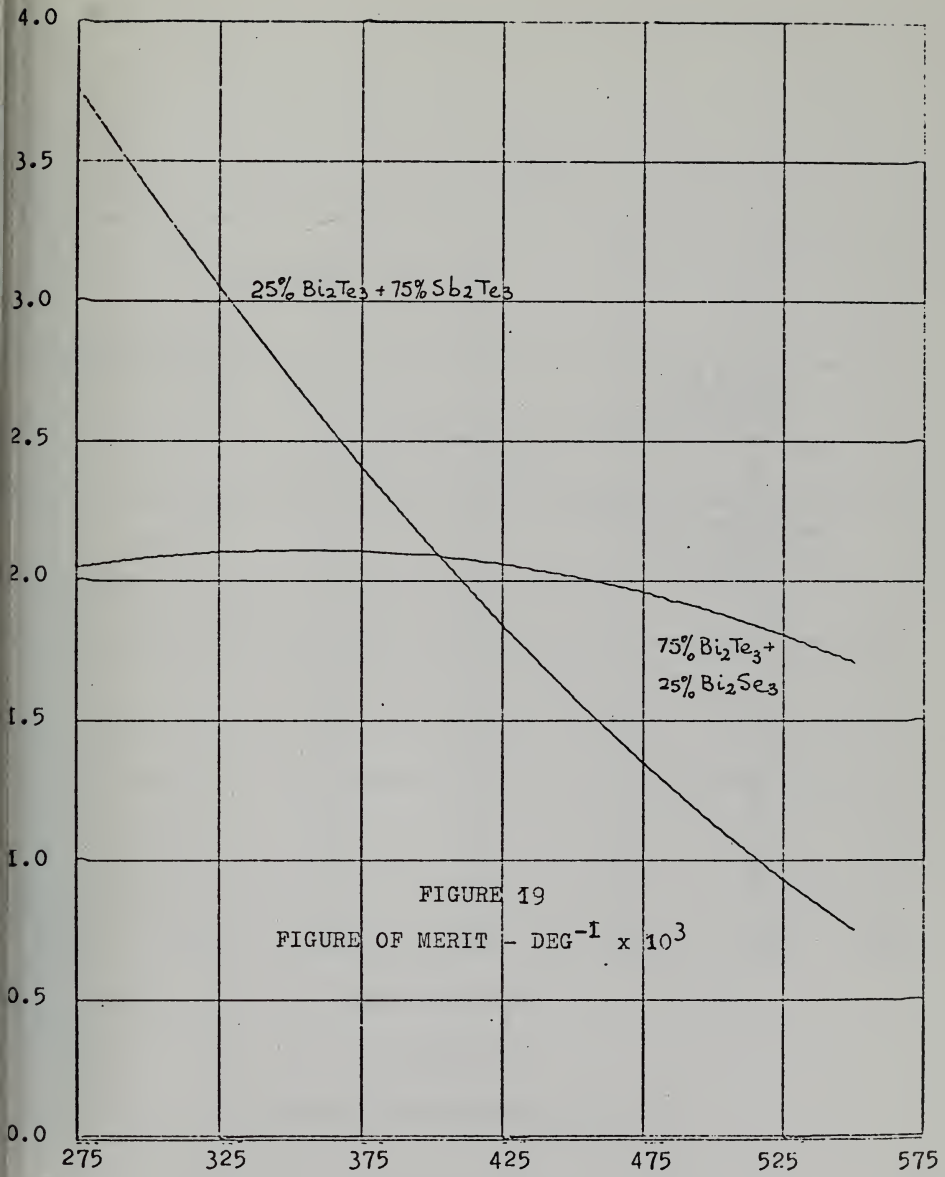

FIGURE 19

FIGURE OF MERIT - $DEG^{-1} \times 10^3$

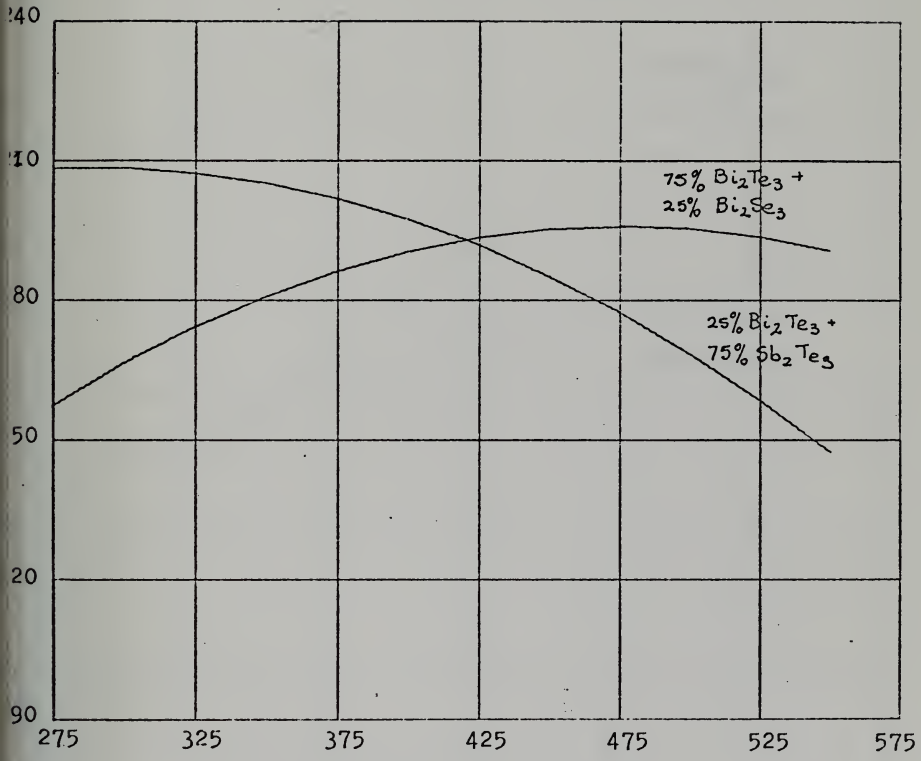

FIGURE 20

SEEBECK COEFFICIENT ($\mu v / K^{\circ}$)

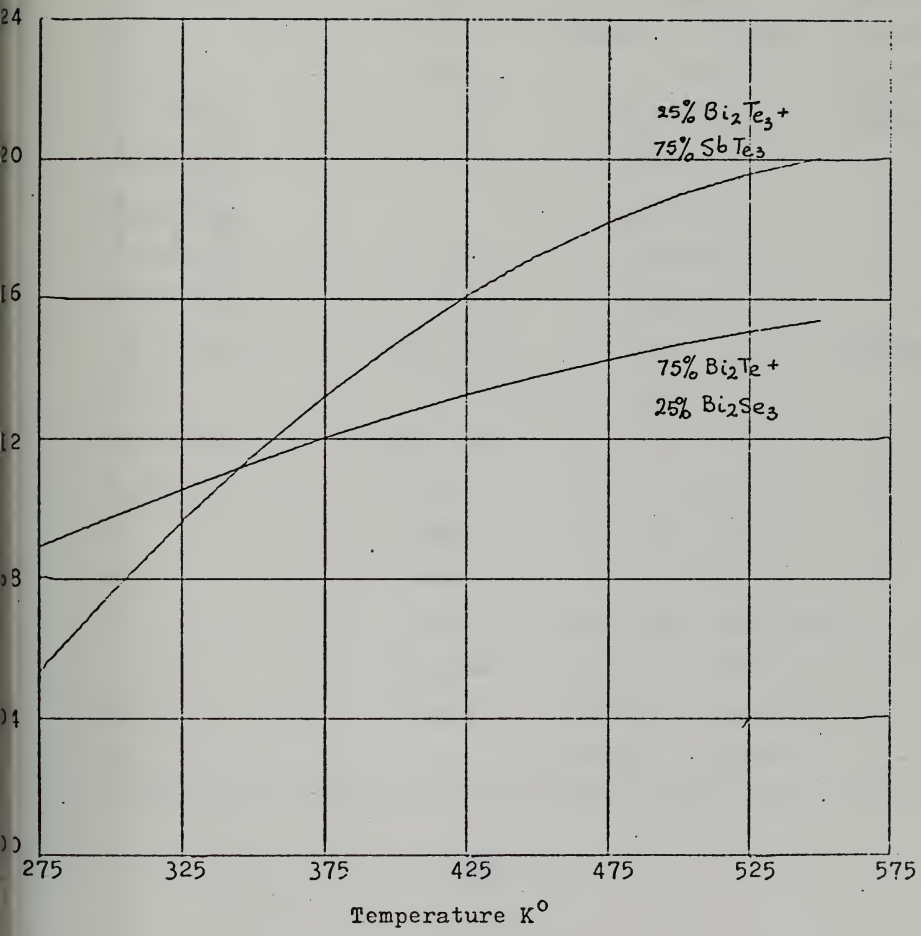

FIGURE 21

ELECTRICAL RESISTIVITY - OHM - CM x 10^3

ITEM	UNIT	VALUE	REMARKS
T_H	K°	720 min - 940 max	Selected
T_C	K°	335	Selected
$L = \ln\left(\frac{R_2}{R_1}\right)$	-	0.25845371	Selected
$\ell_{P1} = \ln\left(\frac{R_x}{R_1}\right)$	-	0.153	
$\ell_{P2} = \ln\left(\frac{R_2}{R_1}\right)$	-	0.10545	
$\ell_{N1} = \ln\left(\frac{R_y}{R_1}\right)$	-	0.22275	
$\ell_{N2} = \ln\left(\frac{R_2}{R_y}\right)$	-	0.0357	
$A_P = (\phi\tau)_P$	rad - cm.	0.2	Selected
A_N/A_P	-	0.5	
$A_N = (\phi\tau)_N$	rad - cm.	0.1	
R_o/R	-	0.272846	
R_o	ohms	1.91×10^{-3}	
R	ohms	7×10^{-3}	
E	volts	min 0.135 - max 0.225	
I	Amperes	min 15.2 - max 23.6	
W	Watts	min 0.44 - max 1.41	
η	-	min 6% - max 9%	

TABLE 10

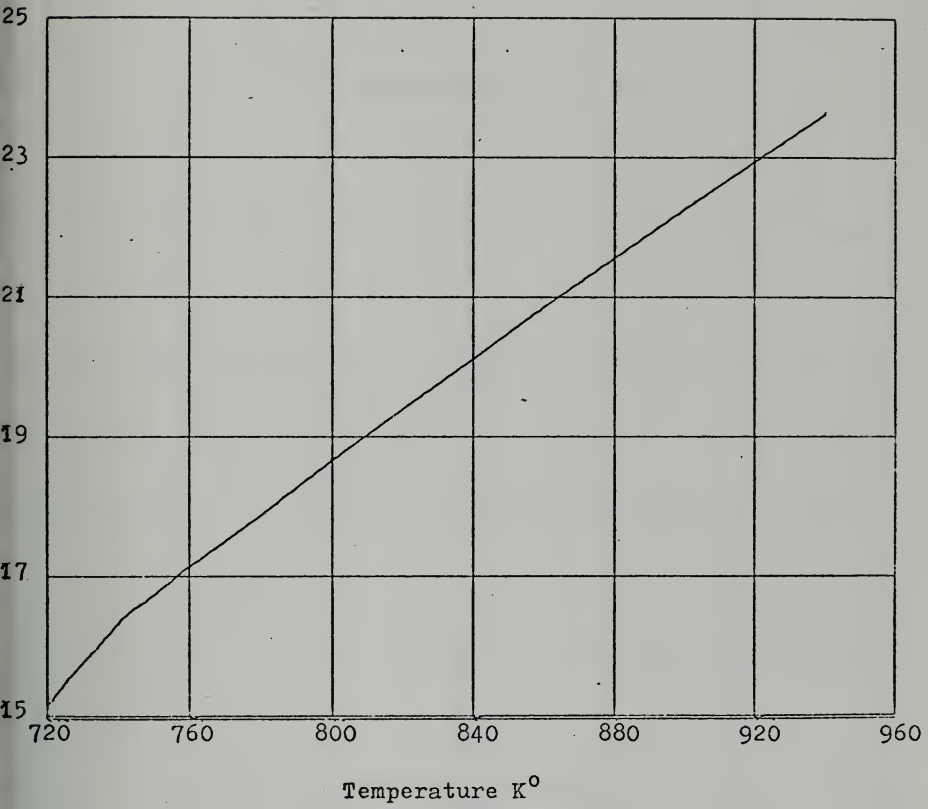

FIGURE 22

CURRENT (AMPERES) VERSUS HOT JUNCTION TEMPERATURE

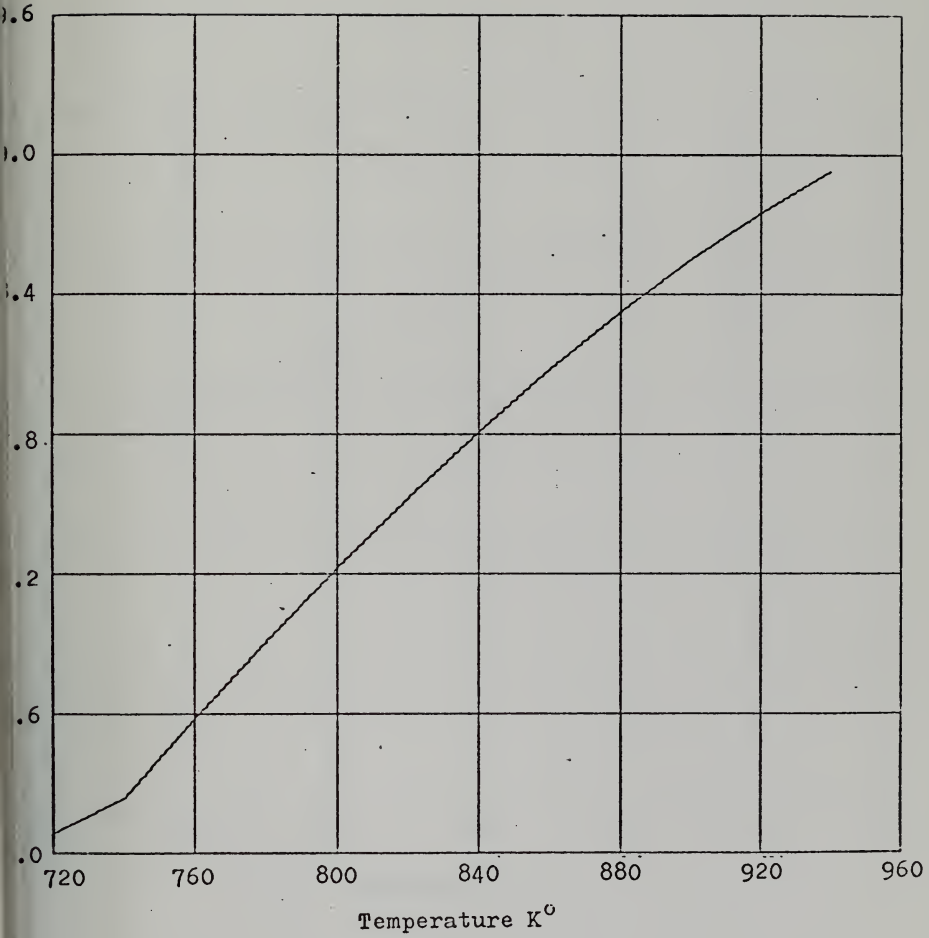

FIGURE 23

EFFICIENCY VERSUS HOT JUNCTION TEMPERATURE

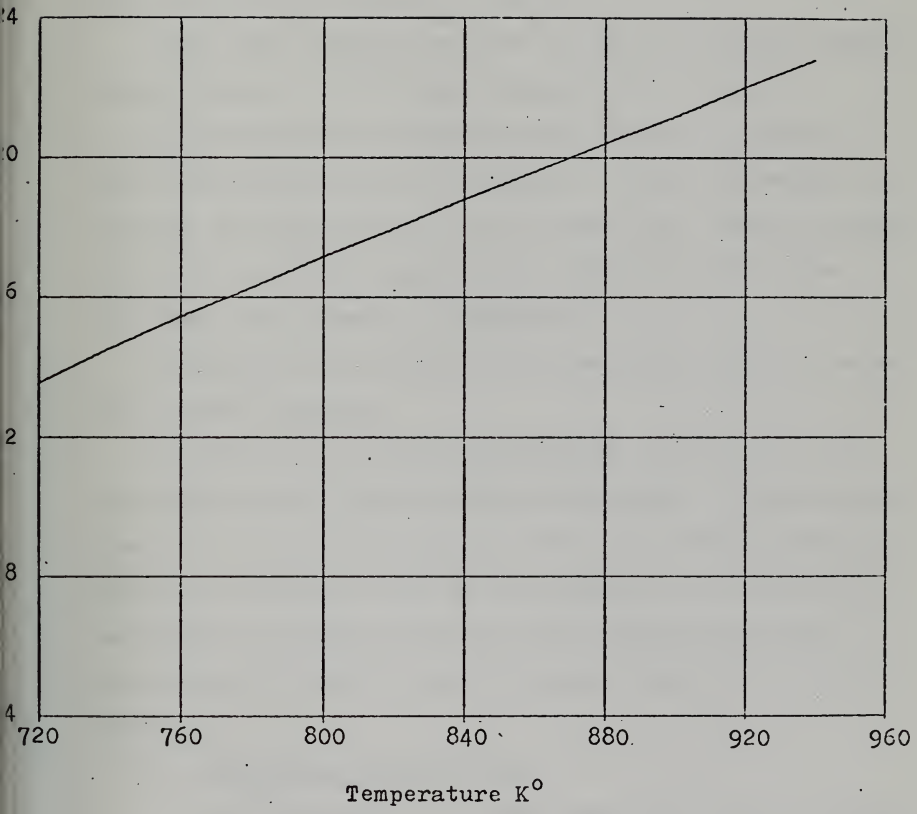

FIGURE 24

VOLTAGE VERSUS HOT JUNCTION TEMPERATURE

E. ESTIMATION OF AVAILABLE HEAT POWER FROM THE EXHAUST GASES

The recently introduced catalytic converter in the exhaust system of automobiles, offers the advantages of additional release of heat and higher temperatures, by oxidation of the unburned CO and H_2.

Heat, also, can be extracted by cooling down the gasses which come out of the output flange of the converter.

The thermodynamic analysis which follows is based on data provided by FORD motor company. A 2300 cm^3 engine is examined and the results of the exhaust gas analysis before and after catalytic converter are summarized, for three different power levels, in Table 11.

The analysis is divided into three parts with the necessary logical sequence.

The first part contains preliminary calculations, as the moles/min and pressure of exhaust gasses. The second is involved with the calculation of the available heat energy from the catalytic action of the converter, and the third is referred to the estimation of the possible extracted heat energy by cooling down the gasses after the catalytic converter.

1. Preliminary Calculations

a) From Table 11 at idle speed, the engine produces exhaust gasses at a rate of 10 ft^3/min or 0.2832 m^3/min. One mole of any gas at the state of 1 atm and 273 K° obtains a volume of 0.0224 m^3 and at standard state — 1 atm, 298 K° —

TABLE 11

	CURB IDLE		60 MPH ROAD LOAD		PEAK POWER	
	EXH. MFLD. FLANGE	CATLTC OUTLET	EXH. MFLD. FLANGE	CATLTC OUTLET	EXH. MFLD. FLANGE	CATLTC OUTLET
EXHAUST GAS VOLUME FT^3/MIN STP	10	10	60	60	230	230
EXHAUST GAS TEMPERATURE F°	760	900	1180	1160	1400	1350
CO_2 MOLE %	6.93	11.50	11.90	12.35	6.50	8.20
CO MOLE %	4.30	0.05	0.50	0.03	4.80	1.50
H_2O MOLE %	9.06	11.70	12.30	12.70	9.20	10.50
H_2 MOLE %	1.61	0.00	0.00	0.00	2.00	0.50
O_2 MOLE %	5.60	1.00	4.80	4.50	3.00	0.00
N_2 BALANCE	BAL.	BAL.	BAL.	BAL.	BAL.	BAL.

0.02445 m^3. Therefore, the flow of the exhaust gasses in terms of gram-moles per minute is 11.583.

Based on the percent mole analysis of Table 11, the actual amount of the several constituents of the exhaust gas can be summarized as follows:

GAS	CURB IDLE gram-mole/min.	60 MPH ROAD LOAD gram-mole/min.	PEAK POWER gram-mole/min.
CO_2	0.80269	8.2700	17.316
CO	0.4981	0.3475	12.787
H_2O	1.0500	8.548	24.509
H_2	0.1865	0.0	5.238
O_2	0.64864	3.3358	7.992
N_2	8.39707	48.995	198.472
TOTAL	11.583	69.497	266.404

TABLE 12

b) The partial pressures of the gasses can be calculated from:

$$P_x = M_x \frac{RT}{V_{TOT}} \qquad (5\text{-}48)$$

where:

M_x = gram-mole of the gas

R = gas constant

T = gas temperature

V_{TOT} = volume occupied by all gasses, comprising the mixture at temperature T.

With M_X taken from Table 12 the partial pressures were calculated for three different power levels, and the results are shown in tabular form as follows:

	CURB IDLE	60 MPH ROAD LOAD	PEAK POWER
GAS	atm	atm	atm
CO_2	0.06931	0.1190122	0.066007
CO	0.04301	0.005001	0.048
H_2O	0.09067	0.123013	0.09201
H_2	0.0161	0.0	0.1967
O_2	0.056007	0.048005	0.030003
N_2	0.725045	0.70508	0.7451
TOTAL	1.000142	1.0001112	1.00079

TABLE 13

Based on the data of Table 13, it is reasonable to consider that the chemical process in the catalytic converter takes place under constant pressure conditions.

2. Released Heat From Converter Action

The change in enthalpy produced by the procedure of a chemical reaction from reactants in their natural state at 25° C and 1 atm to products in their natural state at 25° C and 1 atm is referred to as the "standard heat of reaction" at 25° C.

The "standard heat of formation" is the change in enthalpy resulting from the formation of a compound at 25° C and 1 atm from the elements in their natural states at 25° C and 1 atm. The "standard heat of combustion" is the change in enthalpy resulting from the reaction of a compound with elemental oxygen each initially at 25° C and 1 atm to produce specifically defined products at 25° C and 1 atm.

The heat of a given reaction may be obtained by constructing a set of formation and combustion reactions such that the sum of the individual reactions is the reaction desired. The sum of the enthalpy changes of the individual reactions will then be the standard enthalpy change of the given reaction. If the heats of formation data are available for all compounds involved, the standard heat of reaction may be obtained by subtracting the sum of the heats of formation of the reactants from the sum of the heats of formation of the products. Normally, heats of formation are available for inorganic compounds and heats of combustion are available for organic compounds.

Since the initial and final states differ from 25° C and 1 atm, the change in enthalpy may be evaluated by a series of steps so chosen that the enthalpy change of each individual step can determined. These steps are shown on the following diagram.

The change in enthalpy for steps 1 through 3 and 5 through 16 are calculated from:

$$\Delta H_i = M_i \int_{T_1}^{T_2} c_{Pi}\, dT \qquad (5\text{-}49)$$

where M_i is gram-mole and c_{p_i} is the molal heat capacity of the gas. The molal heat capacity is a strong function of temperature and can be expressed as:

$$c_{Pi} = \alpha_i + b_i T + c_i T^2 \qquad (5\text{-}50)$$

where T is in K°.

The coefficients α_i, b_i and c_i are displayed in Table 14.

COMPOUND	FORMULA	α_i	$b_i \times 10^3$	$c_i \times 10^{-6}$
Carbon dioxide	CO_2	6.214	10.396	- 3.545
Carbon monoxide	CO	6.420	1.665	- 0.196
Water	H_2O	7.256	2.298	0.283
Oxygen	O_2	6.0954	3.2533	- 1.0171
Hydrogen	H_2	6.9469	- 0.1999	0.4808
Nitrogen	N_2	6.4492	1.4125	- 0.0807

TABLE 14

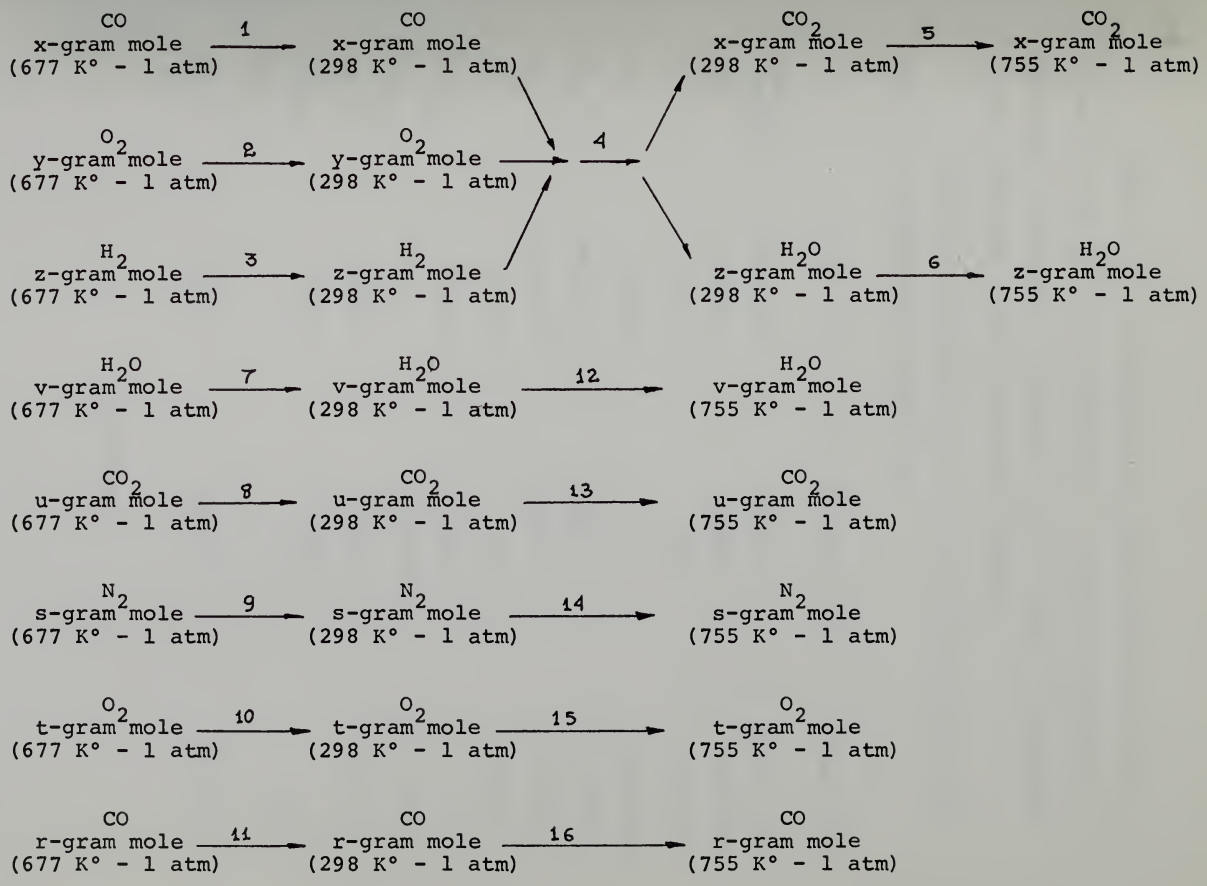
CO
x-gram mole
(677 K° - 1 atm)
1
CO
x-gram mole
(298 K° - 1 atm)
O_2
y-gram mole
(677 K° - 1 atm)
2
O_2
y-gram mole
(298 K° - 1 atm)
H_2
z-gram mole
(677 K° - 1 atm)
3
H_2
z-gram mole
(298 K° - 1 atm)
4
CO_2
x-gram mole
(298 K° - 1 atm)
5
CO_2
x-gram mole
(755 K° - 1 atm)
H_2O
z-gram mole
(298 K° - 1 atm)
6
H_2O
z-gram mole
(755 K° - 1 atm)
H_2O
v-gram mole
(677 K° - 1 atm)
7
H_2O
v-gram mole
(298 K° - 1 atm)
12
H_2O
v-gram mole
(755 K° - 1 atm)
CO_2
u-gram mole
(677 K° - 1 atm)
8
CO_2
u-gram mole
(298 K° - 1 atm)
13
CO_2
u-gram mole
(755 K° - 1 atm)
N_2
s-gram mole
(677 K° - 1 atm)
9
N_2
s-gram mole
(298 K° - 1 atm)
14
N_2
s-gram mole
(755 K° - 1 atm)
O_2
t-gram mole
(677 K° - 1 atm)
10
O_2
t-gram mole
(298 K° - 1 atm)
15
O_2
t-gram mole
(755 K° - 1 atm)
CO
r-gram mole
(677 K° - 1 atm)
11
CO
r-gram mole
(298 K° - 1 atm)
16
CO
r-gram mole
(755 K° - 1 atm)

Step 4 is calculated from tables where the heat of formation for different compounds is given. The change in enthalpy is obtained by subtracting the heat of formation of the reactants from that of the products.

Table 15 displays the change of enthalpy for each step, for three power conditions:

	CURB IDLE	60 MPH ROAD LOAD	PEAK POWER
ENTHALPY CHANGE	Calor/min	Calor/min	Calor/min
H_1	- 1340.11	- 1418.0	- 48025.0
H_2	- 955.36	- 738.7	- 36487.0
H_3	- 492.60	0.0	- 20702.0
H_4	-46303.00	-21285.0	-824828.0
H_5	+ 2394.40	+ 2114.0	+ 70449.0
H_6	+ 728.60	0.0	+ 25102.0
H_{7-12}	+ 741.00	- 930.0	- 6788.0
H_{8-13}	+ 741.30	- 1157.0	- 6354.0
H_{9-14}	+ 4859.00	- 4129.0	- 44372.0
H_{10-15}	+ 714.00	- 282.0	0.0
H_{11-16}	+ 3.40	0.0	+ 885.0
TOTAL	-38909.37	-27826.0	-892886.0

TABLE 15

3. Estimation of Available Heat from Hot Gasses

The gasses flowing out of the catalytic converter have a high thermal content, which partially can be extracted, introducing a heat exhanger in series with the catalytic converter.

A possible arrangement of converter with heat exhanger in series is shown in Figure 25. The change in enthalpy, because of the cooling process of the exhaust gasses, can be estimated from equation (5-49).

For a temperature drop 200 F°, the change in enthalpies, for different load conditions are shown in Table 16.

ENTHALPY DROP	CURB IDLE BTU/min	60 MPH ROAD LOAD BTU/min	PEAK POWER BTU/min
H_{CO_2}	1737	10119	31173
H_{CO}	5	15	3468
H_{O_2}	102	2400	0
H_{H_2O}	1355	7846	30700
H_{H_2}	0	0	1063
H_{N_2}	6894	35080	169892
TOTAL	10090	55460	236296

TABLE 16

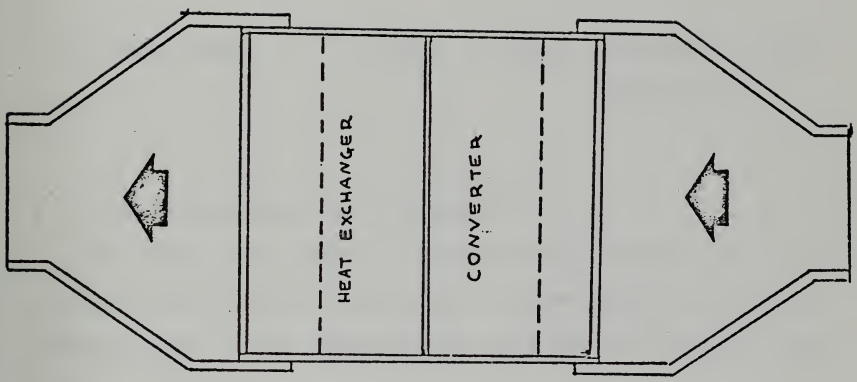

FIGURE 25

CATALYTIC CONVERTER AND HEAT EXCHANGER COMBINATION

In summary, the total amount of available heat power from the exhaust gasses of the examined engine, under the assumed conditions is determined as:

1)	Idle condition	38909 + 10090 =	50000 cal/min
		=	3486 watts
2)	60 MPH ROAD LOAD	278264 + 55460 =	83286 cal/min
		=	5808 watts
3)	PEAK POWER	892886 + 236296 =	1129182 cal/min
		=	78741 watts

F. FINAL CONSIDERATIONS ON GENERATOR

The number of required thermoelectric couples for a typical design of the generator is based on the available thermal power which corresponds to 60 mph road load of the automobile engine.

The design specifications of the thermoelectric generator are shown in Table 17.

ITEM	UNIT	VALUE	REMARKS
Available thermal power	watts	5808	
T_H	K°	900	SELECTED
T_C	K°	335	SELECTED
Efficiency	-	8.9%	
Electrical output power	watts	517	
Current	amps	22.3	
Voltage	volts	23.2	
Number of couples	-	43.2	
R_1	cm.	8.00	
R_2	cm.	10.36	
ϕ_P	rad	0.2	
ϕ_N	rad	0.1	
τ	cm.	1.00	
ϕinsulation	rad	0.1	

TABLE 17

The maximum working temperature of the selected thermoelectric materials is restricted to 900 K°. It is possible to have higher temperatures in the wall of the catalytic converter when the engine is overloaded. In order to protect the hot junction thermoelectric materials from damage, a protective system must be provided. Such system could be a single by-pass line for the exhaust gasses, automatically

operating when a certain temperature is achieved, or introduction of a heat resisting material between the converter's wall and the hot junctions of thermocouples, which will insure a sufficient temperature drop.

The cold junction temperature was arbitrarily selected to be 335 K°. It can be even lower, depending on the heat rejection system which is employed, i.e. water cooling, forced or free air convection.

The hot junction temperature is varying according to the developed power level of the engine. This results in the variation of all design specifications of the thermoelectric generator, as delivered useful power, voltage, current, etc. For this reason, an electrical power conditioning device becomes necessary. The function of this device depends on the special application of the generator. That is, if the generator is employed as the electrical power source of the automobile, constant voltage and variable current is required, and when the generator supplies part of the electrical power to the thermoelectric cooler, constant current and variable voltage is desired.

Contact resistance and conductor losses were not taken into account, because the estimation of the former is a matter of manufacturing procedure and the latter depends on the proper material for the applied contact technique.

Nevertheless, a reasonable figure of contact resistance is of the order of 10 micro-ohms per cm^2, which is very small compared to the resistivity of the thermoelectric materials.

Figure 26 shows the arrangement of catalytic converter with the attached thermoelectric generator.

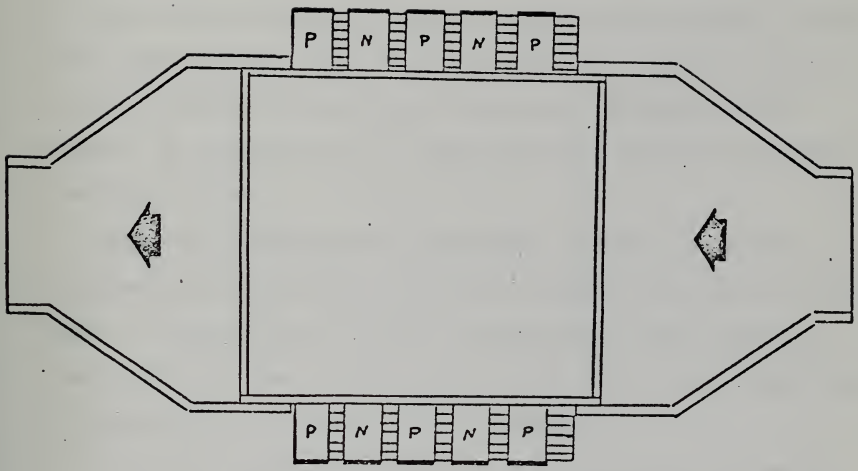

FIGURE 26

T.E. GENERATOR ASSEMBLY

VI. CONCLUSIONS AND RECOMMENDATIONS FOR FURTHER STUDY

The obtained figures for the thermoelectric cooler and generator could be considered as quite promising at least from the standpoint of feasibility of the application.

The thermoelectric cooler for 7000 BTU/hour was found to require 1953.0 watts of electrical power. From this figure 50 watts are dissipated for the required air blowers. If the four units, which comprise the device, are fed in parallel, then an external conventional generator, coupled to the engine, is needed with 33. volts and 57.6 amperes as rating characteristics.

When the thermoelectric generator and the cooler are considered as one system, then the required external electrical power is reduced by 18 to 25%, depending on the operating power level of the engine, and correspondingly the coefficient of performance of the cooler is increasing.

A direct comparison between the conventional air conditioning system and the thermoelectric cooler-generator scheme is not easy, because there are not available enough data for the latter. In Table 18 an attempt for comparison is made in the most broad characteristics.

CHARACTERISTIC	CONVENTIONAL SYSTEM	THERMOELECTRIC SYSTEM
Volume	Both systems have almost the same	
Weight	worst	best
Complexity	complex	simple
Maintenance	required	almost none
Noise level	relatively noisy	quiet
COP	Both systems are in the same level	
Working fluids	yes	no

TABLE 18

From the standpoint of manufacturing cost, the existing figures show that the thermoelectric system is two to three times more expensive from the corresponding conventional. It must be mentioned that the cost of the conventional system is referred to the "series production cost" and the corresponding for the thermoelectric system, to experimental constructions. It is expected that whenever the thermoelectric system will be manufactured in series, the cost will decrease enough and eventually it will be compatible or even cheaper from the conventional system, since the thermoelectric material itself is not expensive.

The analysis showed that the efficiency of the generator depends strongly on the thermoelectric material. The obtained figures – 6% minimum and 9% maximum – for the generator's efficiency, are considered satisfactory compared to

efficiencies reported already in the literature. Bates and Weinstein developed a similar design using PbTe and SiGe which complemented each other over the temperature interval from 50C° to 1000 C°. Their generator achieved an efficiency of 8.7 percent with a hot junction temperature of 800 C° (1073 K°). The present design shows an efficiency of 9% with T_H = 940 K° and T_C = 335 K°.

The requirements for the primary electrical source of a small automobile vehicle are satisfactorily fulfilled from the specifications of the segmented type thermoelectric generator.

Table 19 displays the electrical power requirements for a small size car.

ITEM		WATTAGE (12-Volts)
Head lamps	high beam	45
	low beam	40
Front lamps		21
Tail lamps		21
Other lamps		10
Wiper motor		10
Electrofan motor		11.5
TOTAL		158.5

TABLE 19

The thermoelectric generator provides 230 watts in the idle condition of the engine and 517 watts in the 60 mph road load. So, from this simple examination, the thermoelectric generator can replace the conventional alternator, offering the great advantages of fuel economy and elimination of moving parts.

The realization of the discussed applications requires further theoretical and practical work to be done. The systems must be examined thoroughly from the following standpoints:

1) Stress analysis of T.E. couples for T.E. generator and T.E. cooler.

2) Thermal and electrical insulation.

3) Contact techniques.

4) Fabrication of thermoelectric pellets.

5) Power conditioning circuits for T.E. generator.

6) Control system for the automatic co-operation of cooler, T.E. generator and conventional alternator.

It must be stressed that the present work was developed under the scheme of the feasibility study instead of a detailed design.

APPENDIX A

APPROXIMATE ANALYTIC SOLUTION OF HEAT BALANCE EQUATION

The heat balance equation is:

$$\lambda(T)\, m r \frac{d^2T}{dr^2} + \frac{d[\lambda(T)]}{dT} m r \left(\frac{dT}{dr}\right)^2 + \lambda(T) m \frac{dT}{dr} \pm I\sigma(T)\frac{dT}{dr} + I^2 \frac{\rho(T)}{m r} = 0 \qquad \text{(A-1)}$$

where: $\lambda(T)$, $\rho(T)$, $\sigma(T)$, are functions of temperature.

Equation (A-1) can be written also as:

$$\lambda(T) m^2 r^2 \frac{d^2T}{dr^2} + \frac{d[\lambda(T)]}{dT} m^2 r^2 \left(\frac{dT}{dr}\right)^2 + \lambda(T) m^2 r \frac{dT}{dr} \pm I\sigma(T) m r \frac{dT}{dr} + I^2 \rho(T) = 0 \qquad \text{(A-2)}$$

Expression $r\frac{dT}{dr}$ can be written as $\frac{dT}{\left(\frac{dr}{r}\right)}$ or $\frac{dT}{d(\ln r)}$.

If the variable x is introduced such that $x = \ln r$ then:

$$r\frac{dT}{dr} = \frac{dT}{dx} \qquad \text{(A-3)}$$

$$\frac{dT}{dr} = \frac{1}{r}\frac{dT}{dx} \qquad \text{(A-4)}$$

$$\frac{d}{dr}\left[\frac{dT}{dr}\right] = \frac{d}{dr}\left[\frac{1}{r}\frac{dT}{dx}\right] = \frac{d}{dr}\left[\frac{1}{r}\right]\frac{dT}{dx} + \frac{1}{r}\frac{d^2T}{dx^2}\frac{dx}{dr} \qquad \text{(A-5)}$$

$$\frac{d^2T}{dr^2} = -\frac{1}{r^2}\frac{dT}{dx} + \frac{1}{r^2}\frac{d^2T}{dx^2} \qquad \text{(A-6)}$$

$$r^2\frac{d^2T}{dr^2} = \frac{d^2T}{dx^2} - \frac{dT}{dx} \qquad \text{(A-7)}$$

Applying transformation (A-7) to equation (A-2), it becomes:

$$\lambda(T)m^2\left[\frac{d^2T}{dx^2} - \frac{dT}{dx}\right] + \frac{d[\lambda(T)]}{dT}m^2\left(\frac{dT}{dx}\right)^2 + \lambda(T)m^2\frac{dT}{dx} \pm mI\sigma(T)\frac{dT}{dx} + I^2\rho(T) = 0$$

or:

$$\lambda(T)m^2\frac{d^2T}{dx^2} + \frac{d[\lambda(T)]}{dT}m^2\left(\frac{dT}{dx}\right)^2 \pm I\sigma(T)m\frac{dT}{dx} + I^2\rho(T) = 0 \qquad \text{(A-8)}$$

Dividing by the product mI equation (A-8) becomes:

$$\frac{\lambda(T)m}{I}\frac{d^2T}{dx^2} + \frac{d[\lambda(T)]}{dT}\frac{m}{I}\left(\frac{dT}{dx}\right)^2 \pm \sigma(T)\frac{dT}{dx} + I\frac{\rho(T)}{m} = 0 \qquad \text{(A-9)}$$

The following transformation is introduced:

$$z = -\frac{\lambda(T)m}{I}\frac{dT}{dx} \qquad \text{(A-10)}$$

Differentiation with respect to T, equation (A-10) becomes:

$$\frac{dz}{dT} = -\frac{m}{I}\frac{d[\lambda(T)]}{dT} - \frac{m}{I}\lambda(T)\frac{d^2T}{dx^2}\frac{dx}{dT}$$

or

$$\frac{dz}{dT}\left(\frac{dT}{dx}\right) = -\frac{m}{I}\frac{d[\lambda(T)]}{dT}\left(\frac{dT}{dx}\right)^2 - \frac{m}{I}\lambda(T)\frac{d^2T}{dx^2} \qquad \text{(A-11)}$$

Applying the transformation (A-11) to equation (A-9), the latter becomes:

$$\frac{dz}{dT} + \frac{\rho(T)\lambda(T)}{z} \pm \sigma(T) = 0 \qquad \text{(A-12)}$$

Through the attempted transformation the order of the original differential equation was reduced but the non-linearity remained, so the solution of it at least is not obvious. From this point, the analysis of the problem is based on the assumption that in a first approximation the electric effects are independent. That means, it is assumed that the Thomson effect is not interacting with the Joule effect.

From this standpoint, the electric effects can be studied separately and their influence can be added finally in the interpretation of the formulae for the rate of heat flow in the two ends of the semiconductor element.

1. Influence of Thomson Effect on Heat Conduction

It is assumed that the Joule effect is not present in the system. Then it can be set $\rho(T) = 0$.

Equation (A-12) becomes, for one possible current direction:

$$\frac{dz}{dT} + \sigma(T) = 0 \qquad \text{(A-13)}$$

Integrating and introducing the transformation (A-10), equation (A-13) becomes:

$$-\lambda(T)\, m \frac{dT}{dx} = B - I\int_{T_c}^{T} \sigma(T)\, dT \qquad \text{(A-14)}$$

where B is the integration constant which must be determined. Transforming the independent variable x to the original r, equation (A-14) becomes:

$$-\lambda(T)\, m r \frac{dT}{dr} = B - I\int_{T_c}^{T} \sigma(T)\, dT \qquad \text{(A-15)}$$

The boundary conditions of the system are:

$r = R_1 \qquad T = T_H$

$r = R_2 \qquad T = T_C$

Under these conditions, the rate of heat flow in the two ends of the element is given by:

$$-\lambda(T)\, m r \left.\frac{dT}{dr}\right|_{r=R_1} = B - I\int_{T_c}^{T_H} \sigma(T)\, dT$$

(A-16)

$$-\lambda(T) m r \left.\frac{dT}{dr}\right|_{r=R_2} = B$$

Equation (A-15) can also be written as:

$$-\lambda(T) m r \frac{dT}{dr} = B\left(1 - \frac{I}{B}\int_{T_c}^{T} \sigma(T) dT\right) \qquad \text{(A-17)}$$

Integrating both sides:

$$B = \frac{m}{\ln\left(\frac{R_2}{R_1}\right)} \int_{T_c}^{T_H} \frac{\lambda(T)\, dT}{\left[1 - \frac{I}{B}\int_{T_c}^{T} \sigma(T) dT\right]} \qquad \text{(A-18)}$$

The following notations are used:

Q = rate of conduction heat flow = $\dfrac{m}{\ln\left(\frac{R_2}{R_1}\right)} \int_{T_c}^{T_H} \lambda(T) dT$

q_T = rate of Thomson heat flow = $I\int_{T_c}^{T_H} \sigma(T) dT$

From equations (A-16) it can be seen that $B \geqslant Q$.

The equality sign holds for the low temperature end. Also, for normal conditions, $Q > |q_T|$ and consequently, $\frac{|q_T|}{B} < 1$, which justifies the required conditions in order

to expand the fraction $\dfrac{1}{1-\frac{I}{B}\int_{\tau_c}^{\tau}\sigma(\tau)d\tau}$ in a series of the following form:

$$\frac{1}{1-\frac{I}{B}\int_{\tau_c}^{\tau}\sigma(\tau)d\tau} = 1+\left[\frac{I}{B}\int_{\tau_c}^{\tau}\sigma(\tau)d\tau\right]+\left[\frac{I}{B}\int_{\tau_c}^{\tau}\sigma(\tau)d\tau\right]^2+\cdots+\left[\frac{I}{B}\int_{\tau_c}^{\tau}\sigma(\tau)d\tau\right]^n \quad \text{(A-19)}$$

Equation (A-18) now can be written as:

$$B=\frac{m}{\ln\left(\frac{R_2}{R_1}\right)}\int_{\tau_c}^{\tau_H}\lambda(\tau)\left[1+\left(\frac{I}{B}\int_{\tau_c}^{\tau}\sigma(\tau)d\tau\right)+\left(\frac{I}{B}\int\sigma(\tau)d\tau\right)^2+\cdots+\left(\frac{I}{B}\int_{\tau_c}^{\tau}\sigma(\tau)d\tau\right)^n\right]d\tau \quad \text{(A-20)}$$

Integrating term by term and after some algebra, equation (A-20) can be written as:

$$B = Q\left[1+\frac{q_{T1}}{B}+\frac{q_{T2}^2}{B^2}+\cdots\frac{q_{Ti}^i}{B^i}+\cdots\right] \quad \text{(A-21)}$$

where:

$$q_{Ti} = I\left[\frac{\int_{\tau_c}^{\tau}\lambda(\tau)\left(\int_{\tau_c}^{\tau}\sigma(\tau)d\tau\right)^i d\tau}{\int_{\tau_c}^{\tau_H}\lambda(\tau)d\tau}\right]^{1/i}$$

for $i = 1,2,\ldots,n$

From equation (A-20) it can be set, for a first approximation, $B = Q$. Then, B for the second approximation becomes:

$$B = Q + \frac{q_{T1}}{Q} + \frac{q_{T2}^2}{Q^2} + \cdots + \frac{q_{Tm}^n}{Q^n} \qquad \text{(A-22)}$$

It is sufficient to keep only the first two terms of equation (A-22), since higher order terms are quite small.

$$B = Q + q_{T1} = Q + I\frac{\int_{T_c}^{T_H} \lambda(T) \int_{T_c}^{T} \sigma(T)\, dT\, dT}{\int_{T_c}^{T_H} \lambda(T)\, dT} \qquad \text{(A-23)}$$

Substitution of (A-23) in equation (A-16) yields:

$$-\lambda(T) m r \frac{dT}{dr}\bigg|_{r=R_1} = \frac{m}{\ln\left(\frac{R_2}{R_1}\right)} \int_{T_c}^{T_H} \lambda(T) dT - I\frac{\int_{T_c}^{T_H} \sigma(T) \int_{T_c}^{T} \lambda(T) dT\, dT}{\int_{T_c}^{T_H} \lambda(T) dT}$$

$$-\lambda(T) m r \frac{dT}{dr}\bigg|_{r=R_2} = \frac{m}{\ln\left(\frac{R_2}{R_1}\right)} \int_{T_c}^{T_H} \lambda(T) dT + I\frac{\int_{T_c}^{T_H} \lambda(T) \int_{T_c}^{T} \sigma(T) dT\, dT}{\int_{T_c}^{T_H} \lambda(T) dT} \qquad \text{(A-24)}$$

2. Influence of the Joule Effect on Heat Conduction

Here it is assumed that the Thomson effect is not present, so setting $\sigma(T) = 0$ equation (A-12) becomes:

$$\frac{dz}{dT} + \frac{\rho(T)\lambda(T)}{z} = 0 \qquad \text{(A-25)}$$

Rearranging and integrating, it is obtained:

$$Z^2 = D^2 - 2\int_{T_c}^{T} \lambda(T)\rho(T)\,dT$$

where D is the integration constant.

Introduction of the transformations:

$$z = -\frac{\lambda(T)m}{I}\frac{dT}{dx}$$

$$dx = \frac{dr}{r}$$

in the above equation yields:

$$-\lambda(T)mr\frac{dT}{dr} = \pm D_1\left[1 - \frac{2I^2}{D_1^2}\int_{T_c}^{T}\rho(T)\lambda(T)\,dT\right]^{1/2} \qquad \text{(A-26)}$$

The appearance of two signs in equation (A-26) leads to the conclusion that the temperature distribution along the element will present a local maximum T_m at a point corresponding to some radial distance R_m.

Rearranging equation (A-26), integrating both sides and applying the boundary conditions, the following expression for D_1 is obtained:

$$D_1 = \frac{m}{\ln\left(\frac{R_2}{R_1}\right)}\left[2\int_{T_H}^{T_m}\frac{\lambda(T)\,dT}{\left[1 - \frac{2I^2}{D_1^2}\int_{T_c}^{T}\rho(T)\lambda(T)\,dT\right]^{1/2}} + \int_{T_c}^{T_H}\frac{}{\left[1 - \frac{2I^2}{D_1^2}\int_{T_c}^{T_H}\rho(T)\lambda(T)\,dT\right]^{1/2}}\right] \qquad \text{(A-27)}$$

and for the point (R_m, T_m)

$$D_1 = \bar{I}\left[2\int_{T_c}^{T_m}\rho(T)\lambda(T)dT\right]^{1/2} \qquad \text{(A-28)}$$

There is a certain value of the current which could establish the condition of no back heat flow in the hot end of the element. That means, it is possible to have the point (R_m, T_m) shifted to coincide with the point (R_1, T_H), applying a certain value of current.

This value of current can be found from equations (A-27) and (A-28) and it is:

$$I_o = \frac{m}{\ln\left(\frac{R_2}{R_1}\right)}\int_{T_c}^{T_H}\frac{\lambda(T)dT}{\left[2\int_{T}^{T_m}\lambda(T)\rho(T)dT\right]^{1/2}} \qquad \text{(A-29)}$$

The above result might be important for the thermoelectric cooler, which should operate under the most efficient conditions.

The rate of heat flow at the two element ends is given by the following equations.

$$-\lambda(T)\,m\,r\left.\frac{dT}{dr}\right|_{r=R_1} = D_1\left[1-\frac{2I^2}{D_1^2}\int_{T_c}^{T}\rho(T)\lambda(T)dT\right]^{1/2} \qquad \text{(A-30)}$$

$$-\lambda(T)\,m\,r\left.\frac{dT}{dr}\right|_{r=R_2} = D_1$$

It is obvious from equation (A-26), in order for the left side to be real, the following condition should exist:

$$D_1^2 > 2I^2 \int_{T_c}^{T} \rho(T)\lambda(T)\,dT \qquad \text{(A-31)}$$

for the range of temperature under consideration.
Also, from equation (A-26) by integration of both sides

$$D_1 = \frac{m}{\ln\left(\frac{R_2}{R_1}\right)} \left[\int_{T_c}^{T_H} \frac{\lambda(T)\,dT}{\left[1 - \frac{2I^2}{D_1^2} \int_{T_c}^{T} \rho(T)\lambda(T)\,dT\right]^{1/2}} \right] \qquad \text{(A-32)}$$

The condition declared by equation (A-31) justifies the series expansion of the integrand of equation (A-32), in the binomial form.

$$\left(1 - \frac{2I^2}{D_1^2} \int_{T_c}^{T} \rho(T)\lambda(T)\,dT\right)^{-1/2} = (1+x)^p \qquad \text{(A-33)}$$

where $p = -\frac{1}{2}$ and $x = -\frac{2I^2}{D_1^2} \int_{T_c}^{T} \rho(T)\lambda(T)\,dT$

$$(1+x)^p = 1 + px + \frac{p(p-1)x^2}{2!} + \frac{p(p-1)(p-2)x^3}{3!} + \cdots + \frac{p(p-1)\cdots(p-n+1)x^n}{n!}$$

$$(1+x)^{-\frac{1}{2}} = 1 - \frac{1}{2}x + \frac{3}{4}\frac{x^2}{2!} - \frac{15}{8}\frac{x^3}{3!} + \cdots + \frac{(2n-1)(2n-3)\cdots 1}{2^n}\frac{x^n}{n!}$$

Application of the above expansion in equation (A-32) and integration of it term by term would yield, after algebraic manipulation, the following expression for D_1:

$$D_1 = Q + q_{J1} \sum_{n=1}^{\infty} C_n \frac{q_{Jn}^n}{q_{J1}} \frac{Q}{2^n} \left(\frac{Q}{D_1^2} \right)^n \qquad \text{(A-34)}$$

where:

$$Q = \frac{m}{\ln\left(\frac{R_2}{R_1}\right)} \int_{T_c}^{T_H} \lambda(T)\, dT$$

$$C_n = \frac{2n(2n-1)(2n-2)\cdots(2n-(n-1))}{n!}$$

$$q_{Jn} = I^2 \frac{\ln\left(\frac{R_2}{R_1}\right)}{m} \left[\frac{\int_{T_c}^{T_H} \lambda(T) \left(\int_{T_c}^{T} \rho(T)\lambda(T)\, dT \right)^n dT}{\left(\int_{T_c}^{T_H} \lambda(T)\, dT \right)^{n+1}} \right]^{\frac{1}{n}}$$

Following the same procedure as before, one can set $D_1 = Q$ as a first approximation. Applying this value of D_1 in equation (A-34), D_1 can be calculated in a second approximation as:

$$D_1 = Q \left[1 + \frac{q_{J1}}{Q} + \frac{3}{2} \frac{q_{J2}^2}{q_{J1}} \frac{1}{Q^2} + \cdots \right] \qquad \text{(A-35)}$$

The higher order correction in equation (A-35) might be considered to be quite small to be taken into account in an approximation solution.

It is sufficient to approximate D_1 by:

$$D_1 = Q + q_{J1} \tag{A-36}$$

Applying the above expression for D_1 in equations (A-30) the rate of heat flow at the two ends of the element, now it is given by:

$$-\lambda(T)\, m r \frac{dT}{dr}\bigg|_{r=R_1} = \frac{m}{\ln\left(\frac{R_2}{R_1}\right)} \int_{T_c}^{T_H} \lambda(T)\,dT - I^2 \frac{\ln\left(\frac{R_2}{R_1}\right)}{m} \frac{\int_{T_c}^{T_H} \lambda(T) \int_{T_c}^{T} \rho(T)\lambda(T)\,dT\,dT}{\left(\int_{T_c}^{T_H} \lambda(T)\,dT\right)^2} \tag{A-37}$$

$$-\lambda(T)\, m r \frac{dT}{dr}\bigg|_{r=R_2} = \frac{m}{\ln\left(\frac{R_2}{R_1}\right)} \int_{T_c}^{T_H} \lambda(T)\,dT + I^2 \frac{\ln\left(\frac{R_2}{R_1}\right)}{m} \frac{\int_{T_c}^{T_H} \lambda(T) \int_{T_c}^{T} \rho(T)\lambda(T)\,dT\,dT}{\left(\int_{T_c}^{T_H} \lambda(T)\,dT\right)^2}$$

3. Composite Solution

Based on the assumption that the electric effects — Joule and Thomson — are non-interacting, superposition of the obtained results yield the following composite solution

for the rate of flow of conduction heat in the semiconducting pellet:

$$-\lambda(T)\,m\,r\,\frac{dT}{dr}\bigg|_{\substack{r=R_1\\T=T_H}} = \frac{m}{\ln\left(\frac{R_2}{R_1}\right)}\int_{T_c}^{T_H}\lambda(T)\,dT - I^2\frac{\ln\left(\frac{R_2}{R_1}\right)}{m}\frac{\int_{T_c}^{T_H}\rho(T)\lambda(T)\int_{T_c}^{T}\lambda(T)\,dT\,dT}{\left(\int_{T_c}^{T_H}\lambda(T)\,dT\right)^2} + \\ + I\frac{\int_{T_c}^{T_H}\sigma(T)\int_{T_c}^{T}\lambda(T)\,dT\,dT}{\int_{T_c}^{T_H}\lambda(T)\,dT} \qquad \text{(A-38)}$$

$$-\lambda(T)\,m\,r\,\frac{dT}{dr}\bigg|_{\substack{r=R_2\\T=T_c}} = \frac{m}{\ln\left(\frac{R_2}{R_1}\right)}\int_{T_c}^{T_H}\lambda(T)\,dT + I^2\frac{\ln\left(\frac{R_2}{R_1}\right)}{m}\frac{\int_{T_c}^{T_H}\lambda(T)\int_{T_c}^{T}\rho(T)\lambda(T)\,dT\,dT}{\left(\int_{T_c}^{T_H}\lambda(T)\,dT\right)^2} - \\ - I\frac{\int_{T_c}^{T_H}\lambda(T)\int_{T_c}^{T}\sigma(T)\,dT\,dT}{\int_{T_c}^{T_H}\lambda(T)\,dT} \qquad \text{(A-39)}$$

Equation (A-38) is quite complicated to be used in the analysis of the thermoelectric cooler or generator, and it can be replaced by a simpler but less exact expression as:

$$-\lambda(T)\,m\,r\,\frac{dT}{dr}\bigg|_{r=R_1} = \frac{m}{\ln\left(\frac{R_2}{R_1}\right)}\int_{T_c}^{T_H}\lambda(T)\,dT - \frac{1}{2}I^2\bar{\rho}\frac{\ln\left(\frac{R_2}{R_1}\right)}{m} - I\hat{\sigma}\,\Delta T \qquad \text{(A-40)}$$

where: $\bar{\rho} = \frac{1}{\Delta T}\int_{T_c}^{T_H}\rho(T)\,dT$ $\qquad \hat{\sigma} = \frac{1}{\Delta T}\,\frac{\int_{T_c}^{T_H}\sigma(T)\int_{T_c}^{T}\lambda(T)\,dT\,dT}{\int_{T_c}^{T_H}\lambda(T)\,dT}$

The introduced error in equation (A-40) has been investigated using computer techniques and was found to be in the order of +5.8% and -3% for the resistivity terms of (A-40) for P and N type semiconducting pellets.

Analytically, a semiconducting SiGe allow has been used with electrical resistivity and thermal conductivity as shown in Figures 27 and 28. For $T_H = 645\ K°$ and $T_C = 400\ K°$ the following results were obtained:

P-TYPE	N-TYPE
$\hat{\rho} = 1.12535 \times 10^{-3}$	$\hat{\rho} = 0.64771 \times 10^{-3}$
$\frac{1}{2}\bar{\rho} = 1.275 \times 10^{-3}$	$\frac{1}{2}\bar{\rho} = 0.61 \times 10^{-3}$

where:

$$\hat{\rho} = \frac{\int_{T_c}^{T_H} \rho(T)\lambda(T)\int_{T_c}^{T} \lambda(T)\rho(T)\,dT\,dT}{\left(\int_{T_c}^{T_H} \lambda(T)\,dT\right)^2}$$

These small errors have a very slight effect in the calculated amount of the conduction heat rate of flow as it is calculated by (A-38) and (A-40). The calculated error was of the order of 0.2%.

The validity of the assumption of non-interacting electrical phenomena, in a first approximation, can be justified by replacing the arbitrary relation $\rho(T), \lambda(T), \alpha(T)$ with constant values in equations (A-38) and (A-39). Such a

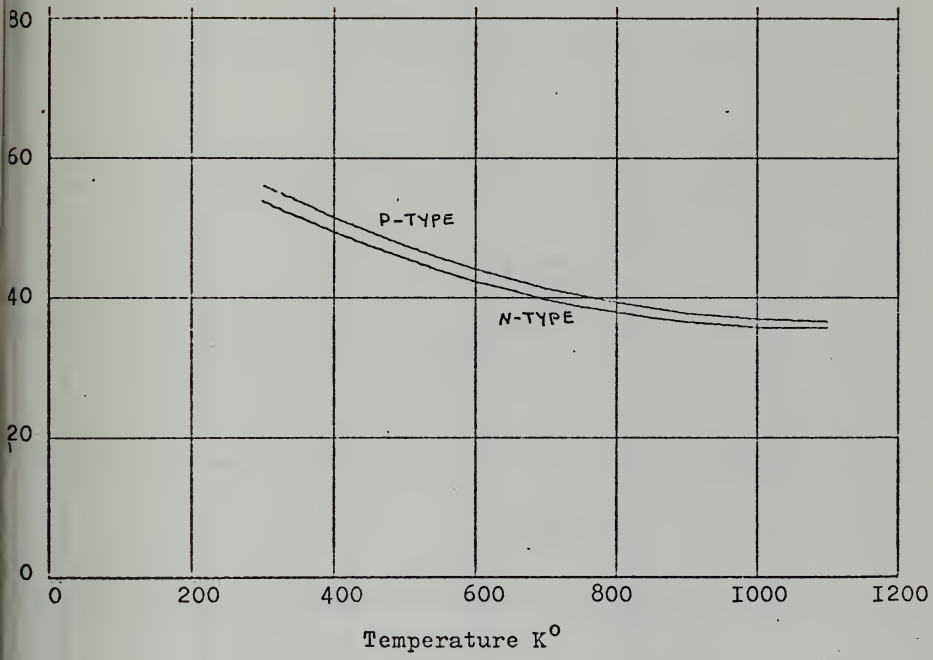

FIGURE 27

THERMAL CONDUCTIVITY x 10^3 - WATT/CM/DEG.

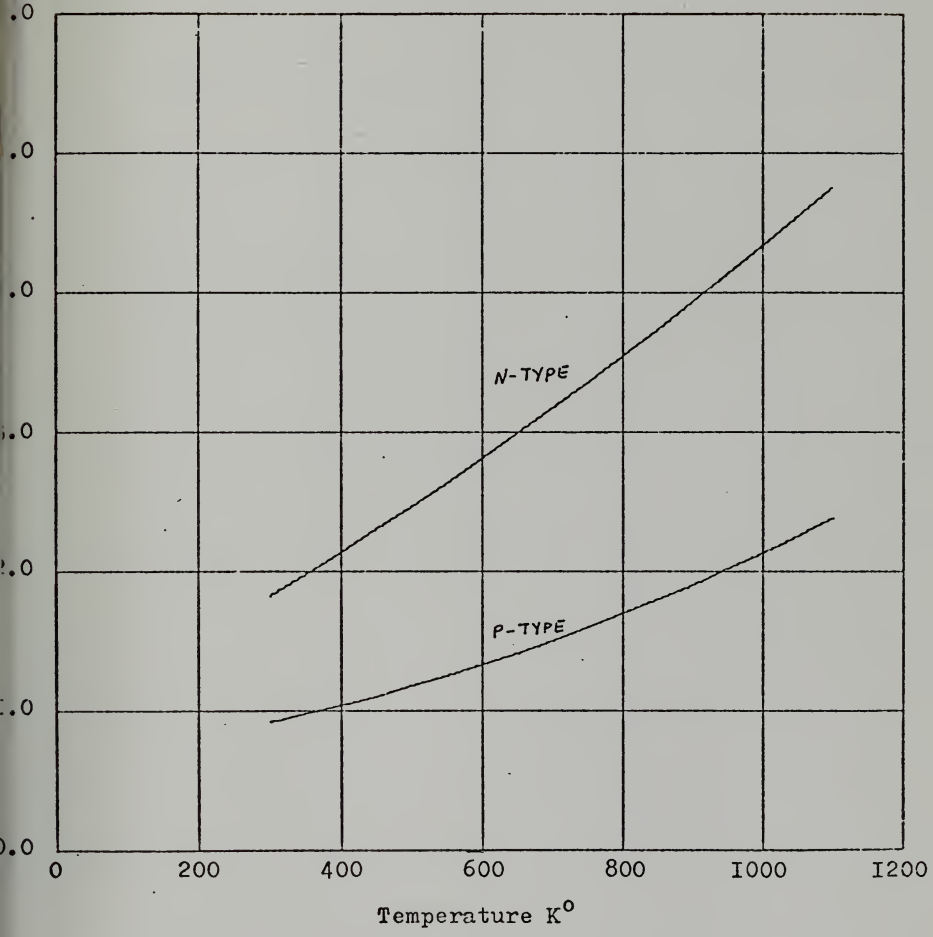

FIGURE 28

ELECTRICAL RESISTIVITY - OHM - CM x 10^3

substitution gives the exact form of the rigorous solution of the simplified differential equation as obtained in Appendix B.

APPENDIX B

SOLUTION OF SIMPLIFIED HEAT BALANCE EQUATION

The heat balance equation in the thermoelectric element with constant properties was defined in Section II as:

$$\frac{d^2T}{dr^2} + \frac{1}{r}\frac{dT}{dr} + \frac{B}{r^2} = 0 \qquad \text{(B-1)}$$

where $B = \dfrac{\rho I^2}{\lambda(\phi\tau)^2}$

Multiplying by r^2, equation (B-1) becomes:

$$r^2\frac{d^2T}{dr^2} + r\frac{dT}{dr} + B = 0 \qquad \text{(B-2)}$$

Introducing the transformation $x = \ln r$, equation (B-2) becomes:

$$\frac{d^2T}{dx^2} = -B \qquad \text{(B-3)}$$

Integration of equation (B-3) yields:

$$\frac{dT}{dx} = -Bx + C_1 \qquad \text{(B-4)}$$

$$T = C_2 + C_1x - \tfrac{1}{2}Bx^2 \qquad \text{(B-5)}$$

Replacing x with ln r equation (B-5) becomes:

$$T = C_2 + C_1 \ln r - \frac{1}{2} B (\ln r)^2 \qquad \text{(B-6)}$$

The initial conditions for the system are:

$r = R_1 \qquad T = T_H$

$r = R_2 \qquad T = T_C$

Introducing the above conditions to equation (B-6), it yields:

$$T_H = C_2 + C_1 \ln R_1 - \frac{1}{2} B (\ln R_1)^2 \qquad \text{(B-7)}$$

$$T_C = C_2 + C_1 \ln R_2 - \frac{1}{2} B (\ln R_2)^2 \qquad \text{(B-8)}$$

From equations (B-7) and (B-8) the constants of integration C_1 and C_2 are determined as:

$$C_1 = \frac{\frac{B}{2}\left[\ln (R_1 R_2) \ln \left(\frac{R_2}{R_1}\right)\right] - \Delta T}{\ln \left(\frac{R_2}{R_1}\right)} \qquad \text{(B-9)}$$

$$C_2 = T_H - C_1 \ln R_1 + \frac{B}{2} \left[\ln (R_1)\right]^2 \qquad \text{(B-10)}$$

The rates of heat flow at the hot junction ($T = T_H$) and at the cold junction are defined as:

$$q_1 = -\lambda(\phi\tau r)\frac{dT}{dr}\Big|_{r=R_1} = \lambda\frac{\phi\tau}{\ln\left(\frac{R_2}{R_1}\right)}\Delta T - \frac{1}{2}I^2\rho\frac{\ln\left(\frac{R_2}{R_1}\right)}{\phi\tau} \qquad \text{(B-11)}$$

$$q_2 = -\lambda(\phi\tau r)\frac{dT}{dr}\Big|_{r=R_2} = \lambda\frac{\phi\tau}{\ln\left(\frac{R_2}{R_1}\right)}\Delta T + \frac{1}{2}I^2\rho\frac{\ln\left(\frac{R_2}{R_1}\right)}{\phi\tau} \qquad \text{(B-12)}$$

The temperature distribution along a SiGe segment is shown in Figure 29.

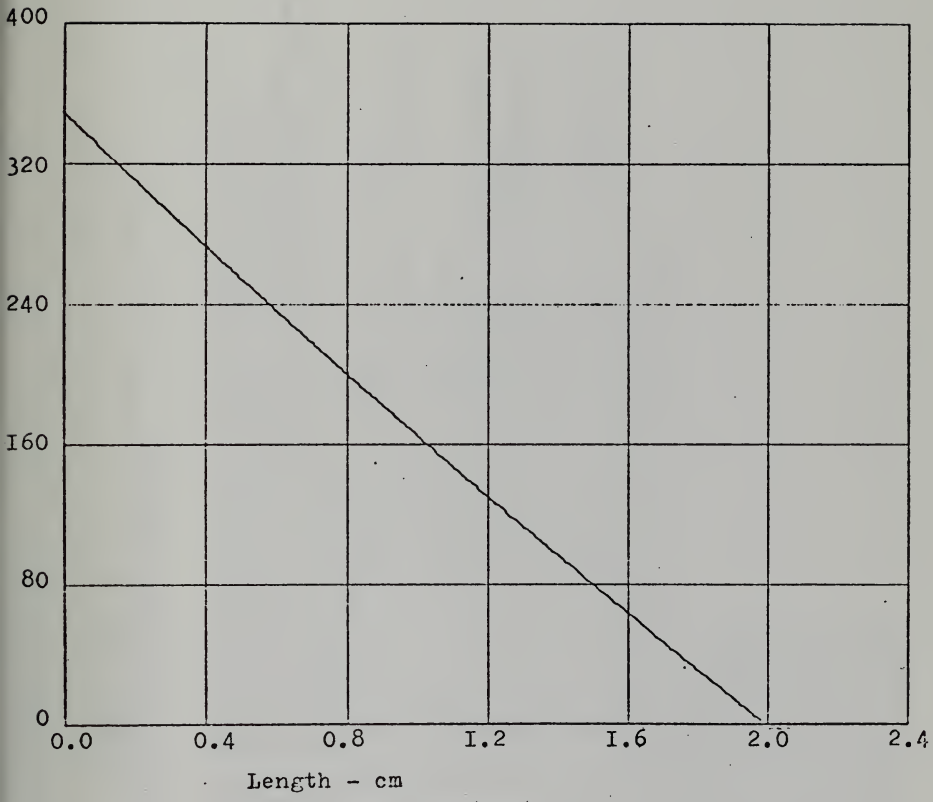

FIGURE 29

TEMPERATURE DISTRIBUTION IN A SiGe SEGMENT

```
C
C           PROGRAM  NO.  1
C     THIS PROGRAM CALCULATES THE CHARACTERISTICS OF THE
C   SEGMENTED THERMOELECTRIC GENERATOR
C
C
      REAL*8 AOP,A1P,A2P,BOP,B1P,B2P,GOP,G1P,G2P,C1P,C2P,TH,TC
      REAL*8 AON,A1N,A2N,BON,B1N,B2N,GON,G1N,G2N,C1N,C2N,LP1,LN1
      REAL*8 APO,AP1,AP2,BPO,BP1,BP2,GPO,GP1,GP2,CP1,CP2,TX,TY
      REAL*8 ANO,AN1,AN2,BNO,BN1,BN2,GNO,GN1,GN2,CN1,CN2,LP2,LN2
      REAL*8 SBP1,SBN1,SBP2,SBN2,SEB1,SEB2,KP1,KN1,RP1,RN1,RU,R2,R3,R4
      REAL*8 L,LTP1,LTP2,LTN1,LTN2,AP,AN,CUR,THP,THN,CDP1,CDP2
      REAL*8 CDN1,CDN2,A,M,N,D1,D2,W1,W2,W3,T1,RETP,RETN,V1,V2,V3
      REAL*8 Q1,Q2,Q3,PAR,EFF,EP,EN
      REAL NH,NHT1,NHT2,NHT3,NHT4,NHT5,NHT6
      DATA AON,A1N,A2N/0.6088288E-3,-0.00269657E-3,0.502E-8/
      DATA BON,B1N,B2N/42.40605128E-3,-0.06403288E-3,0.2953E-7/
      DATA GON,G1N,G2N/257.74918262E-6,-0.97372485E-6,0.0005347E-6/
      DATA C1N,C2N/-0.97372485E-6,0.00010694E-6/
      DATA AOP,A1P,A2P/5.77965414E-3,-0.0025E-3,0.0/
      DATA BOP,B1P,B2P/7.24100618E-3,0.00053692E-3,-0.61E-9/
      DATA GOP,G1P,G2P/88.821555E-6,0.47409667E-6,-0.00037167E-6/
      DATA C1P,C2P/0.47409667E-6,-0.00074334E-6/
      DATA ANO,AN1,AN2/-0.41467871E-3,0.0059497E-3,0.00000435E-3/
      DATA BNO,BN1,BN2/16.10561616E-3,-0.01337126E-3,0.00001714E-3/
      DATA GNO,GN1,GN2/21.96092588E-6,-0.91836756E-6,0.00096716E-6/
      DATA CN1,CN2/-0.91836756E-6,0.00193432E-6/
      DATA APO,AP1,AP2/-3.11792795E-3,0.0172502 2E-3,-0.00001442E-3/
      DATA BPO,BP1,BP2/46.58898533E-3,-0.1277562E-3,0.00012105E-3/
      DATA GPO,GP1,GP2/136.53867102E-6,0.50285533E-6,-0.00087778E-6/
      DATA CP1,CP2/0.50285533E-6,-0.00165556E-6/
      DATA TH,TC,TX,TY,CUR/720.,335.,450.,400.,20./
      DATA EP,EN,L,AP/1.0E-1,1.0E-1,0.258453731,0.2/
      DT=TH-TC
      DTX11=TH-TX
      DTX12=TH**2-TX**2
      DTX13=TH**3-TX**3
      DTX14=TH**4-TX**4
      DTX15=TH**5-TX**5
      DTX16=TH**6-TX**6
      DTX17=TH**7-TX**7
      DTX18=TH**8-TX**8
      DTY11=TH-TY
      DTY12=TH**2-TY**2
      DTY13=TH**3-TY**3
      DTY14=TH**4-TY**4
      DTY15=TH**5-TY**5
```

```
      DTY16=TH**6-TY**6
      DTY17=TH**7-TY**7
      DTY18=TH**8-TY**8
      DTX21=TX-TC
      DTX22=TX**2-TC**2
      DTX23=TX**3-TC**3
      DTX24=TX**4-TC**4
      DTX25=TX**5-TC**5
      DTX26=TX**6-TC**6
      DTX27=TX**7-TC**7
      DTX28=TX**8-TC**8
      DTY21=TY-TC
      DTY22=TY**2-TC**2
      DTY23=TY**3-TC**3
      DTY24=TY**4-TC**4
      DTY25=TY**5-TC**5
      DTY26=TY**6-TC**6
      DTY27=TY**7-TC**7
      DTY28=TY**8-TC**8
C   STEP  1
C
C         CALCULATION OF AVERAGE SEEBEC  COEFFICIENT
C
      SBP1=(G0P*DTX11+(G1P*DTX12/2.)+(G2P*DTX13/3.))/DTX11
      SBP2=(GP0*DTX21+(GP1*DTX22/2.)+(GP2*DTX23/3.))/DTX21
      SBN1=(G0N*DTY11+(G1N*DTY12/2.)+(G2N*DTY13/3.))/DTY11
      SBN2=(GN0*DTY21+(GN1*DTY22/2.)+(GN2*DTY23/3.))/DTY21
      SEB1=SBP1-SBN1
      SEB2=SEB1+SBP2-SBN2
      S1=SBP1*DTX11
      S2=SBP2*DTX21
      S3=SBN1*DTY11
      S4=SBN2*DTY21
      STOT=(S1+S2-S3-S4)/DT
      WRITE(6,10) SBP1,SBN1
   10 FORMAT(3X,'SBP1=',F10.8,3X,'SBN1=',F10.8)
      WRITE(6,11) STOT
   11 FORMAT(3X,'STOT=',F10.8)
      WRITE(6,15) SBP2,SBN2
   15 FORMAT(3X,'SBP2=',F10.8,3X,'SBN2=',F10.8)
      WRITE(6,16) SEB1,SEB2
   16 FORMAT(3X,'SEB1=',F10.7,3X,'SEB2=',F10.7)
C
C         CALCULATION OF CONDUCTIVITY INTEGRALS
C
      LP1=B0P*DTX11+B1P*(DTX12/2.)+B2P*DTX13/3.
      LP2=BP0*DTX21+BP1*(DTX22/2.)+BP2*DTX23/3.
      LN1=B0N*DTY11+B1N*(DTY12/2.)+B2N*DTY13/3.
```

```
      LN2=BNO*DTY21+BN1*(DTY22/2.)+BN2*DTY23/3.
      CDP1=LP1/DTX11
      CDP2=LP2/DTX21
      CDN1=LN1/DTY11
      CDN2=LN2/DTY21
      WRITE(6,20) LP1,LP2
   20 FORMAT(3X,'LP1=',F10.5,3X,'LP2=',F10.5)
      WRITE(6,25) LN1,LN2
   25 FORMAT(3X,'LN1=',F10.5,3X,'LN2=',F10.5)
      WRITE(6,26) CDP1,CDP2
   26 FORMAT(3X,'CDP1=',F10.6,3X,'CDP2=',F10.6)
      WRITE(6,28) CDN1,CDN2
   28 FORMAT(3X,'CDN1=',F10.6,3X,'CDN2=',F10.6)
C
CCC      CALCULATION OF CONSTANT OF INTEGRATION
C
      FP1=BOP*TX+(B1P*(TX**2)/2.0)+B2P*(TX**3)/3.0
      FP2=BPO*TC+(BP1*(TC**2)/2.0)+BP2*(TC**3)/3.0
      FN1=BON*TY+(B1N*(TY**2)/2.0)+B2N*(TY**3)/3.0
      FN2=BNO*TC+(BN1*(TC**2)/2.0)+BN2*(TC**3)/3.0
      WRITE(6,30) FP1,FP2,FN1,FN2
   30 FORMAT(3X,'FP1=',F10.5,3X,'FP2=',F10.5,3X,'FN1=',F10.5,3X,
     C'FN2=',F10.5)
C
CCC      CALCULATION OF THOMSON COEFFICIENT
C
      TMP1=(-0.5*FP1*C1P*DTX12+(C1P*BOP-FP1*C2P)*(DTX13/3.0)
     C+(C2P*BOP+0.5*C1P*B1P)*(DTX14/4.0)
     C+((C1P*B2P/3.0)+0.5*C2P*B1P)*(DTX15/5.0)
     C+C2P*B2P*DTX16/18.0)/LP1
      TMP2=(-0.5*FP2*CP1*DTX22+(CP1*BPO-FP2*CP2)*(DTX23/3.0)
     C+(CP2*BPO+0.5*CP1*BP1)*(DTX24/4.0)
     C+((CP1*BP2/3.0)+0.5*CP2*BP1)*(DTX25/5.0)
     C+CP2*BP2*DTX26/18.0)/LP2
      TMN1=(-0.5*FN1*C1N*DTY12+(C1N*BON-FN1*C2N)*(DTY13/3.0)
     C+(C2N*BON+0.5*C1N*B1N)*(DTY14/4.0)
     C+((C1N*B2N/3.0)+0.5*C2N*B1N)*(DTY15/5.0)
     C+C2N*B2N*DTY16/18.0)/LN1
      TMN2=(-0.5*FN2*CN1*DTY22+(CN1*BNO-FN2*CN2)*(DTY23/3.0)
     C+(CN2*BNO+0.5*CN1*BN1)*(DTY24/4.0)
     C+((CN1*BN2/3.0)+0.5*CN2*BN1)*(DTY25/5.0)
     C+CN2*BN2*DTY26/18.0)/LN2
      WRITE(6,40) TMP1,TMP2
   40 FORMAT(3X,'TMP1=',F10.5,3X,'TMP2=',F10.5)
      WRITE(6,45) TMN1,TMN2
   45 FORMAT(3X,'TMN1=',F10.5,3X,'TMN2=',F10.5)
C
CC                    AVERAGE  RESISTIVITY
```

```
      R1=(AOP*DTX11+0.5*A1P*DTX12+(A2P*DTX13/3.0))/DTX11
      R2=(APO*DTX21+0.5*AP1*DTX22+(AP2*DTX23/3.0))/DTX21
      R3=(AON*DTY11+0.5*A1N*DTY12+(A2N*DTY13/3.0))/DTY11
      R4=(ANO*DTY21+0.5*AN1*DTY22+(AN2*DTY23/3.0))/DTY21
      WRITE(6,60) R1,R2
   60 FORMAT(3X,'R1=',F10.5,3X,'R2=',F10.5)
      WRITE(6,65) R3,R4
   65 FORMAT(3X,'R3=',F10.5,3X,'R4=',F10.5)
C     STEP 2
      THP=DTX11/DT
      THN=DTY11/DT
C    STEP 3
      DO 100 I=1,600,1
      LTP1=FLOAT(I)/2000.
      LTP2=L-LTP1
      DIFP=(CDP1*DTX11/LTP1)-(CDP2*DTX21/LTP2)
      FDIP=ABS(DIFP)
      IF(FDIP.LE.EP) GO TO 200
  100 CONTINUE
  200 WRITE(6,300) DIFP,LTP1,LTP2
  300 FORMAT(3X,'DIFP=',F20.9,3X,'LTP1',F10.8,3X,'LTP2=',F10.8)
      DO 150 J=1,1000,1
      LTN1=FLOAT(J)/4000.
      LTN2=L-LTN1
      DIFN=(CDN1*DTY11/LTN1)-(CDN2*DTY21/LTN2)
      FDIN=ABS(DIFN)
      IF(FDIN.LE.EN) GO TO 250
  150 CONTINUE
  250 WRITE(6,350) DIFN,LTN1,LTN2
  350 FORMAT(3X,'DIFN=',F20.9,3X,'LTN1=',F10.8,3X,'LTN2=',F10.8)
C    STEP 4
  360 RESP=R1*LTP1+R2*LTP2
      RESN=R3*LTN1+R4*LTN2
      CONP=CDP1/LTP1
      CONN=CDN1/LTN1
      WRITE(6,365) RESP,RESN
  365 FORMAT(3X,'RESP=',F10.8,3X,'RESN=',F10.8)
      WRITE(6,370) CONP,CONN
  370 FORMAT(3X,'CONP=',F10.8,3X,'CONN=',F10.8)
C    STEP 5
      RAT1=(THP*CONP*RESN)/(THN*CONN*RESP)
      A=SQRT(RAT1)
      WRITE(6,380) A
  380 FORMAT(3X,'A=',F10.5)
      AN=A*AP
C    STEP 6
      Z1=THP*CONP*RESP
      Z2=THN*CONN*RESN
```

```
      WRITE(6,385) Z1,Z2
  385 FORMAT(3X,'Z1=',F10.5,3X,'Z2=',F10.5)
      W1=SQRT(Z1)
      W2=SQRT(Z2)
      WRITE(6,386) W1,W2
  386 FORMAT(3X,'W1=',F10.5,3X,'W2=',F10.5)
      W3=W1+W2
      D1=TH*STOT**2
      D2=4.*W3**2
      M=D1/D2
      WRITE(6,400) M,D1,D2
  400 FORMAT(3X,'M=',F10.8,3X,'D1=',F10.8,3X,'D2=',F10.8)
C     STEP 7
      N=1./4.*M
      T1=SEB1/STOT
      T2=(TMP1-TMN1)/STOT
      T3=TH*(N+T1)
      T4=(TH/N)-T2
      T5=T3/T4
      PAR=SQRT(T5)
      WRITE(6,450) PAR
  450 FORMAT(3X,'PARAM=',F10.5)
C     STEP  8
      RETP=(R1*LTP1/AP)+(R2*LTP2/AP)
      RETN=(R3*LTN1+R4*LTN2)/AN
      WRITE(6,500) RETP,RETN
  500 FORMAT(3X,'RETP=',F10.6,3X,'RETN=',F10.6)
C     STEP  9
      R=RETP+RETN
      RO=R*M
      WRITE(6,550) R,RO
  550 FORMAT(3X,'R=',F10.5,3X,'RO=',F10.5)
C     STEP  10
      RTP=0.5*R1*LTP1/AP
      RTN=0.5*R3*LTN1/AN
      WRITE(6,600) RTP,RTN
  600 FORMAT(3X,'RTP=',F10.6,3X,'RTN=',F10.6)
      CUR=STOT*DT/(R+RO)
      WRITE(6,680) CUR
  680 FORMAT(3X,'CUR=',F10.5)
      PHT1=0.5*R1*(LTP1/AP)*CUR**2
      PHT2=0.5*R2*(LTP2/AP)*CUR**2
      PHT3=(TMP1+TMP2)*CUR
      PHT4=(SBP2-SBP1)*TX*CUR
      PHT5=(AP/LTP1)*LP1
      PHT6=(AP/LTP2)*LP2
      PH=PHT1+PHT2-PHT3-PHT4+PHT5
      DFP=PH-PHT6
```

```
      ADFP=ABS(DFP)
      WRITE(6,700) ADFP
  700 FORMAT(3X,'ADFP=',F10.5)
      IF(ADFP.LT.0.1) GO TO 690
      LTP1=LTP1+0.001
      LTP2=L-LTP1
      GO TO 360
  690 NHT1=0.5*R3*(LTN1/AN)*CUR**2
      NHT2=0.5*R4*(LTN2/AN)*CUR**2
      NHT3=(TMN1+TMN2)*CUR
      NHT4=(SBN2-SBN1)*TY*CUR
      NHT5=(AN/LTN1)*LN1
      NHT6=(AN/LTN2)*LN2
      NH=NHT1+NHT2+NHT3-NHT4+NHT5
      DFN=NH-NHT6
      ADFN=ABS(DFN)
      WRITE(6,760) ADFN
  760 FORMAT(3X,'ADFN=',F10.5)
      IF(ADFN.LT.0.1) GO TO 750
      LTN1=LTN1+0.001
      LTN2=L-LTN1
      GO TO 360
  750 WRITE(6,800) LTP1,LTP2
  800 FORMAT(3X,'LTP1=',F10.5,3X,'LTP2=',F10.5)
  850 FORMAT(3X,'LTN1=',F10.5,3X,'LTN2=',F10.5)
      WRITE(6,850) LTN1,LTN2
C   STEP  11
      D=(RTP+RTN)/RO
      V1=(TMP1-TMN1)*(1.+(1./PAR))/(STOT*DT)
C   STEP  12
      V2=1.+(1./PAR)
      V3=1.+PAR
      Q1=TH*V3*V2/(4.*M*DT)
      Q2=TH*T1*V2/DT
      Q3=Q1+Q2-D-V1
      EFF=1./Q3
      WRITE(6,650) EFF
  650 FORMAT(3X,'EFFICIENCY=',F10.6)
      STOP
      STOP
      END
```

```
C
C         PROGRAM NO. 2
C     THIS PROGRAM DEVELOPS THE TEMPERATURE RELATIONS
C    OF THE T.E CHARACTERISTICS OF THE USED
C    SEMICONDUCTOR MATERIALS
C
C
C
      DIMENSION X(9),Y(9),A(9),RX(9),RH(9),R(9)
      REAL*8 X,Y,A,RX,RH
      INTEGER R
      DATA M,N/2,9/
      DATA X(1),X(2),X(3),X(4),X(5)/323.,373.,473.,573.,673./
      DATA X(6),X(7),X(8),X(9)/773.,873.,973.,1073./
      DATA Y(1),Y(2),Y(3),Y(4)/25.952,21.482,20.414,16.558/
      DATA Y(5),Y(6),Y(7),Y(8),Y(9)/13.286,12.27,11.855,9.878,6.547/
      CALL DCHBFT(X,Y,N,A,M,RX,RH,R)
      DO 500 I=1,7
      WRITE(6,1000) A(I)
 1000 FORMAT(5X,F15.8)
  500 CONTINUE
C     SUBROUTINE DCHBFT
C
C     PURPOSE:
C         SUBROUTINE DCHBFT EVALUATES THE COEFFICIENTS OF AN MTH ORDER
C         POLYNOMIAL P(X)=A(1)+A(2)*X+A(3)*X**2+...+A(M+1)X**M  SUCH
C         THAT THE MAXIMUM ERROR ABS(P(X(I))-Y(I)) IS A MINIMUM OVER
C         THE N (N.GT.M+1) SAMPLE POINTS X(I),Y(I), I=1,2,...,N.  THE
C         X(I) MUST FORM A STRICTLY MONOTONIC SEQUENCE; I.E.,
C         X(1).LT.X(2).LT.X(3).LT....X(N). THIS SUBROUTINE IS A
C         CONVERSION FROM ALGOL TO FORTRAN OF ALGORITHM 318, CHEBYSCHEV
C         CURVE-FIT FROM"COMMUNICATIONS OF THE ACM"VOL.10,NUMBER 12,
C         DECEMBER,1967. THE AUTHOR OF THE ALGOL VERSION WAS
C         J. BOOTHROYD FROM THE UNIVERSITY OF TASMANIA.
C
C     USAGE:
C         CALL DCHBFT(X,Y,N,A,M,RX,RH,R)
C
C         DESCRIPTION OF PARAMETERS:
C         X     -ARRAY OF ABSCISSAE DIMENSIONED REAL*8 X(N)
C         Y     -ARRAY OF ORDINATES DIMENSIONED REAL*8 Y(N)
C         N     -NUMBER OF SAMPLE POINTS  (INTEGER)
C         A     -ARRAY OF THE OUTPUTTED POLYNOMIAL COEFFICIENTS
C                DIMENSIONED AT LEAST A(M+2) (REAL*8)
C         M     -ORDER OF DESIRED APPROXIMATING POLYNOMIAL
C        RX    -WORK ARRAY DIMENSIONED AT LEAST  REAL*8 RX(M+2)
C         RH    -WORK ARRAY DIMENSIONED AT LEAST REAL*8 RH(M+2)
C         R     -INTEGER WORK ARRAY DIMENSIONED AT LEAST R(M+2)
```

```
C
C     REMARKS:
C         THE POLYNOMIAL P(X) IS A BEST-FIT POLYNOMIAL IN THE CHEBYSCHEV
C         SENSE AS DESCRIBED BY STIEFEL(NUMERICAL METHODS OF
C         TCHEBYCHEFF APPROXIMATION), IN LANGER(ED.),"ON NUMERICAL
C         APPROXIMATION",U.OF WISCONSIN PRESS, 1959, PP. 217-232.
C         STIEFEL (P.221) SHOWS THAT THE PROCEDURE MUST TERMINATE AFTER
C         A FINITE NUMBER OF STEPS. AT EXIT THE ABSOLUTE VALUE OF
C         A(M+1) YIELDS THE FINAL REFERENCE DEVIATION. NEGATIVE A(M+1)
C         INDICATES THAT THE PROCEDURE HAS BEEN TERMINATED FOLLOWING
C         THE DETECTION OF CYCLING.
C
C     NOTE:  DIVIDED DIFFERENCES AND NEWTON'S INTERPOLATING FORMULA IS
C         USED FOR COMPUTING THE POLYNOMIAL COEFFICIENTS.
C
      SUBROUTINE DCHBFT(X,Y,N,A,M,RX,RH,R)
      IMPLICIT REAL*8(A-H,O-Z)
      REAL*8 NEXTHI
      INTEGER RI,RJ,R(1)
      DIMENSION X(1),Y(1),A(1),RX(1),RH(1)
      MPLUS1=M+1
      MPLUS2=M+2
      PREVH=0.0
C     DETERMINE INDEX VECTOR FOR INITIAL REFERENCE SET
      R(1)=1
      R(MPLUS2)=N
      D=(N-1)/MPLUS1
      H=D
      DO 1 I=2,MPLUS1
      R(I)=H+1.0
    1 H=H+D
    2 H=-1.0
C     SELECT M+2 REFERENCE PAIRS AND SET ALTERNATIVE DEVIATION VECTOR
      DO 3 I=1,MPLUS2
      RI=R(I)
      RX(I)=X(RI)
      A(I)=Y(RI)
      H=-H
    3 RH(I)=H
C     COMPUTE M+1 LEADING DIVIDED DIFFERENCES
      DO 4 J=1,MPLUS1
      I1=MPLUS2
      AI1=A(I1)
      RHI1=RH(I1)
      I=MPLUS1
    5 DENOM=RX(I1)-RX(I-J+1)
      AI=A(I)
```

```
      RHI=RH(I)
      A(I1)=(AI1-AI)/DENOM
      RH(I1)=(RHI1-RHI)/DENOM
      I1=I
      AI1=AI
      RHI1=RHI
      I=I-1
      IF(I-J) 4,5,5
    4 CONTINUE
C     EQUATE (M+1) THE DIFFERENCE TO ZERO TO DETERMINE H
      H=-A(MPLUS2)/RH(MPLUS2)
C     WITH H KNOWN, COMBINE THE FUNCTION AND DEVIATION DIFFERENCES
      DO 6 I=1,MPLUS2
    6 A(I)=A(I)+RH(I)*H
C     COMPUTE POLYNOMIAL COEFFICIENTS
      J=M
    7 XJ=RX(J)
      I=J
      AI=A(I)
      JPLUS1=J+1
      DO 8 I1=JPLUS1,MPLUS1
      AI1=A(I1)
      A(I)=AI-XJ*AI1
      AI=AI1
    8 I=I1
      J=J-1
      IF(J-1) 9,7,7
    9 CONTINUE
C     IF THE REFERENCE DEVIATION IS NOT INCREASING MONOTONICALLY
C     THEN EXIT
      HMAX=DABS(H)
      IF(HMAX.GT.PREVH) GO TO 29
      A(MPLUS2)=-HMAX
      RETURN
C     FIND THE INDEX,IMAX,AND VALUE,HIMAX, OF THE LARGEST ABSOLUTE
C     ERROR FOR ALL SAMPLE POINTS
   29 A(MPLUS2)=HMAX
      PREVH=HMAX
      IMAX=R(1)
      HIMAX=H
      J=1
      RJ=R(J)
      DO110 I=1,N
      IF(I.EQ.RJ) GO TO 11
      XI=X(I)
      HI=A(MPLUS1)
      K=M
   12 HI=HI*XI+A(K)
```

```
      K=K-1
      IF(K-1)112,12,12
  112 HI=Y(I)
      ABSHI=DABS(HI)
      IF(ABSHI.LE.HMAX) GO TO 11
      HMAX=ABSHI
      HIMAX=HI
      IMAX=I
      GO TO110
   11 IF(J.GE.MPLUS2) GO TO110
      J=J+1
      RJ=R(J)
  110 CONTINUE
C     IF THE MAXIMUM ERROR OCCURS AT A NONREFERENCE POINT, EXCHANGE THIS
C     POINT WITH THE NEAREST REFERENCE POINT HAVING AN ERROR  OF THE
C     SAME SIGN AND REPEAT
      IF(IMAX.EQ.R(1)) RETURN
      DO 14 I=2,MPLUS2
      IF(IMAX.LT.R(I)) GO TO 15
   14 CONTINUE
      I=MPLUS2
   15 NEXTHI=H
      IF((I-I/2*2).NE.0) NEXTHI=-H
      IF(HIMAX*NEXTHI.GE.0) GO TO 115
      IF(IMAX.GE.R(1))      GO TO 116
      J1=MPLUS2
      J=M
  117 R(J1)=R(J)
      J1=J
      J=J-1
      IF(J-1)118,117,117
  118 R(1)=IMAX
      GO TO 2
  116 IF(IMAX.LE.R(MPLUS2)) GO TO 120
      J=1
      DO 121 J1=1,MPLUS2
      R(J)=R(J1)
  121 J=J1
      R(MPLUS2)=IMAX
      GO TO 2
  115 R(I)=IMAX
      GO TO 2
  120 R(I-1)=IMAX
      GO TO 2
      END
C                     JOB COMPLETE
```

```
C
C                PROGRAM NO. 3
C    THIS PROGRAM CALCULATES THE CHARACTERISTICS OF
C  ELEMENTARY T.E COOLER UNDER MAXIMUM COEFFICIENT OF
C PERFORMANCE CONDITIONS
C
C
C
      DIMENSION TIN1(15),TOUT1(15),TX(15),TC(15),NUM(15),DT(15)
      DIMENSION CUR(15),VOL(15),PWR(15),PUMP(15),COEF(15)
      DIMENSION TIN2(15),TOUT2(15),TY(15),TH(15),TAV(15),FM(15)
      DIMENSION TZ(15),PMPO(15),XZ(15),XX(15)
      REAL*8 TITLE(12)/'THOMAS  ',11*'          '/
      REAL LABEL/'    '/
      REAL*8 LNTH,NUM,LOAD
      DATA GP,GN/205.E-6,220.E-6/
      DATA RP,RN/1.20E-3,1.08E-3/
      DATA R1,R2/7.,8.5/
      DATA CP,CN/0.012,0.0149/
      DATA Z,PHP,PHN/1.0,0.174533,0.19455/
      DATA A,A1/7.389,1.8682/
      DATA LOAD/7000./
      AP=PHP*Z
      AN=PHN*Z
      W=R2/R1
      LNTH=ALOG(W)
      RES=(RP/AP+RN/AN)*LNTH
      WRITE(6,50) RES
   50 FORMAT(3X,'RES=',F10.5)
      CND=(CP*AP+CN*AN)/LNTH
      DO 1000 I=1,15
      X1=FLOAT(I)-1.
      TIN1(I)=100.-X1
      TOUT1(I)=75.-(X1/5.)-5.
      WRITE(6,100) TIN1(I),TOUT1(I)
  100 FORMAT(3X,'TIN1=',F10.5,3X,'TOUT1=',F10.5)
      TX(I)=(A*TOUT1(I)-TIN1(I))/(A-1.)
      TC(I)=(5.*(TX(I)-32.)/9.)+273.
      WRITE(6,120) TC(I)
  120 FORMAT(3X,'TC=',F10.5)
      TIN2(I)=TIN1(I)
      TOUT2(I)=TIN2(I)+10.
      WRITE(6,140) TOUT2(I)
  140 FORMAT(3X,'TOUT2=',F10.5)
      TY(I)=(A1*TOUT2(I)-TIN2(I))/(A1-1.)
      TH(I)=(5.*(TY(I)-32.)/9.)+273.
      WRITE(6,160) TH(I)
  160 FORMAT(3X,'TH=',F10.5)
```

```
      DT(I)=TH(I)-TC(I)
      XX(I)=DT(I)-20.
      SBC=GP+GN
      TAV(I)=(TH(I)+TC(I))/2.0
      Y1=CP*RP
      Y2=SQRT(Y1)
      Y3=CN*RN
      Y4=SQRT(Y3)
      Y5=Y2+Y4
      Y6=1./Y5
      Y7=Y6**2
      Y8=Y7*SBC**2
      Y9=Y8*TAV(I)+1.
      FM(I)=SQRT(Y9)
      TZ(I)=TH(I)/TC(I)
      COEF(I)=((FM(I)-TZ(I))/(FM(I)+1.))*(TAV(I)/DT(I))
      VOL(I)=SBC*DT(I)*FM(I)/(FM(I)-1.)
      CUR(I)=SBC*DT(I)/((FM(I)-1.)*RES)
      PWR(I)=VOL(I)*CUR(I)
      PUMP(I)=FM(I)*DT(I)*(TC(I)*FM(I)-TH(I))*SBC**2/
     C(RES*(FM(I)+1.)*(FM(I)-1.)**2)
      PMPO(I)=FM(I)*DT(I)*(TH(I)*FM(I)-TC(I))*SBC**2/
     C(RES*(FM(I)+1.)*(FM(I)-1.)**2)
      XZ(I)=PMPO(I)-1.
      NUM(I)=LOAD*0.293/PUMP(I)
      WRITE(6,170) CUR(I),VOL(I),PWR(I)
  170 FORMAT(3X,'CUR=',F10.5,3X,'VOL=',F10.5,3X,'PWR=',F10.5)
      WRITE(6,180) PUMP(I),COEF(I),NUM(I)
  180 FORMAT(3X,'PUMP=',F10.5,3X,'COEF=',F10.5,3X,'NUM=',F10.5)
      WRITE(6,185) PMPO(I)
  185 FORMAT(3X,'PMPO=',F10.5)
      WRITE(6,190) TAV(I),FM(I),TZ(I)
  190 FORMAT(3X,'TAV=',F10.5,3X,'FM=',F10.5,3X,'TZ=',F10.5)
 1000 CONTINUE
      CALL DRAW(15,XX,XZ,0,0,LABEL,TITLE,3.,0.,0,0,0,0,6,8,1,LAST)
      STOP
      END
```

```
C
C                PROGRAM NO. 4
C     THIS PROGRAM COMPARES THE TWO MODES OF
C     T.E COOLER DESIGN
C
C
      DIMENSION X(43),Q1(43),Q2(43),K1(43),K2(43),X1(43)
      REAL LNTH,M,K1,K2
      REAL*8 TITLE(12)/'THOMAS  ',11*'        '/
      REAL LABEL/'    '/
      DATA TC/291./
      DATA GP,GN/205.E-6,220.E-6/
      DATA RP,RN/1.20E-3,1.08E-3/
      DATA R1,R2/7.,8.5/
      DATA CP,CN/0.012,0.0149/
      DATA Z,PHP,PHN/1.0,0.174533,0.19455/
      AP=PHP*Z
      AN=PHN*Z
      W=R2/R1
      LNTH=ALOG(W)
      RES=(RP/AP+RN/AN)*LNTH
      WRITE(6,50) RES
   50 FORMAT(3X,'RES=',F10.5)
      SBC=GP+GN
      Y1=CP*RP
      Y2=SQRT(Y1)
      Y3=CN*RN
      Y4=SQRT(Y3)
      Y5=Y2+Y4
      Y6=1./Y5
      Y7=Y6**2
      Y8=Y7*SBC**2
      DO 1000  I=1,43
      X(I)=1.+(FLOAT(I)/100.)
      X1(I)=X(I)-1.
      SBC1=SBC**2
      TC1=TC**2
      TH=TC*X(I)
      TAV=(TC+TH)/2.
      Y9=Y8*TAV+1.
      M=SQRT(Y9)
      Z1=SBC1*TC1/(2.*RES)
      Z2=M-X(I)
      Z3=M+X(I)
      Z4=Z2*Z3
      Z5=M-1.
      Z6=M+1.
```

```
      Z7=Z5*Z6
      Q1(I)=Z1*Z4/Z7
      DT=TH-TC
      T1=SBC1/RES
      T2=Z5**2
      T3=TC*M-TH
      T4=T1*M*T3*DT
      Q2(I)=T4/(T2*Z6)
      D1=TC/DT
      D2=Z2/Z6
      K1(I)=D1*D2
      D3=2.*X(I)
      D4=1./D3
      D5=Z2*Z3
      D6=Z5*Z6
      D7=D5/D6
      K2(I)=D4*D7
      WRITE(6,500) Q1(I),Q2(I),X(I),K1(I),K2(I)
  500 FORMAT(3X,F10.5,3X,F10.5,3X,F10.5,3X,F10.5,3X,F10.5)
 1000 CONTINUE
      CALL DRAW(43,X1,K1,1,0,LABEL,TITLE,0.1,1.0,0,0,0,0,6,6,1,LAST)
      CALL DRAW(43,X1,K2,3,0,LABEL,TITLE,0.1,1.0,0,0,0,0,6,6,1,LAST)
      STOP
      END
```

LIST OF REFERENCES

1. The General Electric Report on, Optimization of Thermo-Electric Energy Converters, by L. Luft, 1961.

2. The Radio Corporation of America, Report on Thermo-Electric Materials for Power Conversion, F.D. Rossi, 1961.

3. The General Electric Report on, Optimization of Energy Converters, by G. Klein, 1960.

4. The Ford Motor Company Letter to Professor Wilcox, M.L., Subject: Data on Catalytic Converter, Feb. 10, 1975.

REFERENCES NOT CITED:

1. Sutton, G.W., Direct Energy Conversion, McGraw-Hill, Inc., 1966.

2. Spring, K.H., Direct Generation of Electricity, Academic Press, 1965.

3. Rogers, G.F., Engineering Thermodynamics, John Wiley, 1962.

4. Angrist, S.W., Direct Energy Conversion, Allyn and Bacon, Inc., 1971.

5. Kraus, A.D., Extended Surfaces, Spartan Books, Inc., 1964.

6. Allen, J.R., Heating and Air Conditioning, McGraw-Hill, Inc., 1946.

7. Howertor, M.T., Engineering Thermodynamics, Van Nostrand, Inc., 1962.

8. Burshteyn, A.I., Semiconductor Thermoelectric Devices, Temple Press Book Ltd., 1964.

9. Jacob, M., Heat Transfer, John Wiley, Inc., 1949.

10. Swanson, B.W., Optimization of a Sandwiched Thermoelectric Device, Journal of Heat Transfer, vol. 83, 1961.

11. Sheehan, W.F., Physical Chemistry, Allyn and Bacon, Inc., 1961.

INITIAL DISTRIBUTION LIST

		No. Copies
1.	Defense Documentation Center Cameron Station Alexandria, Virginia 22314	2
2.	Library, Code 0212 Naval Postgraduate School Monterey, California 93940	2
3.	Department Chairman, Code 52 Department of Electrical Engineering Naval Postgraduate School Monterey, California 93940	2
4.	Assoc. Professor M. Wilcox, Code 52Wx Department of Electrical Engineering Naval Postgraduate School Monterey, California 93940	3
5.	Assoc. Professor P. Marto, Code 53Mx Department of Mechanical Engineering Naval Postgraduate School Monterey, California 93940	1
6.	Hellenic Navy Headquarters Holargos Athens, Greece	1
7.	Lieutenant Thomas Tsoukalas, HN 19, Vikella - Eftzxia Str. Kato Patissia Athens, Greece	3

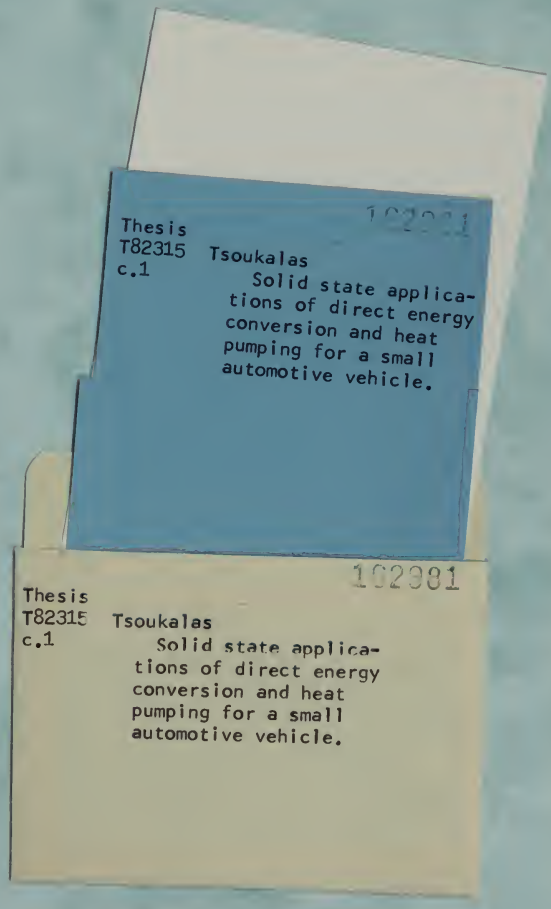
Thesis
T82315
c.1
Tsoukalas
Solid state applications of direct energy conversion and heat pumping for a small automotive vehicle.
102981
Thesis
T82315
c.1
Tsoukalas
Solid state applications of direct energy conversion and heat pumping for a small automotive vehicle.